FUNCTIONAL ROLES OF UBIQUITIN LIGASE GP78 IN ENDOPLASMIC
RETICULUM DOMAINS

by

Pascal St-Pierre

B.Sc., Université de Sherbrooke, 2003

A THESIS SUBMITTED IN PARTIAL FULFILLMENT OF
THE REQUIREMENTS FOR THE DEGREE OF

Doctor of Philosophy

in

THE FACULTY OF GRADUATE STUDIES

(Anatomy and Cell Biology)

THE UNIVERSITY OF BRITISH COLUMBIA

(Vancouver)

September 2012

Abstract

The ubiquitin ligase gp78, involved in ER-associated degradation, has been extensively studied using the 3F3A monoclonal antibody, and correlates with increaeed metastasis incidence in cancer patients (review in Chiu et al. 2008) The 3F3A-labeled ER characterized as an ER domain in close association with mitochondria distinct of the reticulon-labeled ER tubules, the juxtanuclear and the perinuclear ER. Overexpression of gp78 saw 3F3A expansion to the peripheral ER, but remained in association with mitochondria. This association is calcium-sensitive as elevation in cytosolic calcium levels disrupted contact with mitochondria. Similarly, induction of calcium released from the ER through thapsigargin or ATP stimulation of purinegic receptors promoted dissociation of 3F3A labeled ER and mitochondria. Upon ER-mitochondria dissociation, the IP3R-labeled ER dissociated in a distinct domain from the 3F3A-labeled ER, indicating that regulation of the ER-mitochondria association by free cytosolic calcium is a characteristic of smooth ER domains and that multiple mechanisms regulate the interactions between these organelles.

Upon overexpression of gp78, the 3F3A labeled peripheral ER was identified as the site of gp78-mediated ubiquitylation. Gp78 polyubiquitylated substrates where stabilized through Cue domain interaction in the peripheral ER. Derlin-1 and derlin-2, involved in retrotranslocation of ERAD substrates, localized to a juxtanuclear ER domain, where ubiquitylated proteins accumulate upon proteasome inhibition. This segregation was shown in a non-overexpressing system using HT-1080 fibrosarcoma cells expressing elevated levels of endogenous gp78. This shows the special segraqgation of ERAD by gp78-mediatedubiquitin ligase activity in the peripheral ER. This may function in ER quality control and regulate the expression of smooth ER-associated substrates in response to physiological change.

Finally, we found that stimulation of gp78 at the cell surface by its ligand AMF disrupts ER-mitochondria interaction, calcium coupling and decreases gp78 ubiquitin ligase activity. Disruption of the ubiquitin ligase activity via mutation of gp78 RING domain or expression of ubiquitin mutant unable to form elongated polyubiquitin chains disrupts ER-mitochondria

coupling. The increased fragmentation and reduced mobility of mitochondria upon gp78 overexpression were dependant on ubiquitin ligase activity and prevented by AMF treatment. These results describe a novel mechanism regulating mitochondrial dynamics via the ER ubiquitin ligase gp78.

Preface

Chapter 2 is based on a paper published in Journal of Cell Science titled: "Reversible interactions between smooth domains of the endoplasmic reticulum and mitochondria are regulated by physiological cytosolic Ca^{2+} levels" (Goetz JG., Genty., St-Pierre., Dang T., Joshi B., Sauve R., Vogl W., Nabi IR., 2007). Dr. Jacky Goetz, Hélène Genty and myself are co-first author, Thao Dang, Dr. Bharat Joshi, Dr. Rémi Sauvé, Dr. Wayne Vogl, have also participated in this paper with Dr. Ivan Robert Nabi as the corresponding author. My contribution was the quantification of the siRNA knockdown of gp78 using a dicer gp78 siRNA developed by Bharat Joshi (Figure 2.1). I also did the immunofluorescence of 3F3A and different ER subdomain shown in Figure 2.2, with the exception of the mitochondria labeling, which was done by Thao Dang. The immunofluorescences and calcium measurements shown in the subsequent figures were done by either Dr. Jacky Goetz or Hélène Genty. I participated in the redaction and revision of the manuscript.

I was involved in every experiments presented in Chapter 3. Thao Dang did the p97 immunoprecipitation (Figure 3.2c), and immunofluorescence (Figure 3. 4b), as well as the 3F3A western blot (Figure 3.2a). Thao Dang also did few experiments leading to the ubiquitin ligase activity quantification (Figurte 3.2b). Dr. Bharat Joshi helped to produce the viruses used for the gp78 shRNA stable cell lines (Figure 3.7). I wrote the manuscript under the supervision of Dr. Ivan Robert Nabi, and the manuscript has been accepted in Journal of Cell Science, titled: "Peripheral Endoplasmic Reticulum Localization of Gp78 Ubiquitin Ligase Activity" (St-Pierre, P., et al. 2011).

Chapter 4 was based on a manuscript in which Dr. Min Fu and I are co-first author. Experiments presented in Figure 4.1 and 4.2 were conducted by Min Fu. Results in Figure 4.3 and 4.4 were obtained following a protocol of ubiquitin ligase activity quantification (Figure 4.4a) that I developed. Transfected cells in calcium quantification experiments were identified by FlAsH/ReAsH labeling using the tetracystein tag protocol that I cloned and optimized. I designed and cloned all the gp78 constructs used in this

manuscript. I generated the 4D quantification of mitochondria dynamics and the FRAP data presented in Figure 4.6 and 4.7.

Table of Contents

List of Tables

List of Figures

List of Schematics

Chapter 1: Introduction

The endoplasmic-reticulum (ER) is an organelle present in all eukaryotic cells. It is composed of an extensive network of membrane that spreads throughout the cytoplasm. It is a central component to membrane and secreted protein biosynthesis, as well as calcium homeostasis and regulation of lipid and cholesterol production. This wide variety of functions is organized in subdivisions of the ER called subdomains. The subdomains are defined by the ER morphology, contact with other organelles or by the enrichment of resident proteins. For example, rough ER (RER) was identified as the site of protein biosynthesis and entry into the secretory pathway and ER-mitochondria contact sites as the site of calcium transfer between the two organelles. The organization of these subdomains is highly dynamic and adaptive to the cellular physiological states.

In my thesis, I will first describe and characterize a new subdomain of the ER defined by a subpopulation of the ubiquitin ligase gp78. I will then discuss the function of this ER subdomain and its role in the ER-associated degradation (ERAD) pathway. I will finally examine the involvement of gp78 ubiquitin ligase function on the regulation of ER-mitochondria interaction and mitochondrial dynamics.

1.1 Endoplasmic reticulum structure

The first structural studies by electronic microscopy (EM) divided the ER in two distinct domains, smooth ER (SER) and rough ER (RER), based on the presence of cytoplasmic studded ribosome and polysomes to define the RER reviewed in (Voeltz et al., 2003). EM studies of SER have further defined the presence of a tubular meshwork and tripartite junctions while the rough ER is classically formed of parallel ribosome studded sheets. More recent studies using live cell microscopy have revisited this classification and morphologically classified the ER into two domains: the tubular ER and the ER sheets, the later including the perinuclear membrane (Shibata et al.2011; Shibata et al., 2006; Voeltz et al., 2006).

1.1.1 The tubular ER

The tubular ER is a network of tubules, as indicated by its name, interconnected by three-point junctions and is also called the peripheral ER, as it extends throughout the cell. Its structure is generated by the reticulon protein family (Voeltz et al., 2006). These proteins have transmembrane domains containing a hairpin motif that form a wedge in the ER membrane inducing a positive curvature of ER tubules and also form stable homo-oligomers in the ER, thereby forming a scaffold that stabilizes the tubular shape (Shibata et al., 2008). This hydrophobic insertion together with the formation of a scaffold is sufficient to form tubules *in vitro*, with any individual member of these protein families are able to generate tubules in proteoliposomes (Hu et al., 2008).

The tubular structure of the peripheral ER is also highly interconnected, forms three-way junctions with one another generating a dynamic polygonal network (Lee and Chen, 1988). This branched network is maintained by a dynamin-like class of GTPases called the atlastins. Atlastin GTPases are membrane bound and directly interact with DP1 and the reticulons. When a dominant negative mutant of atlastin 1 is overexpressed ER branching is diminished drastically (Hu et al., 2009).

ER assembly/disassembly of three-way junctions is important during mitosis where the ER network is broken down to allow separation in the two daughter cells. Following mitosis, the reformation of the ER network is accomplished through two sequential fusion reactions. The first process is performed by the N-ethylmaleimide-sensitive fatcor (NSF) that bring disconnected tubules together. The second fusion is performed by the ATPase p97 and its cofactor p47and VCIP135 (Kano et al., 2005). During interphase, p37, another co-factor of p97, has been shown to maintain the number of three-way junction (Uchiyama et al., 2006).

1.1.2   ER sheets

ER sheets represent juxtanuclear ER domains that are composed of two membranes aligned in parallel way (Bernales et al., 2006). Reticulons and DP1 proteins maintain the curve at the edge of a folded membrane by stabilizing a sheet domain. A recent study established that the relative amount of reticulons and DP1 determine the ratio of sheet:tubule in a given cell; their increased expression results in more tubules and their decreased expression results in more sheets (Hu et al. 2011). The luminal space in the sheet is regulated by the coiled-coil membrane protein CLIMP-63.   The luminal coiled-coil domains of individual proteins located on opposite sides of the sheets flatten the membranes and stabilize the luminal space at 50nm (30nm in yeast). Interestingly, translocon proteins, coiled-coil proteins and other sheet-enriched proteins are concentrated in ER sheets upon interaction with polysomes, therefore establishing peripheral ER tubules as SER and juxtanuclear ER sheets as the RER (Hu et al. 2011).

However, segregation of the ER into only two structurally distinct domains remains simplistic. The ER is also organized into sub-domains that are functionally distinct. Some of the key questions remaining to understand the ER organization are related to the localization of biochemical processes in relation to its architecture. The ER comprises 50% of cell membranes and interacts with multiple organelles including mitochondria, the plasma membrane, Golgi apparatus, nucleus (nuclear membrane) and endosomes (Chao and Loewen, 2010). How these various ER specializations are defined, interact and contribute to ER domain function represents a major challenge of future research on this organelle.

1.2   The ER quality control

Secretory and transmembrane proteins acquire their tertiary structure in the ER prior to their export. Protein folding is a slow succession of intermediate conformations directed by interaction with multiple chaperones as the polypeptide acquires post-translational modifications. Multiple receptors have to form homo- or heteromers with precise

stoichiometry prior to exit the ER. Misfolded or misassemble subunits can lead to aggregate accumulation, a dominant negative phenotype or an improper function, resulting in conformational diseases such as Alzheimer's disease, Parkinson disease and diabetes for example (reviewed in (Yoshida, 2007)). The ER has a specially elaborated quality control system to prevent accumulation of misfolded proteins called the unfolded protein response (UPR). The UPR is divided in three different steps; transcriptional induction, translational attenuation and ER-associated degradation (ERAD). In this section, the UPR system, the ERAD pathway and the existence of a ER quality control compartment (ERQC) or subdomain will be detailed and discussed.

1.2.1   The unfolded protein response (UPR)

Molecular chaperones in the ER, such as BiP and GRP94, and folding enzymes such as protein disulfide isomerase (PDI) assist and facilitate nascent polypeptides to acquire their proper tertiary structure (Schroder and Kaufman, 2005). These chaperones, especially BiP, also monitor the amount of misfolded proteins in the ER. In normal condition, a subpopulation of BiP binds to the major inducer of the UPR pathway, namely IREs, ATF6 and PERK to keep the UPR suppressed. Competition for BiP/GFP78 binding by accumulation unfolded proteins releases these effectors leading to UPR induction. IREs and ATF6 are involved in transciptional induction of folding chaperones and PERK is involved in transcriptional attenuation, preventing further increase in ER stress due to the accumulation of newly translated proteins. ER stress is resolved by disposal of misfolded protein, either via chaperones interaction achieving proper folding or degradation by the ERAD pathway. If UPR fails to resolve the folding problem, aggregates will accumulate in the ER lumen, causing sustained ER stress and apoptosis.

1.2.1.1   Transcriptional induction

Competition for BiP by misfolded proteins releases the sensor molecule ATF6. ATF6, another translational induction protein, is also retained in the ER via interaction of its luminal

domain with BiP. Upon competition with BiP, ATF6 is trafficked to the Golgi where a pair of proteases, S1P and S2P, sequentially cleave ATF6, releasing its cytosolic fragment. This cytosolic fragment translocates to the nucleus where it acts as a transcription factor for gene under control of the ER-stress response element (ERSE), and such as BiP, GRP95 and calreticulin.

The inositol requirement 1 protein (IRE1) is a sensor molecule of ER stress in the ER membrane responsible for transcriptional induction. Upon its release from BiP, IRE1 is activated by dimerization, which induces transphosphorylation via a kinase domain, which subsequently activates an endonuclease domain (Iwawaki et al., 2001; Tirasophon et al., 1998). Activated IRE1 convert the XBP1 mRNA into a mature mRNA, leading to the translocation of transcription factor. XPB-1 has been shown to promotes transcription of members of the ERAD pathway, such as EDEM, HDR1, Derlin-2 and -3 (Oda et al., 2006; Yoshida et al., 2003). Interestingly, XBP1 also induces expression of lipid synthesis and ER biogenesis genes, thought to increase the ER volume and therefore, accommodate accumulated folding proteins (Calfon et al., 2002; Sriburi et al., 2004).

The transcriptional induction also increased transcription of proteins not known to be involved in the folding process. Using microarray techniques (Travers et al., 2000), a total of 381 genes were found to be up- or down-regulated in response to UPR in yeast. These findings suggest that the purpose of UPR is not simply increasing the folding capacity of the ER but also inducing mechanisms to remove misfolded proteins and restore ER integrity.

1.2.1.2   Transductional attenuation

UPR also involves translational attenuation in response to ER stress. The continuous flow of newly synthesized proteins may be problematic when proper folding is impaired in the ER. The attenuation of translation is initiated by the ER type I transmembrane protein kinase PERK (Shi et al., 1998). Once released from BiP, PERK is activated through oligomerization and auto-transphosphorylation (Bertolotti et al., 2000). The activated PERK induces

phosphorylation of the α subunit of eukaryotic translation factor 2 (eIF2-α) on serine 51 (Harding et al., 1999; Koumenis et al., 2002). The phosphorylated eIF2-α interferes in the assembly of the ribosomal 60S and 40S subunits by leading to the formation of a 43S initiation complex (Fernandez et al., 2002). The inactivation of eIF-2 by PERK induces increase of transcription factor AFT4 mRNA and activates the GRP/78 promoter independently of the ERSE element (Luo et al., 2003) but no specific ribosomal binding factors allowing transduction of those factors in the absence of eIF-2 were discovered yet.

The UPR pathway not only increases transcription of chaperones and attenuates translation of other proteins but also increases degradation of misfolded/misassembled proteins via the ERAD pathway. The third function of the UPR is the degradation of misfolded proteins. This complex mechanism is active at a basal level in non-stress condition and will be discussed in detail in the next section.

1.2.2   ER-associated degradation (ERAD)

Endoplasmic reticulum-associated degradation (ERAD) is a cellular pathway targeting ER proteins for proteasomal degradation; this pathway functions to eliminate misfolded and misassembled proteins and also occurs in response to specific physiological conditions (reviewed in (Meusser et al., 2005; Vembar and Brodsky, 2008)). This pathway comprises three general steps: 1. substrate recognition by chaperones in the ER lumen; 2. ubiquitylation and translocation from the ER to the cytosol; and 3. degradation by the proteasome.

1.2.2.1   Substrate recognition

The maturation of secreted and transmembrane protein is slow and inefficient (Ellgaard and Helenius, 2003). Post-translational modifications such as N-linked glycosylation, disulfide-bond formation and cleavage that are essential to proper folding require interaction with multiple chaperones, glycosidases and protein disulphide isomerases that requires time. Misfolded or misassembled proteins are recognized by ER luminal chaperones. As explained

in the previous section, the UPR system detects such misfolded proteins, and signaling from the ER lumen to the nucleus stimulates expression of folding chaperones to correct the folding/assembly problem and of others chaperones to facilitate their degradation (Casagrande et al., 2000; Friedlander et al., 2000; Travers et al., 2000). However, in the normal folding process of a protein, the same hydrophobic polypeptide segment can be transiently exposed. To explain how misfolded proteins are individualized from proteins still into their folding process, a molecular "timer" was proposed for glycoproteins.

1.2.2.1.1   Glycosylation-deglycosylation cycle

Soon after its translocation in the ER membrane, a nascent glycoprotein is conjugated to the carbohydrate polymer $Glc_3Man_9GlcNac_2$ on a specific asparagines residues, and from there, it starts along the folding pathways (Schematic 1.1). The sugar polymer attached is sequentially trimmed by glucosidase I and II and, as long as the polypeptide remains unfolded, the UDP-glucose glycosyltransferase (UGGT) adds a glucose to the sugar chain that will be cleaved again by glucosidase II. The monoglucosylated form of the sugar chain is recognized by calnexin and calreticulin, two ER chaperones that retained the folding polypeptide in the ER, preventing its export. This process, from chaperones to glucosidase II and back to chaperones, passes through an unknown number of cycles while the protein acquires its native conformation. The mono- or- non glycosylated form of the sugar chain can be recognized by the enzyme mannosidase I. The mannosidase I reaction is slow, so only unfolded proteins that spent an excessive amount of time will have a sugar moiety $Man_8GlcNAc_2$ (Jakob et al., 1998). $Man_8GlcNAc_2$-tagged protein are recognized by ER degradation-enhancing α-mannosidase-like protein 1 and 2 (EDEM), a lectin that targets misfolded proteins to retro-translocation complexes (Molinari et al., 2003).

The importance of this pathway is underscored by the fact that treatment of cells with tunicamycin, an inhibitor for *N*-glycosylation, results in the accumulation of misfolded proteins in the ER and UPR induction (Okuda-Shimizu and Hendershot, 2007). Although glycosylation seems to be a critical element for the recognition of ERAD substrates, it is less

clear how non-glycosylated misfolded proteins are recognized and targeted for degradation. It was recently proposed that monoubiquitylation could be involved in a sensing mechanism for membrane proteins on the cytosolic side of the ER (Feldman and van der Goot, 2009)
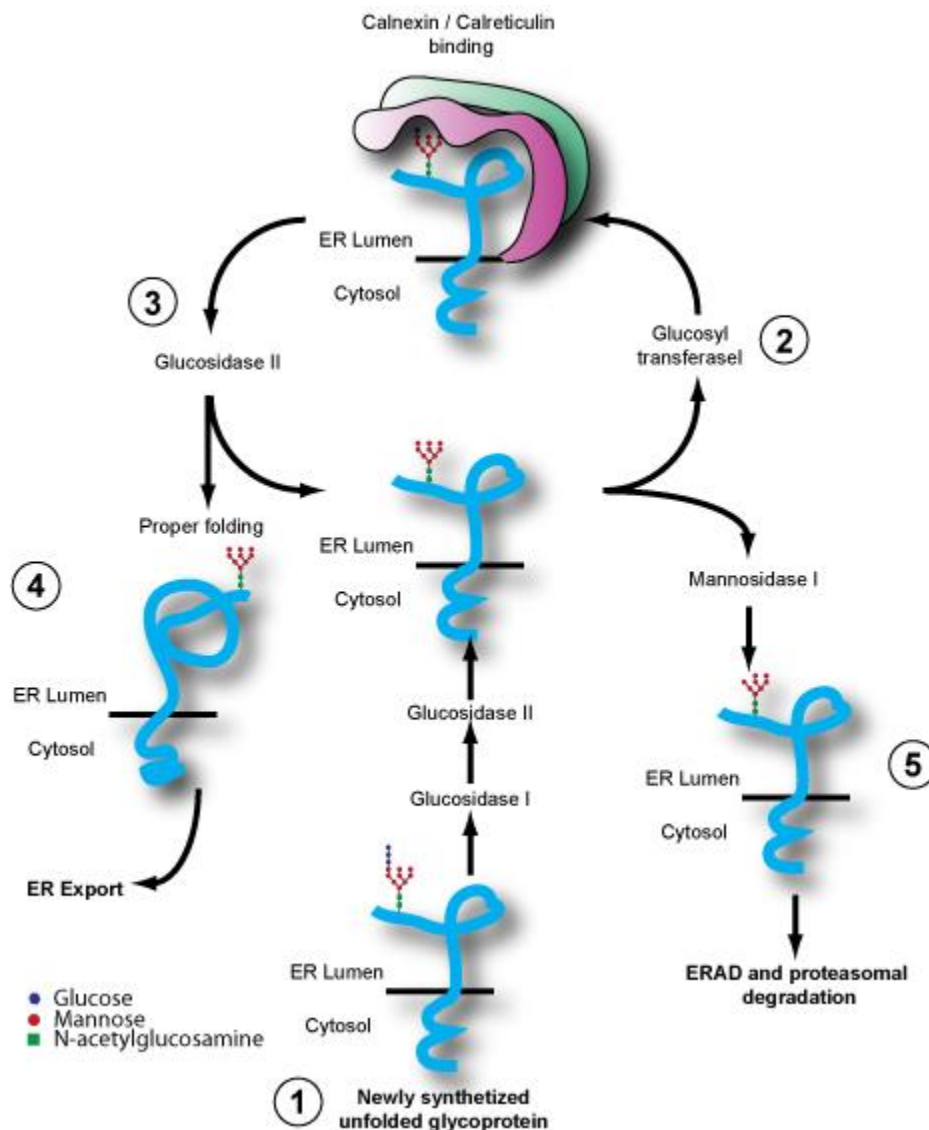
Schematic 1-1 The glycosylation de-glycosylation cycle

After the insertion of a newly synthesized glycoprotein in the ER membrane, (1) sugar polymers $Glc_3Man_9GlcNac_2$ are conjugated to asparagine residues. The sugar polymer attached is sequentially trimmed by glucosidase I and II and, as long as the polypeptide remains unfolded, the UDP-glucose glycosyltransferase (UGGT) adds a glucose to the sugar (2) which promote binding with the folding chaperones calnexin and calreticulin. The sugar

chain is then cleaved by the glycosidase II (3). If the polypeptide achieved proper folding it will be recruited for ER export (4), if folding is not achieved, the polypeotide will re-enter the glycosylation cycle. In case of permanent misfolding, resulting in excessive time in the glycosylation cycle, the glycosylated protein will be trimmed by mannosidase I to form $Man_8GlcNAc_2$ and the polypeptide will be recognized as an ERAD substrates. The mannosidase I reaction is slow, so only unfolded protein that spend an excessive amount of time will have a trimmed sugar moiety (adapted from (Feldman and van der Goot, 2009)).

1.2.2.1.2   Ubiquitylation-deubiquitylation cycle

Studies of the biogenesis of the lipoprotein receptor-related protein-6 (LRP6) found that palmitoylation-deficient mutants were not only retained in the ER, but were also monoubiquitylated on a juxtamembranous-lysine residue (Abrami et al., 2008). This monoubiquitylated form of LRP6 was not targeted to proteasome via ERAD. Interestingly, palmitoylation-deficient mutants carrying a mutation preventing monoubiquitylation were delivered at the plasma membrane, identifying monoubiquitylation as an ER retention signal. These observations lead to the proposition of an ubiquitin-dependent quality mechanism control in the ER involving an ubiquitin-chain editing process (Abrami et al., 2008).

Ubiquitylation is a dynamic and reversible protein modification. It is well known that polyubiquitin acts as a degradation signal by the proteasome. On the other hand, monoubiquitin is involved in regulatory functions. For example, at the plasma membrane, monoubiquitylation of the epidermal growth factor receptor (EGFR) leads to its recruitment in clathrin coated pits (Mosesson et al., 2003). Ubiquitin-chain editing, a process that regulates ubiquitin chain assembly has been suggested to be involved in ERAD (Feldman and van der Goot, 2009). Ubiquitin-chain editing has been observed for the cystic fibrosis transmembrane regulator (CFTR). CFTR is first monoubiquitylated by the ubiquitin ligase RMA1 prior to being polyubiquitylated by gp78 and targeted to the proteasome (Morito et al., 2008a).

Proteins undergoing the folding process would be monoubiquitylated and protected from polyubiquitylation via interaction with ubiquitin-binding chaperones. After proper folding, monoubiquitylated-proteins would then recruit de-ubiquitylating enzymes and allow the newly synthesized protein to be exported. Inversely, misfolded proteins would see their monoubiquitylation being extended to polyubiquitin chain and subsequently sent for degradation. A potential de-ubiquitylating enzyme playing this role could be ataxin 3. Ataxin 3 has a de-ubiquitylation and a ubiquitin binding domain and it interacts with p97 (Stirling and Lord, 2006; Wang et al., 2006; Zhong and Pittman, 2006). This process is still hypothetical but deserved further investigation.
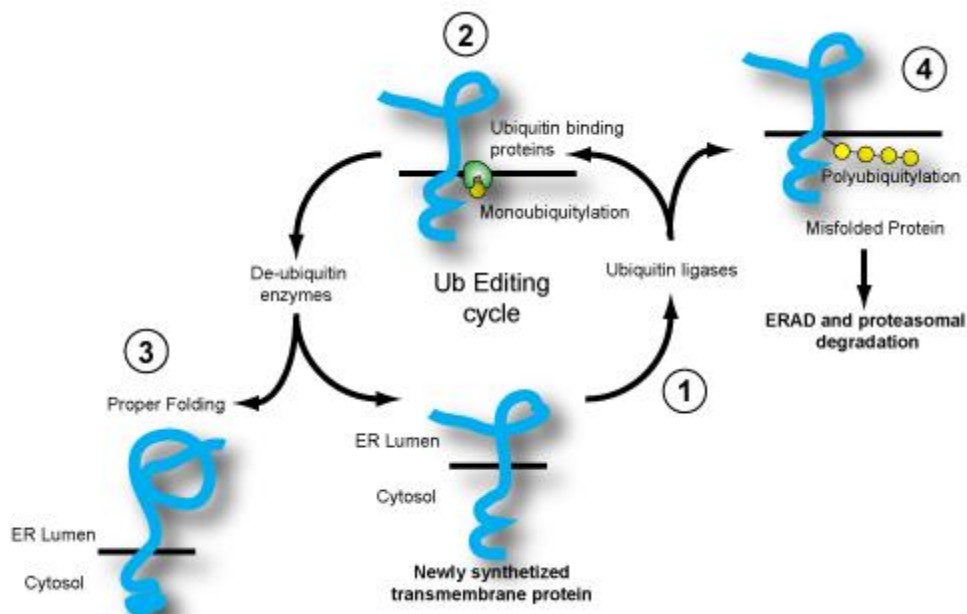
Schematic 1-2 The ubiquitylation de-ubiquitylation cycle
Upon co-translational insertion of a newly synthesized polypeptide in the ER membrane, a ubiquitin molecule is added to a cytoplasmic juxtamembrane lysine residue (1). This monoubiquitylation is then recognized by membrane anchored ubiquitin-binding proteins (2), retaining the polypeptide in the ER. De-ubiquitin enzyme removes the monoubiquitin tag allowing ER export of protein achieving a native conformation (3). Misfolded proteins whose monoubiquitin is extended to polyubiquitin are sent for ERAD (4).

1.2.2.2   Retro-translocation to the cytoplasm

Once recognized as folding incompetent, misassembled or targeted for degradation, ERAD substrates are retro-translocated to the cytoplasm for subsequent ubiquitylation and proteasomal delivery. ERAD substrates are polyubiquitylated at the membrane in a process that complements retro-translocation. Ubiquitylation will be discussed at length in a later section but it is important to note that ubiquitylation alone is sufficient to release some substrates into the cytosol.

In yeast, the ERAD pathways have been divided into three categories, based on the localization of the misfolded domain on the substrates. Luminal misfolded domain are retro-translocated through the ERAD-L pathway and the membrane and cytosolic misfolded domain through ERAD-M and –C, respectively (Carvalho et al., 2006). These pathways are distinct in their requirement of different co-factors to achieve cytoplasmic delivery of their substrates. ERAD-L and –M retro-translocation machinery is composed of hdr1p/hdr3p ubiquitin ligases in complex with der1p and the linker protein Usa1p. Der1p and its mammalian homologues Derlin-1, -2 and -3 are found in complexes with multiple ERAD-L and M substrates, such as the superoxide dismutase 1 (SOD1), apolipoprotein B 100 (apoB) , cystic fibrosis transmembrane regulator (CFTR) and the V2 vasopressin receptor (Mori et al., 2011; Rutledge et al., 2009; Wang et al., 2008); (Schwieger et al., 2008). It was proposed that the derlins forms the long sought retro-translocation pore (Ye et al., 2004). Later studies have shown that the derlins, in interaction with gp78 and Hrd1 ubiquitin ligases, promote cholera toxin retro-translocation to the cytosol (Bernardi et al., 2008; Bernardi et al., 2010; Dixit et al., 2008). However, a growing number of substrates are shown to be retro-translocated by the translocon complex Sec61; this will be discussed below. The membrane bound ubiquitin ligase Doa10 is required for the ERAD-C pathway and does not required a membrane bound adaptor (Carvalho et al., 2006).

The translocon channel Sec61, by which the polypeptides are inserted in the ER membrane or lumen during translation, is also implicated in the retro-translocation process of some ERAD-M and –L substrates. The initial evidence for the implication of Sec61 comes from

co-immunoprecipitation experiments. The human cytomegalovirus genome encodes US2 protein that triggers destruction of newly synthesized major histocompatibility complex (MHC) class I molecules. In infected cells, or cells expressing US2 viral protein, MHC class 1 polypeptide could be immunoprecipitated using antibody to Sec61 (Wiertz et al., 1996a; Wiertz et al., 1996b). It was also the first evidence that viruses can target the ERAD pathway to selectively destroy cellular proteins, in this case, to impair immune defense of his host. Other substrates found to co-immunoprecipitate with the Sec61 translocon are CFTR, robophorin 1, human δ-opioid receptor and the A-chain of the toxin ricin (Bebok et al., 1998; de Virgilio et al., 1998; Petaja-Repo et al., 2001; Wesche et al., 1999). Other evidence of the role of Sec61 in retro-translocation were obtain using yeast temperature-sensitive mutants of Sec61p (Pilon et al., 1997). At the non permissive temperature, the degradation of a mutant form of pro-α-factor was inhibited and 92% was still present in a microsome preparation. Although, there is strong evidence of retro-translocation through the Sec61 channel for both ERAD-M and –L substrates, some studies suggest the presence of a parallel or complementary pathway. Ubc6, an ER membrane protein with a carboxyl TM domain, is not affected by Sec61p mutation in yeast (Lenk et al., 2002)

One point of convergence of all ERAD pathways, whether Sec61 or the derlins are required, is the necessity to recruit p97, CDC48 in yeast, at the ER membrane. In each case, p97/cdc48 specifically binds the ubiquitylated target protein and, by pulling out substrates, disassembles the protein complex. P97 forms a hexameric ring and catalyzes ATP hydrolysis via its two triple ATPase domain (AAA) domains to perform mechanical work in the cells. p97, like the other AAA-ATPases, acts as a molecular chaperone in many cellular activities, such as membrane fusion, cell cycle regulation, stress response, apoptosis, transcriptional regulation and regulation of cytosolic and ERAD substrates (Wang and Chang, 2003).

1.2.2.3   Targeting to proteasome degradation

Once the substrate reached the cytoplasm, p97 in conjugation with its two cofactors Ufd1 and Npl4, escort the ubiquitylated substrates from the ER membrane to the proteasome. Other

p97 cofactors regulate ubiquitin chain extension. In yeast, p97 (cdc48) recruits Ufd2, an E4 enzyme that promotes chain extension of mono- or diubiquitylated substrates (Koegl et al., 1999). Interestingly, p97 and Npl4 seem to restrict ubiquitin chain length to 4 to 6 moieties. Classically, proteins tagged with polyubiquitin are recognized by the subunit Rpn10p of the proteasome but Rpn10p has a weak affinity for these size restricted chain (Wilkinson et al., 2001). These restricted ubiquitin chains are targeted to the proteasome by RAD23, a soluble protein. The interaction between RAD23 and size restricted ubiquitin chain suggests the existence of a specific pathway to deliver polyubiquitylated ERAD substrates to the proteasome.

Two proteasome delivery models have been proposed for integral membrane proteins: 1. The degradation could be tightly coupled to retro-tranlocation and occur on the cytosolic side of the ER membrane 2. The membrane protein could be completely solubilized from the lipid bilayer, with the hydrophobic segments of its transmembrane domains maintained in solution, prior to proteasome delivery. Large ERAD substrates, such as MHC and CFTR have been shown to accumulate in the cytoplasm when the proteasome is inhibited, in accordance with the second model (Johnston et al., 1998; Wiertz et al., 1996a). However, other substrates such as cholera toxin and the yeast mating pheromone (pαF) are retro-translocated by the driving force of the proteasome itself, on the 19S particle (Kothe et al., 2005; Lee et al., 2004; Wahlman et al., 2007). Therefore there is evidence for both models.

1.2.3   Specialized quality control domains in the ER

The ER is a dynamic organelle and its subdivision in specialized domains is highly dynamic and adaptable to the cell's physiological states. ER is the site of membrane and secretory protein biogenesis and, as described above, this involves multiple quality control pathways. The existence of ER domains specialized in protein folding, quality control and degradation will be discussed in this section.

1.2.3.1   The ER folding and sensing domain

Increasing the size of a specific domain of the ER in response to the stimulation of a metabolic pathway shows that the ER is a highly dynamic organelle that can adapt to various stresses. For example upon phenobarbitol treatment, which increases liver microsomal enzyme and HMG-CoA reductase, the amount of SER increased in the hamster liver cells (Jones and Armstrong, 1965; Sudjana-Sugiaman et al., 1994). Similarly, expansion of the SER has been reported when HMG-CoA reductase was overexpressed resulting in its accumulation in crystalloid hexagonal arrays (Chin et al., 1982; Orci et al., 1984). A similar expansion of the SER has been observed in mice that lack the peptide transporter TAP. TAP imports antigenic peptides to the ER lumen, where they are assembled into the major histocompatibility complex (MHC) class 1 and then exported for display at the plasma membrane. Assembly of the heavy chain (HC) and β_2-microglobulin (β_2m) subunits of the complex in the ER lumen is dependent on TAP-peptide association. In absence of the TAP transporter, HC and β_2m accumulate in the tubular ER and are found associated with ubiquitin, suggesting the presence of a subcompartment of the ER where misassembled proteins are recognized and ubiquitylated for degradation (Raposo et al., 1995b) The peripheral accumulation of HC and β_2m in TAP-deficient mice (Raposo et al., 1995b) suggest that the peripheral ER could be the folding/assembly domain of the ER.

1.2.3.2   The ER quality control compartment (ERQCC)

The maturation of secreted and transmembrane proteins is slow and inefficient (Ellgaard and Helenius, 2003). Post-translational modifications require interaction with multiple chaperones, glycosidases and protein disulphide isomerase to acheive N-linked glycosylation, disulfide-bond formation and cleavage. The glycosylation-deglycosylation cycle and the ubiquitylation-de-ubiquitylation cycle described above are mechanisms that time the folding of newly synthesized protein. The ER quality control compartment (ERQCC) was identified as being a site of ERAD substrates and p97 accumulation in mammalian cells treated with a proteasome inhibitor (Kamhi-Nesher et al., 2001a; Wojcik et

al., 2004). ERQCC is distinct from the ER-Golgi intermediate compartment and ER-exit sites (Wakana et al., 2008), and both are located in a juxtanuclear ER domain. Expression of a dominant negative mutant of theATPase function of p97 was sufficient to induce accumulation of p97 itself, derlin-1 and polyubiquitylated substrates in the ERQCC, identifying this site as the potential retro-translocation site in the ER (Wakana et al., 2008).

Different ER chaperones are distributed differentially in the ERQCC or the peripheral ER upon proteasome inhibition. For example, the thiol oxidoreductase ERp57, a folding chaperone, acts on glycoprotein by forming a complex with calnexin or calreticulin during the glycosylation-deglycosylation cycle. Both ERp57 and calnexin bind the nascent glycoprotein but can dissociate independently. Calnexin association persists with misfolded glycoprotein and accumulates at the ERQCC while ERp57 dissociate rapidly. Using asialoglycoprotein receptor as a model, ERp57 was found to protect substrate undergoing proper folding from ERAD and export them to the peripheral ER network. (Frenkel et al., 2004; Lederkremer, 2009). It is tempting to propose that the tubular ER is the folding site and, once a protein failed to achieve proper folding and will not reach its native conformation, the misfolded ERAD substrate is recruited back to the juxtanuclear ER sheet where it is retro-translocated for delivery to the proteasome. The translocon localization to ER sheets suggests that the sheets are the site of protein biosynthesis as well as of degradation. This hypothesis is attractive but remains to be proven.

1.3   The identification of gp78

Gp78 was first named after a glycoprotein of 78 kDa purified from metastatic B16-F1 melanoma cells (Nabi and Raz, 1987; Nabi and Raz, 1988). Protein-protein binding assay identified gp78 as the cell surface receptor of the autocrine motility factor (AMF), also called phosphoglucose isomerase (PGI), and therefore gp78 is also called autocrine motility factor receptor (AMFR) in the literature. The gp78 notation will be used in this thesis. In the past 25 years, multiple groups have linked gp78 and its ligand to increased metastasis development and poor prognosis in cancer patient (Chiu et al., 2008). This led to extensive studies on the

physiological role of both proteins in normal and cancer cells (review in (Fairbank et al., 2009)).

A monoclonal antibody (mAb), called 3F3A, has been used to study gp78 distribution and its possible role in cell motility (Nabi et al., 1990b). Binding of 3F3A mAB induced cell movement in a similar fashion to AMF (Nabi et al., 1990b; Nabi et al., 1991). The cellular distribution of gp78 was assessed by immunoelectron microscopy using the 3F3A antibody. Gp78 was found on the plasma membrane in caveolae structures and on smooth ER tubules in close contact with mitochondria (Benlimame et al., 1998a; Benlimame et al., 1995a; Goetz et al., 2007a; Wang et al., 1997b; Wang et al., 2000).
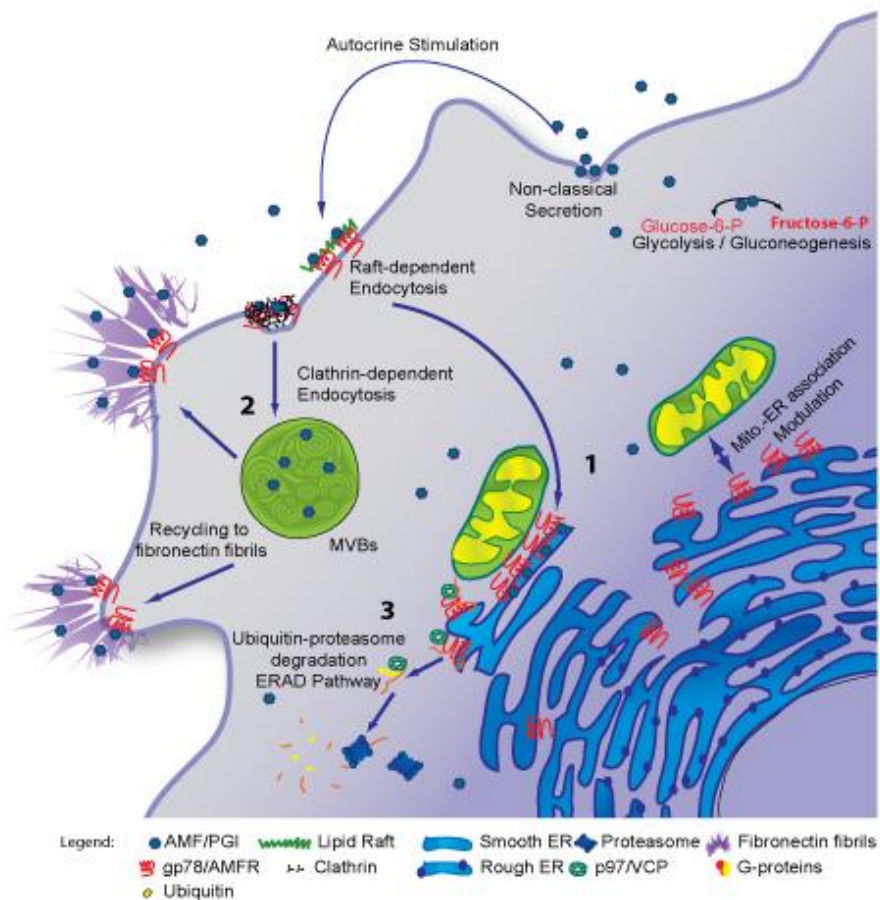
Schematic 1-3 Gp78 is involved in multiple cellular pathways.

The ligand AMF/PGI and its receptor gp78 have been reported to be involved in many cellular pathway linked to metastasis development. These include (1) Endocytosis to the ER-mitochondria contact site where it protects against ER stress and apoptosis, (2) Endocytosis to multi vesicular bodies (MVBs) and recycling to the fibronectin fibrils, inducing matrix remodeling and (3) ER-associated degradation of KAI-1, a metastasis suppressor gene, and other proteins.

1.3.1   Cloning of gp78

The first sequence reported for human gp78 was in 1991 (Watanabe et al., 1991) using expression cloning with the 3F3A antibody. The cDNA fragment identified was 1.9 kilobases long and gave an open reading frame (ORF) of 321 amino acids (GenBank accession number L35233). In 1999, a second sequence from a mouse EST cloned library was published that was 74% homologous to the previous sequence but with a remarkably different ORF of 643 amino acids (GenBank accession number AA260491). The difference was explained by four non-consecutive base deletions and two one base insertions in the first published sequence. Isolation of a cDNA cloned from HeLa human cells confirmed the second reading frame with a 94.7% homology to the mouse gene (Shimizu et al., 1999a).

1.3.2   Ubiquitin ligase function of gp78

1.3.2.1   The ubiquitylation reaction

Gp78 is amongst the best characterized ubiquitin ligases (Ballar et al., 2006; Cao et al., 2007; Chen et al., 2006b; Fang et al., 2001a; Lee et al., 2006a; Liang et al., 2003; Morito et al., 2008a; Song et al., 2005; Tsai et al., 2007; Zhong et al., 2004). Ubiquitylation has been described as a three step process requiring the enzymes E1, E2 and E3. E1, the ubiquitin activating protein, forms a thiol ester bond with ubiquitin using ATP and transfers the "activated" ubiquitin to the E2, known as ubiquitin conjugating protein. The ubiquitin is then transferred from the E2 to the substrate by the ubiquitin ligase (E3**).** This reaction is repeated

to form a polyubiquitin chain and targets the substrate for proteasomal degradation (Hershko and Ciechanover, 1998). However, an *in vitro* ubiquitylation assay using gp78 has changed the sequential model of ubiquitin chain elongation (described above) for a preassembled ubiquitin chain model (Schematic 1.4). Gp78 can catalyze elongation of an ubiquitin chain on an E2 (in this case Ube2g2) and then transfer this preassembled chain to a substrate (in this case Herpc) (Li et al., 2007) (Schematic 1.4 and 1.5).
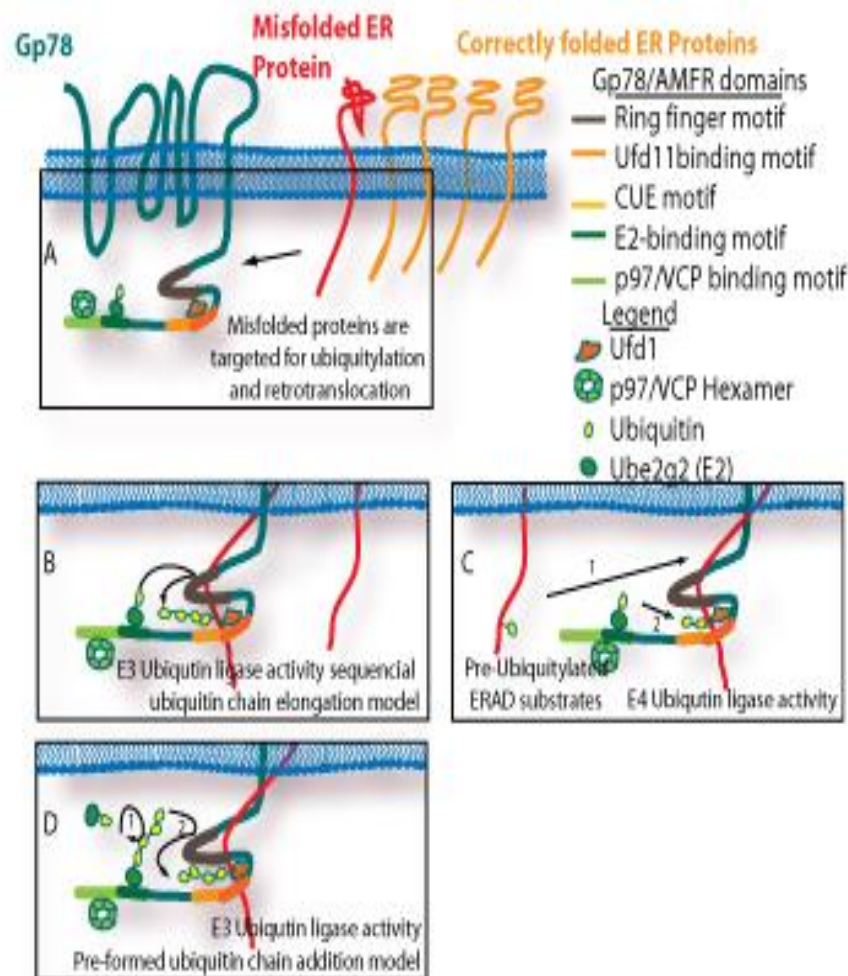
Schematic 1-4 Gp78 ubiquitin ligase function

Gp78/AMFR forms a complex with p97/VCP, an E2 and the cofactor Ufd1. There is three different models by which gp78/AMFR performed its ubiquitin ligase activity; (A) The E2 conjugated to ubiquitin is recruited and a polyubiquitin chain is formed by sequential addition of ubiquitin moieties. (B) 1- gp78/AMFR first pre-assembled a polyubiquitin chain on a E2 conjugating enzyme and 2- transfers the pre-assembled ubiquitin chain directly to the substrates. (C) 1- Short ubiquitin chain is assembled on an ERAD substrates and 2- gp78/AMFR functions as an E4 ubiquitin ligase by elongating the ubiquitin chain.

1.3.2.2   E3/E4 activity of gp78

Gp78 was first proposed to be an ubiquitin ligase (E3) after sequence analysis identified a catalytic RING finger and CUE motif, responsible for ubiquitin ligase activity and ubiquitin binding, respectively (Schematic 1.4 and 1.5)(Ponting, 2000; Shimizu et al., 1999a). The RING finger domain is composed of eight conserved cysteines (Cys) and histidines (His) that coordinate two Zn ions in a "cross-braced" fashion. The domain is classified as RING-H2 or RING-HC depending on whether position 5 is occupied by His (-H2) or Cys (-HC). Gp78 is a RING-H2 ubiquitin ligase with two His residues in position 4 and 5 and six Cys residues in positions 1–3, 6–8. The ubiquitin binding motif family CUE has been identified by a database search for homologous sequence of the yeast protein Cue1p (Ponting, 2000); (Biederer et al., 1997). Gp78's role as an ubiquitin ligase has been confirmed experimentally and the RING finger, CUE motif and an E2 binding site have all been shown to be essential to its E3 function (Chen et al., 2006b; Fang et al., 2001a; Li et al., 2007).
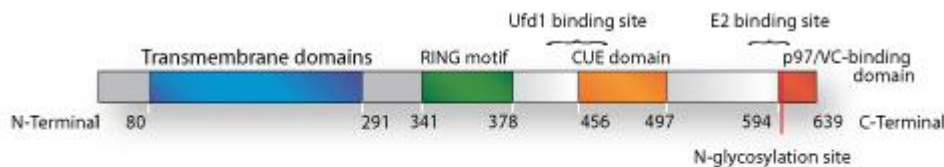
Schematic 1-5 Gp78 motifs

The cytosolic C-terminal tail of gp78/AMFR includes a RING finger motif, responsible for the ubiquitin ligase activity, a ubiquitin-binding CUE motif that partially overlaps with the binding site of the co-factor Ufd1, a E2 binding domain and a p97/VCP binding domain.

In addition to E3 ligase activity, gp78 also has been recently reported to have E4 ligase activity, in which gp78 elongates the ubiquitin chain of previously ubiquitylated substrates (Schematic 1.4). Gp78 is involved in the recognition and degradation of mutant cystic fibrosis transmembrane regulator (CFTRΔ508). Gp78 binds to CFTRΔ508 via its ubiquitin binding domain CUE in a complex including p97, Derlin-1 and BAP31, the latter being

implicated in ER export of membrane proteins (Carlson et al., 2006; Morito et al., 2008a; Sun et al., 2006; Wang et al., 2008). Interestingly, silencing of RMA1 ubiquitin ligase prevents ubiquitylation of CFTRΔ508 by gp78 while knockdown of another E3 ubiquitin ligase involved in CFTRΔ508 ubiquitylation, namely CHIP, has no effect (Morito et al., 2008a). These findings propose that gp78 can function as an E4 ligase in cooperation with other ubiquitin ligases.

1.3.3   Gp78 is involved in ERAD

Gp78 directly binds to the cytosolic p97 ATPase, also known as VCP or CDC48, via its C-terminal domain (Ballar et al., 2006; Zhong et al., 2004). P97 is a hexameric ATPase with multiple cellular activities belonging to the AAA family that provides the "driving force" to extract ERAD substrates from the lipid bi-layer at the retro-translocation site (Ye et al., 2005b). The gp78-p97 interaction is also important for the recruitment of gp78 to the retro-translocation complex composed of the valosin-interacting membrane protein (VIMP), Derlin-1 and peptide N-glycanase (PNGase) (Li et al., 2006; Ye et al., 2005b; Ye et al., 2004). As shown by a GST pull-down assay, gp78 does not physically interact with any other member of the complex (Li et al., 2006). Gp78 recruitment to the retro-translocation complex is regulated by Small p97/VCP-Interacting Protein (SVIP) (Ballar et al., 2007). P97 binds to SVIP and gp78 in a mutually exclusive manner, whereby SVIP sequesters the p97-Derlin-1 complex and prevents gp78 binding to p97.

Ufd1 is another cofactor that binds directly gp78 and has been implicated in the regulation of its ubiquitin ligase activity (Cao et al., 2007). Ufd1 was previously identified in a complex with p97 and Npl4 that delivers the ubiquitylated substrates to the proteasome (Bays and Hampton, 2002; Meyer et al., 2002; Ye et al., 2001; Ye et al., 2003). It was proposed that this complex forms a ring-like structure providing the driving force to dislocate ERAD substrates across the membrane into the cytosol (DeLaBarre and Brunger, 2003; Pye et al., 2007). Although both proteins, gp78 and Ufd1, recruit p97, this happens in a mutually exclusive manner (Ballar et al., 2006). Ufd1 has two ubiquitin binding domains in its N-terminus for mono- and polyubiquitin (Park et al., 2005). Using the gp78 substrate HMG-CoA reductase,

Cao at al. (2007) have determined that the monoubiquitin binding site of Ufd1 is essential to enhance the ubiquitin ligase activity of gp78 (Cao et al., 2007). Subsequently, Ufd1 affinity for polyubiquitin increases upon its recruitment to p97 (Park et al., 2005; Ye et al., 2003). This is promoting ubiquitin chain elongation on mono-ubiquitylated substrates, once the chain is long enough, Ufd1 promote p97/Npl4 recruitment to dislocate the substrate and subsequent proteasome delivery.

1.4 Physiological roles of gp78-mediated ERAD

1.4.1 Cholesterol homeostasis

Gp78 plays an important role in cholesterol homeostasis via the sterol-regulated ubiquitylation of HMG CoA reductase and its co-factor Insig-1 (Lee et al., 2006a; Song et al., 2005). HMG-CoA reductase is involved in the reduction of 3-hydroxy-3-methylglutaryl coenzyme A to mevalonate, a critical step in cholesterol synthesis. In the presence of high sterol levels, mevalonate synthesis is no longer required and Insig-1 binds to HMG-CoA reductase and promotes the recruitment of gp78-p97, resulting in HMG-CoA reductase degradation. It still remains to be determined if Insig-1 is degraded along with HMG-CoA reductase in the presence of sterol (Song et al., 2005). When the level of sterol is low, gp78 targets Insig-1 for proteasomal degradation, protecting HMG-CoA reductase and promoting cholesterol synthesis (Lee et al., 2006a). Gp78 is also implicated in the degradation of apolipoprotein B100 (ApoB), the single protein component of atherogenic low and very low density lipoprotein (Liang et al., 2003).

1.4.2 Metastasis development

It was recently reported that KAI1, also called CD82, is a substrate of gp78 (Tsai et al., 2007) representing the first reported evidence that the ubiquitin ligase activity of gp78 is involved in metastasis development. KAI1 is a tetra-spanning protein known as a metastasis suppressor. The loss of its expression is correlated with metastasis development in several cancers (Abe et al., 2008; Briese et al., 2008; Protzel et al., 2008; Xu et al., 2008; Yang et al.,

2008). Knockdown of gp78 results in increased KAI1 expression and reduced morbidity in an experimental metastasis model. The CUE and the RING domains are essential to restore metastasis development. Interestingly, replacement of the membrane spanning domains of gp78, believed to be the AMF binding site, by a single pass transmembrane domain restored ubiquitylation and degradation of KAI1 and enhanced its metastatic potential (Tsai et al., 2007). This suggests that AMF-gp78 signaling may affect tumor and metastasis development independently of its cytokine function.

1.5 Gp78 is a cell surface receptor

1.5.1 The ligand: the autocrine motility factor

The autocrine motility factor (AMF) is also the phosphoglucose isomerase (PGI) that catalyzes the interconversion of glucose 6-phosphate and fructose-6-phosphate critical to glycolysis and gluconeogenesis (Watanabe et al., 1996). It is expressed in all tissues and plays a vital role in metabolism. Throughout this thesis, it will be referred to as AMF. AMF first was purified from serum-free conditioned medium of human A2058 melanoma cells and first described as a tumor secreted cytokine that stimulates direct and random migration (Liotta et al., 1986).

AMF also plays important roles in development. It function as a neuroleukin that facilitates survival and growth of embryonic spinal and sensory neurons, as well as maturation of B cells (Gurney et al., 1986) ; a critical protein for embryo implantation in ferrets (Schulz and Bahr, 2003); a sperm antigen-36 implicated in sperm agglutination (Yakirevich and Naot, 2000); and a myofibril-bound serine proteinase inhibitor (Cao et al., 2000). AMF can therefore act as a cytosolic glycolytic enzyme and an extracellular cytokine.

1.5.2   AMF endocytosis

Upon interaction with gp78 at the cell surface, AMF can be internalized via two different pathways: a raft-dependent, dynamin-dependent endocytosis to the SER and clathrin-dependent endocytosis to multivesicular bodies (Benlimame et al., 1998a; Le et al., 2000; Le et al., 2002; Le and Nabi, 2003). The membrane protein caveolin-1 (Cav-1) is a negative regulator of the raft-dependent endocytosis pathway of AMF to the SER. In Abl-transformed NIH-3T3 cells and in invasive breast cancer cells, AMF uptake increased upon reduction of Cav1 expression and also involved PI3K/Akt signaling pathway (Le et al., 2002, Tsutsumi et al., 2003b, Kojic et al., 2007). Transformation and survival is also promoted in NIH-3T3 cells when AMF is overexpressed (Tsutsumi et al., 2003b). A highly significant correlation between gp78 and Akt phosphorylation was observed in invasive breast cancers by tissue microarray analysis (TMA) (Kojic et al., 2007). Of particular interest, a recent study has shown that a paclitaxel conjugated AMF is able to inhibit tumor cell proliferation and induce tumor regression upon intratumoral injection into mouse melanoma tumors (Kojic et al., 2008). This suggests that the PI3K-dependent uptake of AMF by gp78 might be associated with a prosurvival role in cancer and might also represent a promising route for drug delivery to tumor cells.

1.5.3   AMF signaling in tumor cell motility and tumorigenesis

AMF-induced cell motility in tumor cells is an important process in cancer metastasis, as correlation between AMF protein expression and increased tumor aggressiveness has been established (Dobashi et al., 2006). Stable overexpression of AMF induces (1) morphological changes typical of neoplastic transformation, (2) invasive ability *in vitro*, and (3) tumorigenicity *in vivo* (Tsutsumi et al., 2003b; Yanagawa et al., 2004). Importantly, these effect of high AMF expression were shown to be gp78-dependent and occurs via a MAPK pathway in HT-1080 cells. (Haga et al., 2008). In hepatoma cells, AMF induction of cell motility has been linked to the degradation of the extracellular matrix (ECM) by matrix metalloproteinase–3 (MMP-3) (Yu et al., 2004). This was correlated to matrix remodeling in

23

low metastatic K1735-Cl11 cells and matrix degradation in high-metastatic K-1735- M1 cells after AMF treatment (Silletti et al., 1998).

1.5.4   Gp78 induction of tumor cell motility and tumorigenesis

Gp78 overexpression induces increased cell motility, and the presence of this receptor seems to be sufficient to produce tumors in nude mice (Onishi et al., 2003). In fact, several studies have shown that there is a correlation between gp78 expression and cellular transformation. Invasive Moloney sarcoma virus (MSV) transformed MDCK cells are characterized by a loss of epithelial phenotype and increased cell motility that is associated with a decrease in E-cadherin and an increase in gp78 expression (Simard and Nabi, 1996). Likewise, NIH-3T3 fibroblast cells transfected with gp78 display morphological changes resembling neoplastic transformation and are able to grow in the presence of low serum in an anchorage-independent manner (Onishi et al., 2003).

Recently, both AMF and gp78 have been implicated in mesenchymal-to-epithelial transition, where AMF was down-regulated in mesenchymal human fibrosarcoma HT-1080 cells using small interfering RNA technology. This study argued that the AMF-gp78 protein complex plays a significant role in tumor cell motility, invasion, contact-dependent inhibition and tumorigenesis (Funasaka et al., 2007).

Human fibrosarcoma HT-1080 cells secreting high levels of AMF are resistant to drug-induced apoptosis via the down-regulation of two essential pro-apoptotic proteins, namely apoptotic protease activating factor-1 (Apaf-1) and caspase-9 (Haga et al., 2003). To further investigate the apoptotic pathway following AMF-gp78 binding, HT-1080 cells were treated with inhibitors of protein kinase C (PKC), phosphatidylinositol-3 kinase (PI3K) and mitogen-activated protein kinase (MAPK) and through quantitative RT-PCR, it was observed that Apaf-1 and caspase-9 mRNA levels were restored and comparable to control cells (Haga et al., 2003). Overexpression and secretion of AMF may thereby contribute to tumor cell growth and survival in response to anti-cancer agents.

1.6   ER-mitochondria contact-sites

1.6.1   Mitochondria-associated membrane

A well-characterized ER domain is the mitochondria–associated ER. Exchange of Ca2+ between the ER and mitochondria regulates cell signaling, ER chaperone assisted folding of newly synthesized proteins, the mediation of mitochondria-localized ATP associated dehydrogenases and the activation of calcium-dependent enzymes that execute cell death programs (Berridge, 2002; Breckenridge et al., 2003; Brough et al., 2005; Hajnoczky et al., 2000; Rizzuto et al., 1998).

Electron microscopy studies have long identified close contact sites between ER and mitochondria and electron tomography showed that these measure about 15 nm (Perkins et al., 1997). In a wide variety of cells, conventional transmission electron microscopy images have shown mitochondria in close apposition to ER (Shore and Tata, 1977; Sommer and Johnson, 1970) and high-resolution 3D electron tomography also reveals that the extended ER closely contacts with the mitochondria (Marsh et al., 2001; Rizzuto et al., 1998). Initial studies identified fragmented ER proteins that copurified with mitochondria and called these ER membranes domains mitochondria-associated membranes (MAM). They play a role in lipid biosynthesis (Rizzuto et al., 1998; Shore and Tata, 1977) as well as ER homoeostasis and Ca^{2+} signalling and apoptosis (Berridge, 2002; Rizzuto et al., 1998). Biochemical studies have identified MAMs that contain multiple phospholipid- and glycosphingolipid-synthesizing enzymes, and support direct transfer of lipids between the ER and mitochondria (Piccini et al., 1998; Stone and Vance, 2000; Vance, 1990).

A tethering complex linking ER to mitochondria composed of Mmm1/ Mdm10/ Mdm12/ Mdm34 has recently been uncovered in yeast (Kornmann et al., 2009). In mammalian cells, mitofusin 2 (de Brito and Scorrano, 2008) and its regulator Trichoplein/mitostatin (TpMs) (Cerqua et al. 2011) also regulate dynamic ER-mitochondria interactions. Another physical bridge between ER and mitochondria is composed of the cytosolic chaperone GRP75 that

links the mitochondrial dependent anion channel (VDAC) to IP3R on the ER (Szabadkai et al., 2006).

The existence of MAM domains suggest that the ER-mitochondria communication may occur by direct transfer rather than vesicular traffic. It remains to be determined to what extent multiple MAM domains exist.

1.6.2   Calcium homeostasis

1.6.2.1   The ER is a calcium store

The ER releases Ca2+ through the inositol-1,4,5-phosphate receptor IP3R channel to mitochondria at their contact site (Mendes et al., 2005; Rizzuto et al., 2004). The ER serves as the principal internal store of calcium ions (Meldolesi and Pozzan, 1998). Free Ca2+ calcium levels are kept under tight control by pumps, exchangers, and buffering mechanisms including storage by organelles (Pozzan et al., 1994). For example, the Ca2+ uptake pump like the sarcoplasmic endoplasmic reticulum calcium ATPase family of Ca2+-ATPases (SERCAs) are complemented by Ca2+ release channels including InsP3Rs, ryanodine receptors (RyRs), and cyclic ADP-ribose (cADPR) and nicotinic acid adenine dinucleotide phosphate (NAADP) receptors to accomplish ER Ca2+ homeostasis. A high concentration of Ca2+ is maintained in the ER lumen by a member of the SERCAs that pump Ca2+ into the ER, counterbalancing a leak of Ca2+ ions through the ER membrane into the cytoplasm (Lytton et al., 1991). The two major Ca2+ release channels in the ER are the IP3R and the ryanodine receptor (RyR) which mediates IP3-induced Ca2+ release or Ca2+-induced Ca2+ release, respectively (Miyazaki et al., 1993).

1.6.2.2   Mitochondrial signalling and calcium

Under normal conditions, mitochondria buffers cytosolic increases in calcium influx from the plasma membrane or released from the ER. Multiple calcium pumps and transporters are involved in mitochondrial calcium uptake. Increased cytosolic calcium concentration first activates the VDAC pump and the calcium uniporter (UP) on the outer mitochondrial membrane leading to increase calcium concentrations in the mitochondrial matrix. Calcium ions are then transported across the inner mitochondrial membrane (IMM) through the

Na+/Ca2+ exchangers (NCX) and H+/Ca2+ exchangers (HCX) (Pfeiffer et al., 2001). The matrix Ca2+ induces the permeability transition pore (PTP) formation that traverses both the IMM and OMM and allows free passage of Ca2+. Furthermore, the rise in mitochondrial Ca2+ stimulates the generation of factors, including ROS and free fatty acids, which also promote the opening of the PTP. Opening of the PTP causes dissipation of the membrane potential and release of Ca2+. Finally, impairment of the mitochondrial function and activation of cytoplasmic mechanisms by the released mitochondrial factors leads to apoptosis (Scorrano et al., 2001; Starkov et al., 2004).

1.6.2.3   Calcium release at ER-mitochondria contact sites

The release of Ca2+ from ER stores by IP3Rs has been implicated in apoptosis, which is directly responsible for mitochondrial Ca2+ overload (Hajnoczky et al., 2002). Regions of the ER apposed to mitochondria are enriched with IP3R, identifying these zones as 'hotspots' of calcium transfer from the ER to the mitochondria (Szabadkai et al., 2006). VDAC mediates metabolic flow through the OMM, forming an ATP microdomain close to the ER and SERCAs and take part in metabolic and apoptotic protein complexes (Cheng et al., 2003; Colombini, 2004; Vendelin et al., 2004; Ventura-Clapier et al., 2004). VDAC is physically linked to the ER Ca2+-release channel IP3R through grp75, highlighting chaperone-mediated conformational coupling between the IP3R and the mitochondrial Ca2+ uptake machinery (Szabadkai et al., 2006).

1.6.3   Gp78 is associated with mitochondria

In cultured cells, EM analysis showed that the ER in close association with mitochondria is predominantly SER (Goetz et al., 2007b; Wang et al., 2000).Using the 3F3A antibody, gp78 was shown to be located to a mitochondria-associated domain of the SER (Benlimame et al., 1998a; Benlimame et al., 1995a; Wang et al., 1997b). Studies of the gp78 ubiquitin subpopulation recognized by the 3F3A antibody showed that this mitochondria-associated ER domain was distinct from the ER marker calnexin (Goetz et al., 2007b; Registre et al.,

2004). Distinction between the gp78-labeled SER domain and the central RER is supported by the selective alteration of morphology of the gp78-labeled SER, but not the RER, by the drug ilimaquinone (Wang et al., 1997b).

Association of the gp78-labeled smooth ER with mitochondria is highly sensitive to variations of cytosolic calcium concentrations in permeabilized cells using the calcium ionophore ionomycin (Goetz et al., 2007b; Wang et al., 2000). Cytosolic calcium concentrations under 100 nM favor dissociation of the 3F3A-labeled SER domain and mitochondria, while concentrations over 1 mM favors their close association (Wang et al., 2000)

1.6.3.1   AMF-gp78 signaling regulates ER Ca2+ release and cell apoptosis

AMF protection against thapsigargin- and tunicamycin-induced ER stress and apoptosis is receptor-mediated by gp78. The reduced ER stress response as well as cytosolic Ca2+ elevation and mitochondrial Ca2+ uptake induced by thapsigargin and tunicamycin was mediated only partially through PI3K/Akt activation. AMF reduction of the elevation of cytosolic Ca2+ in response to either thapsigargin or IP3R activation with ATP was gp78-dependent, independent of mitochondrial depolarization and not associated with changes in ER calcium content. These results implicate regulation of ER Ca2+ release in AMF protection against ER stress and apoptosis. These results suggest that by regulating ER Ca2+ release, AMF interaction with gp78 therefore protects against ER stress identifying novel roles for these cancer-associated proteins in promoting tumor cell survival (Fu et al. 2011).

1.6.4   Mitochondrial dynamics

Mitochondria are highly mobile organelles in constant movement in the cell. Mitochondrial dynamics referred to the antagonist activities of fusion and fission (Schematic 1.6). In mammals, mitochondrial dynamics are differentially balanced to accommodate the function of different cell types. For example, in cardiomyocytes, fused mitochondria are the favored

phenotype and this leads to an interconnected mitochondria network (Skulachev, 2001). This highly interconnected mitochondrial network serves as a system of distribution of membrane potential throughout the cell or across multiple sarcomeres (Amchenkova et al., 1988; Huser and Blatter, 1999). Inversely, a phenotype of small distinct rod shape mitochondria is favour in large extended cells, such as neurons. Mitochondria need to be distributed along the dendritic spines and at distant synapses, which are sites of high energy demand (Li et al., 2004).

Maintenance of mitochondrial membrane potential, integrity and distribution is dependent on their dynamics. In this section, I will summarize mitochondrial fusion and fission mechanisms as well as their role in the maintenance of mitochondrial function (Schematic 1.6).
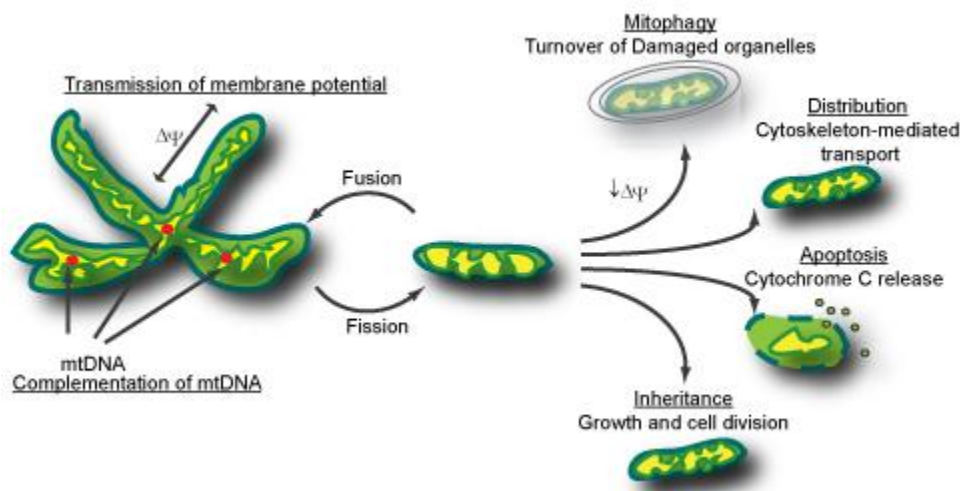
Schematic 1-6 Mitochondrial fusion and fission

Fusion and fission are involved in many mitochondrial functions. Fusion is essential for complementation of mitochondrial DNA (mtDNA) gene products and maintaining respiratory functions. It also dissipates metabolic energy through transmission of membrane potential along mitochondrial filaments. Fission allows disposal of damage mitochondria (low membrane potential) by mitophagy, intracellular distribution and partitioning during cell division, and the release of pro-apoptotic factors from the intermembrane space (adapted from (Westermann, 2011).

1.6.4.1   Fusion machinery

Fusion of mitochondria is a particularly complex process, as mitochondria are double membrane bound and the fusion of two mitochondria involves the coordination of four membranes. The first fusion effectors involved are the mitofusin proteins. Mammals have two different mitofusins, MNF1 and MNF2 that have similar structures (Santel and Fuller, 2001). They are composed of transmembrane segments in the outer membrane, with a short loop in the intermembrane space and a large GTPase domain on the cytosolic side (Rojo et al., 2002). Inner membrane fusion is controlled by the optic atrophy protein 1 (OPA1). Together with mitofusin 1, they compose the core component of mitochondria fusion (Cipolat et al., 2004).

Mitofusins first tether two mitochondria by the coiled-coil domain and initiate the bilayer mixing through their GTPase domains, providing the biomechanical energy for outer membrane fusion (DeVay et al., 2009; Koshiba et al., 2004). The subsequent inner membrane fusion is operated by OPA1 that, like mofusins, is responsible for both inner membrane tethering and fusion. Mutation of OPA1 selectively disrupts inner membrane fusion without affecting outer membrane fusion, indicating that both fusions operate independently of each other but must be coordinated (Meeusen et al., 2004). In yeast, the protein Ugo1 is an essential linker of yeast homologue of mitofusins and OPA1 (Fzo1 and Mgm1 respectively) that coordinate inner and outer membranes fusion with each other. A structural or functional equivalent in higher eukaryotes has not yet been identified.

Levels of the mitofusin yeast homologue Fzo1 are controlled by Mdm30, a subunit of the ubiquitin ligase complex Skp1-cullin-F-box (SCF), which promote Fzo1 degradation by the proteasome (Cohen et al., 2008). Interestingly, GTPase-deficient Fzo1 mutant shows reduce degradation, suggesting that fusion activity also promotes degradation (Amiott et al., 2009).

The regulation of OPA1 expression and activity appears to be more complex. OPA1 exists as two isoforms, a long and a short one that act in trans to promote inner membrane fusion. In yeast these two isoforms are generated at the translocation step. A mitochondrial translocase imports Mgm1 (the yeast OPA1) through the outer membrane. Once in the intermembrane space, first transmembrane domain of Mgm1 is inserted in the inner membrane, generating the first long isoform. As translocation in the inner membrane is ATP dependent, a matrix that is ATP-rich would promote further translocation of Mgm1 into the inner membrane, exposing the second hydrophobic region to Pcp1, a mitochondria protease, that would cleaves and releases the second short isoform into the intermembrane space. Because the level of ATP dictates the speed of insertion, mitochondrial energy levels dictate the processing of Mgm1. Since both isoforms are needed for mitochondrial inner membrane fusion, ATP levels regulate mitochondria fusion activity (Herlan et al., 2004).

In mammals, OPA1 is regulated in a more complex manner but still depends on the energetic state of mitochondria. Low membrane potential, low ATP level and apoptosis favored the expression of the short isoform, which is the opposite of what is observed in yeast (Griparic et al., 2007; Ishihara et al., 2006). The processing of OPA1 involves many proteases, the best caracterized being OMA1. OMA1 is an inner membrane protease up-regulated by low membrane potential (Head et al., 2009). Therefore, damaged mitochondria would see their pool of OPA1 being converted to the short form, preventing fusion with healthy mitochondria. Mammalian OPA1 processing is not restricted to newly imported protein, in contrast to yeast, allowing for a rapid response in case of stress.

1.6.4.2 Fission machinery

The dynamin-related protein 1 (DRP1) is a self-assembled GTPase that forms rings around mitochondria and direct fission (Smirnova et al., 1998). The regulation of the fission mechanisim is best understood in yeast, where DRP1 is named Dnm1. Dnm1 is recruited to the outer mitochondrial membrane via its interaction with the mitochondrial fission protein 1 (Fis1) and the mitochondrial division protein (Mdv1) (Mozdy et al., 2000; Tieu and Nunnari, 2000). Fis1 is an outer membrane protein that recruits the scaffolding protein Mdv1, forming

a scaffold binding Dnm1. Mdv1 function as nucleator of GTP-bound Dnm1, forming helical restriction sites around the mitochondria. These restriction sites finally sever mitochondria after GTP hydrolysis. In mammal, there is no equivalent of Mdv1, FIS1 is sufficient to recruit and initiate oligomerization of DRP1, inducing mitochondrial fission (Tieu et al., 2002; Zhang and Chan, 2007). Interestingly, the mitochondrial fission factor (MFF) is a recently identified outer mitochondrial membrane protein that performs the same role as DPR1, suggesting the existence of two parallel pathways of DPR1 recruitment (Gandre-Babbe and van der Bliek, 2008).

The severing of the inner membrane is not as well understood. It is possible that DPR1 constriction of the outer membrane is sufficient to sever the inner membrane. However, possible candidates have been identified in yeast, Mdm33, and in mammals, MTP18. They are not homologous genes but are both localized on the mitochondria inner membrane and induce fragmentation when overexpressed and elongation when depleted (Messerschmitt et al., 2003; Tondera et al., 2005). Their regulation and mechanism are not well understood.

Mitochondrial fission is principally regulated by a ubiquitin ligase located in the outer membrane of the mitochondria, MARCH5, that targets for degradation DRP1 and FIS1 (Karbowski et al., 2007; Yonashiro et al., 2006). Interestingly, the increased fission resulting from loss of MARCH5 results in mitochondrial elongation and triggers cell senescence (Park et al., 2010). Another ligase, the mitochondrial-anchored protein ligase (MAPL), attaches a small ubiquitin-like modifier (SUMO) to DRP1, stimulates DRP1 activity and increases fission (Braschi et al., 2009). In addition to sumoylation, phosphorylation on Ser residues can modulate DRP1 activity. The CDK1/cyclin kinase B complex phosphorylates DRP1 on serine 658 at the beginning of mitosis, increasing its activity and enabling a fragmented phenotype and distribution to the daughter cells (Taguchi et al., 2007). DRP1 is also phosphorylated by cAMP-dependent protein kinase (PKA) at serine 656, reducing its activity and conferring resistance to diverse apototic stimuli (Cribbs and Strack, 2007). Its dephosphorylation by calcineurin, induced by calcium levels, determine apoptotic sensitivity and provide a mechanism for calcium regulation of mitochondria morphology (Cereghetti et al., 2008).

1.6.4.3 Role of mitochondrial dynamics

The principal roles of mitochondrial dynamics, namely fission and fusion, are biogenesis, distribution throughout the cytosol, partition during cell division, quality control and disposal of damaged mitochondria. Mitochondria cannot be generated de novo and grow from division of pre-existing organelles. They have their own genome coding mostly for proteins required for respiration and protein translation. Even if most mitochondrial proteins are encoded by the nucleus, transmission of the mitochondrial genome is essential to their function. Because their dynamics do not require the transmission of genetic material, the mitochondrial genome is not evenly distributed in all mitochondria in the cell and fusion is essential to replenish the mitochondria-encoded proteins in all mitochondria. Yeast cells with fusion mutations lose their mitochondrial genome in a few generations and show defects in respiration (Merz and Westermann, 2009). Therefore, mitochondrial fusion is crucial to maintain the mitochondrial genome throughout the cell life and prevent heterogeneity and dysfunction (Chen et al., 2005).

Mitochondrial fission is observed as the cell enters mitosis and undergoes cytokinesis, allowing partition of mitochondria in the daughter cells (Ishihara et al., 2009; Taguchi et al., 2007). Interestingly, DPR1 knockout mouse fibroblast can still divide and transmit their mitochondria to both daughter cells (Ishihara et al., 2009), presumably by the sole action of the cytokinesis mechanical forces or perhaps by an unidentified DPR1-independent pathway. Although DPR1 fission is dispensable for cytokinesis, DRP1 and mitofusin knockout mice are embryonic lethal (Chen et al., 2003; Ishihara et al., 2009; Wakabayashi et al., 2009), suggesting that mitochondria dynamics are crucial for cell survival but dispensable for cell division.

Mitochondrial division also allows for distribution throughout the cell, something that is particularly important in large extended cells such as neurons. Fusion is essential in the maintenance of dentritic spines and synapse, which are sites of important energy demand (Li

et al., 2004). Inversely, a large interconnected mitochondria network is important for other cell type such as muscle cells. These mitochondrial networks act as electrical systems that transmit membrane potential generated by the proton gradient of the respiratory chain (Amchenkova et al., 1988). This connects mitochondria in the oxygen-rich cell periphery to the mitochondria of the muscle core, making possible ATP production over the whole muscle fiber (Skulachev, 2001) .

The respiratory chain produces reactive oxygen species (ROS) as a by product of oxidative phosphorylation. This is a major cause of mutation and lesion in mtDNA, leading to a loss of functional respiratory chain complexes and decline in bioenergetic capacity (Balaban et al., 2005). Mitochondrial dynamics act as a quality control check point for mutated mitochondria: restoration of non-functional organelles by fusion and elimination of overly damaged organelles by fission. Fusion restores respiratory activity by re-introducing an intact allele of a mutated gene and synthesizing functional gene product, a process call inter-mitochondrial complementation (Ono et al., 2001).

Inter-mitochondrial complementation is not always sufficient to restore respiratory activity and counteract ROS-induced damage. To prevent proliferation of mutated mtDNA, mitochondria are removed from the cells by a process called mitophagy. Mitophagy is similar to autophagy, a process by which double-membrane autophagosomes sequester organelles and cytosol and then fuse with lysosomes for degradation by hydrolytic enzymes (He and Klionsky, 2009). Mitophagy is part of a normal mitochondrial quality control in the cell. Mitochondrial division frequently produces two mitochondria, one with normal membrane potential and another with decreased membrane potential and OPA1 levels (Twig et al., 2008). Decreased OPA1 level prevent subsequent fusion and favor elimination by mitophagy, constituting a quality control mechanism.

Decreased membrane potential induces mitophagy by stabilizing PINK1 (*PTEN-induced putative kinase* 1) on the outer membrane. In normal, polarized mitochondria PINK1 is degraded by voltage-dependent proteolysis. A low membrane potential favors accumulation of PINK1 which in turn recruits and translocates the cytosolic ubiquitin ligase Parkin to

34

mitochondria (Narendra et al., 2010). This recruitment of parkin activates its ubiquitin ligase activity and mitofusins-1 and -2, among others, have been identified as substrates therefore, parkin activity prevents damaged mitochondria from fusing with healthy mitochondria (Matsuda et al., 2010; Rakovic et al., 2011; Ziviani et al.). There is evidence that mitophagy is a mitochondrial quality control mechanism. Mutations in PINK1 or parkin have been linked to Parkinson's disease, underlining the importance of mitochondrial quality control for proper disposal of damaged or uncoupled mitochondria generating excessive reactive oxygen species (Chen and Chan, 2009; Gandhi et al., 2009; Piccoli et al., 2008).

1.7   Hypothesis

At the beginning of this work, it was well establish that the expression of gp78 as well as its ligand correlated with metastasis development. Using the 3F3A antibody, gp78 was found to be mainly localized in a smooth ER domain associated with mitochondria. My general hypothesis was that gp78 ubiquitin ligase activity regulates the ER-mitochondria interaction. The basic hypothesis of my thesis is that the subpopulation of gp78 labeled by 3F3A is involved in its ubiquitin ligase function, define a specific ER subdomain involved in ERAD and impact on calcium homeostasis at the ER-mitochondria contact site. More precisely, I made the hypothesis that 3F3A defined a specific domain of the ER where association with mitochondria was regulated by calcium concentration. Mitochondria being the energy sources in the cell and ERAD being an energy demanding process, I hypothesizedthat gp78-mediated ubiquitylation would be mainly localized at the ER mitochondria interface. The complementing hypothesis was also tested: that mitochondria dynamics would be influenced by gp78 ligase activity and play a role in ERAD. Finally, gp78 being as well a cell surface receptor of AMF, I hypothesized that AMF treatment would modulate both gp78 ubiquitin ligase activity and mitochondrial dynamics.

In this thesis, I first described an ER domain specific for gp78-mediated ubiquitylation. I investigate the interplay between the cell surface stimulation of gp78 with AMF and its impact of ER-mitochondria dynamics and calcium homeostasis.

Chapter 2: Reversible interactions between smooth domains of the endoplasmic reticulum and mitochondria are regulated by physiological cytosolic Ca2+ levels

2.1 Introduction

An association between the ER and mitochondria was first noted soon after electron microscopy enabled the morphological visualisation of the ER (Dempsey, 1953). More recently, confocal imaging, using recombinant proteins specifically targeted to the ER and mitochondria, has confirmed the association of these two organelles and demonstrated the importance of this interaction in Ca^{2+} homeostasis (Montero et al., 2000; Rizzuto et al., 1993; Rizzuto et al., 1998; Simpson et al., 1997; Szabadkai et al., 2003). Mitochondria are able to sense domains of elevated Ca2+ concentrations generated by the IP3R and/or plasma membrane Ca2+ channel activation (Rizzuto, 1993). These local elevated concentrations enable rapid mitochondrial accumulation of Ca^{2+} that stimulates mitochondrial metabolism (Montero et al., 2000). Mitochondrial Ca^{2+} uptake is greater when triggered either by quantal incrementation of the Ca^{2+} concentration (Csordas et al., 1999) or by sustained Ca^{2+} release from the ER (Szabadkai et al., 2003). Such increases might arise from the simultaneous activation of several Ca^{2+} channels, such as IP3R and the ryanodine receptor (RyR), clustered at sites of close apposition between the ER and mitochondrial membranes (Csordas et al., 1999). In addition, uptake of Ca^{2+} by mitochondria has been documented to feedback, through a currently undefined mechanism, on the ER Ca^{2+}-release process by controlling the frequency or intensity of IP3R or RyR channel activation (Csordas et al., 1999; Jouaville et al., 1995; Straub et al., 2000; Zimmermann, 2000). Ca^{2+} exchange between the two organelles is therefore a finely tuned cellular process that impacts on cellular Ca^{2+} homeostasis as well as Ca^{2+} signaling.

Changes in ER morphology during cellular processes such as fertilisation and oocyte maturation affect its capacity to release free cytosolic Ca^{2+} ($[Ca^{2+}]_{cyt}$) in response to increases

in Ins(1,4,5)P_3 (Shiraishi et al., 1995; Terasaki et al., 1996; Terasaki et al., 2001). Other studies have shown that artificial increases of [Ca^{2+}]$_{cyt}$ dramatically reorganise the ER (Ribeiro et al., 2000; Subramanian and Meyer, 1997). The ER is heterogeneous with respect to its Ca^{2+} storage function owing in part to the presence of microdomains enriched in Ca^{2+}-binding proteins (Papp et al., 2003). Mitochondria are also functionally heterogeneous (Collins et al., 2002; Park et al., 2001) and intracellular segregation of mitochondria is crucial for the spatial regulation of Ca^{2+} signaling and the control of secretion in pancreatic acinar cells and chromaffin cells (Montero et al., 2000; Tinel et al., 1999). The heterogeneous nature of the ER and mitochondria together with the importance of the ER-mitochondria association in regulating cellular Ca^{2+} dynamics suggest that specific, local interactions should necessarily respond to subtle changes in intracellular Ca^{2+} levels.

The 3F3A monoclonal antibody (mAb) raised against gp78 (Nabi and Raz, 1987), stimulates cell motility and metastasis, mimicking ligand activation, and competes with autocrine mobility factor (AMF) for receptor binding (Nabi et al., 1990b; Silletti et al., 1991). In cells transfected with FLAG-tagged gp78, 3F3A labeling of gp78 is increased, but the label only partially colocalises with the exogenously expressed protein, indicating that it is identifying a subpopulation of cellular gp78 (Registre et al., 2004). We previously identified a smooth ER (SER) subdomain that is labeled with the 3F3A mAb against gp78 that selectively associates with mitochondria (Benlimame et al., 1995a; Goetz and Nabi, 2006b; Wang et al., 1997b; Wang et al., 2000). The association between this SER subdomain and mitochondria in digitonin-permeabilised cells is dependent on [Ca^{2+}]$_{cyt}$ (Wang et al., 2000); however, the nature of this interaction in intact cells has yet to be determined. Here, we show that the 3F3A-labeled ER domain is distinct from the tubular ER labeled for reticulon (Voeltz et al., 2006), does not label the nuclear membrane and only partially colocalises with the rough ER marker Sec61α. Importantly, we demonstrate that physiological modulation of [Ca^{2+}]$_{cyt}$ induces the reversible dissociation of this ER domain from mitochondria.

2.2 Results

2.2.1 The 3F3A mAb recognises a mitochondria-associated ER domain

The 3F3A mAb was originally generated against purified gp78 (Nabi et al., 1990b). Judged by immunoelectron microscopy, in addition to plasma membrane labeling, the 3F3A mAb also labels smooth ER tubules that frequently extend from the ribosome-studded rough ER (Benlimame et al., 1998a; Benlimame et al., 1995a; Wang et al., 1997b). In cells rapidly fixed with very cold methanol-acetone, 3F3A immunofluorescent labeling defines an ER domain distinct from the calnexin- and calreticulin-labeled ER and ER-Golgi intermediate compartment (ERGIC) (Benlimame et al., 1998a; Benlimame et al., 1995a; Wang et al., 1997b; Wang et al., 2000). 3F3A labeling is highly stable and persists after 16 hours of cycloheximide treatment (Benlimame et al., 1995a). We therefore used a Dicer siRNA approach to knockdown gp78, resulting in a 60-70% reduction in 3F3A labeling judged by western blot. By quantitative immunofluorescence, we observed a similar reduction in 3F3A labeling of the mitochondria-associated ER domain, demonstrating that 3F3A labeling of ER tubules is specific for gp78/AMFR (Figure 2.1).

In contrast to the distribution of 3F3A labeling, which is restricted to mitochondria-associated ER tubules, exogenously expressed FLAG- or GFP-tagged gp78 is localized throughout the ER (Fang et al., 2001a; Registre et al., 2004). Reticulon4a/NogoA (Rtn4a) defines and maintains tubular ER domains preferentially associated with the peripheral ER, as opposed to the saccular or perinuclear ER that includes the nuclear membrane (Voeltz et al., 2006). In Cos-7 cells, the 3F3A-labeled ER does not localize with transfected MYC-tagged Rtn4a or the perinuclear GFP-Sec61β-expressing ER and 3F3A does not label the nuclear membrane (Figure 2.2A). 3F3A-labeled tubules do, however, exhibit partial colocalization with the translocon component Sec61α (Figure 2.2B). Upon transfection of FLAG-tagged gp78, the antibody against FLAG, but not 3F3A, labels the nuclear membrane (Figure 2.2C) and colocalizes with the ER marker calnexin (data not shown). In the cell

periphery, anti-FLAG and 3F3A labeling colocalize extensively and show only minimal association with Sec61α (Figure 2.2C). They also show extensive colocalisation with Rtn4a (Figure 2.2D). Importantly, both anti-FLAG and 3F3A still label mitochondria-associated ER domains (Figure 2.2E).

2.2.2 ER Ca2+ release regulates SER tubule-mitochondria interaction in intact cells

In digitonin-permeabilised cells, association of the 3F3A-labeled ER domain and mitochondria is favored at high $[Ca^{2+}]_{cyt}$ and reduced at low $[Ca^{2+}]_{cyt}$ (Wang et al., 2000). To study this interaction in intact cells, we modulated $[Ca^{2+}]_{cyt}$ by using the Ca^{2+} ionophore ionomycin in the presence of varying extracellular Ca^{2+} concentrations ($[Ca^{2+}]_{ex}$). While we were able to disrupt the morphology of the calnexin-labeled ER in MDCK cells exposed to 10 μM ionomycin in 10 mM extracellular Ca^{2+} ($[Ca^{2+}]_{ex}$; data not shown), these conditions were found to be highly toxic and resulted in cell rounding and detachment. Reducing the ionomycin concentration led to conditions that selectively affected the 3F3A-labeled SER domain and not the calnexin-labeled ER. As demonstrated in Figure 2.3, 3F3A-labeled SER tubules remained associated with mitochondria in MDCK cells incubated with 1 μM ionomycin and 200 μM EGTA (Figure 2.3A-C). Increasing $[Ca^{2+}]_{ex}$ to 1 mM disrupted the tubular pattern of the 3F3A-labeled ER, which became punctate, dispersed throughout the cell and exhibited reduced colocalization with mitochondria (Figure 2.3D-F) Increasing $[Ca^{2+}]_{ex}$ to 10 mM resulted in mitochondrial rounding and close association with the 3F3A-labeled SER domain. Relative to total cytoplasmic 3F3A pixel intensity, the intensity of 3F3A-labeled pixels that do not overlap with mitochondria provides a relative measure of dissociation of this SER domain from mitochondria. In parallel, $[Ca^{2+}]_{cyt}$ was measured using the cell-permeable Ca^{2+} probe Fura-2-AM (Figure 2.3J). Cells incubated with 1 μM ionomycin in a buffer containing EGTA, essentially R_{min}, presented no measurable $[Ca^{2+}]_{cyt}$. The extensive dissociation of the two organelles detected in the presence of 1 μM ionomycin and 1 mM $[Ca^{2+}]_{ex}$ corresponded to $[Ca^{2+}]_{cyt}$ of 115 ± 17 nM. In the presence of 1 μM ionomycin and 10 mM $[Ca^{2+}]_{ex}$, $[Ca^{2+}]_{cyt}$ increased to 1651 ± 62 nM and resulted in the reassociation of the two organelles (Figure 2.3J).

Thapsigargin is a specific and irreversible inhibitor of the sarco/endoplasmic reticulum Ca^{2+}-ATPases (SERCA), and its application results in the depletion of intracellular ER Ca^{2+} stores (Thastrup et al., 1990). MDCK cells treated with 10 μM thapsigargin in a buffer containing 200 μM EGTA present a dissociation of the 3F3A-labeled SER domain from mitochondria similar to that of cells treated with 1 μM ionomycin and 1 mM $[Ca^{2+}]_{ex}$ (Figure 2.3K). We did not observe alteration in the distribution of the calnexin-labeled ER under these conditions (data not shown), as previously reported (Ribeiro et al., 2000). Incubation of the cells in an EGTA-containing buffer in the presence of both 10 μM thapsigargin and 1 μM ionomycin also resulted in SER tubule-mitochondria dissociation after 20 minutes (Figure 2.3K). The $[Ca^{2+}]_{cyt}$ of cells treated with thapsigargin alone for 20 minutes was measured to be 211±42 nM, and the concomitant addition of 1 μM ionomycin and 10 μM thapsigargin caused a slight reduction of $[Ca^{2+}]_{cyt}$ to 148±19 nM owing to the efflux of some Ca^{2+} into the extracellular medium. Incubation for 60 minutes in 1 μM ionomycin plus 10 μM thapsigargin-EGTA resulted in a further decrease of $[Ca^{2+}]_{cyt}$ to 35±7 nM and reassociation of the 3F3A-labeled SER tubules and mitochondria (Figure 2.3K). Therefore, depletion of free ER Ca^{2+} with thapsigargin does not modify the response of the 3F3A-labeled SER domain to a reduction in $[Ca^{2+}]_{cyt}$.

Using electron microscopy, cells incubated with 1 μM ionomycin in EGTA buffer displayed elongated smooth and rough ER tubules, the latter defined by the presence of a linear array of membrane-bound ribosomes, often closely associated with mitochondria (Figure 2.4A-E). Incubation of cells with 1 μM ionomycin and 1 mM $[Ca^{2+}]_{ex}$ reduced the association between SER tubules and mitochondria (Figure 2.4B,F). Increasing $[Ca^{2+}]_{ex}$ to 10 mM increased the association between mitochondria and ER (Figure 2.4C,G). The shortest distance of ER tubules from the nearest mitochondria was measured from cells plated on plastic, fixed, scraped and embedded as a cell pellet (Wang et al., 2000) and from cells grown on filters and fixed and embedded in situ. As demonstrated in Figure 2.4H, I, the minimal distance of each ER tubule from mitochondria varies greatly. Nevertheless, a cluster of ER tubules in close proximity (<50 nm) to mitochondria was observed predominantly for SER tubules in cells treated with 1 μM ionomycin and EGTA and disrupted in cells treated with 1 μM ionomycin and 1 mM $[Ca^{2+}]_{ex}$. Addition of 10 mM $[Ca^{2+}]_{ex}$ enhanced the number of both smooth and

rough ER tubules in close proximity to mitochondria. Similar results were obtained for cells fixed as pellets (n=3) and on filters (n=2). We therefore counted the number of ER tubules within 50 nm of individual mitochondria and combined data from all five experiments. The number of SER tubules in proximity to mitochondria was significantly greater (4-5 fold) than RER tubules in the presence of 1 µM ionomycin plus EGTA and selectively reduced upon treatment with 1 µM ionomycin plus 1 mM $[Ca^{2+}]_{ex}$. Treatment with ionomycin plus 10 mM $[Ca^{2+}]_{ex}$ resulted in increased association of both SER and RER tubules with mitochondria (Figure 2.4J). These results confirm the Ca^{2+} sensitivity of the SER tubule-mitochondria association detected by 3F3A labeling of AMFR (Figure 2.3) and identify 3F3A labeling as a valid marker for a Ca^{2+}-sensitive mitochondria-associated SER domain.

ATP is a physiological agonist that stimulates purinergic receptors in the plasma membrane, thereby inducing production of Ins(1,4,5)P_3 and IP3R activation, resulting in a transient increase in $[Ca^{2+}]_{cyt}$ (Jan et al., 1999). Upon application of 10 µM ATP to MDCK cells, $[Ca^{2+}]_{cyt}$ measured with Fura-2-AM reached 190±13 nM in less than 20 seconds and then rapidly decreased to a plateau in the 60 nM range after 1 minute (Figure 2.5J). The transient increase was followed at 2 minutes by dissociation of the 3F3A-labeled SER from mitochondria (Figure 2.5A-F'), comparable to what we observed in the presence of ionomycin plus 1 mM $[Ca^{2+}]_{ex}$ or 10 µM thapsigargin (Figure 2.3). After 5 minutes, the mitochondrial association of 3F3A-labeled SER tubules was restored (Figure 2.5G-I'). Quantification of the extent of 3F3A SER tubule-mitochondria association shows clearly that transient dissociation of the two organelles follows the IP3R-mediated Ca^{2+} transient (Figure 2.5J). Pretreatment of MDCK cells with 2 µM xestospongin C, an inhibitor of IP3R (Gafni et al., 1997), for 15 minutes at 37°C before ATP application, limited the ATP-induced $[Ca^{2+}]_{cyt}$ increase to below 65 nM. In the presence of xestopongin C, basal dissociation levels were reduced relative to untreated cells and the ATP-induced dissociation of the two organelles was prevented (Figure 2.5J). Dissociation of 3F3A-labeled SER tubules and mitochondria is therefore a physiological response to ATP-stimulated release of Ins(1,4,5)P_3-sensitive Ca^{2+} pools.

2.2.3 The 3F3A mAb against AMFR defines a distinct Ca^{2+}-sensitive SER domain

In MDCK cells, the ER tubules labeled by 3F3A immunoelectron microscopy include smooth extensions of RER tubules as determined by electron microscopy (Benlimame et al., 1995a; Wang et al., 1997b). Continuities between the 3F3A- and calnexin-labeled ER are observed under conditions where the 3F3A-labeled SER domain remains associated with mitochondria (Figure 2.6A-B). After a two minute ATP treatment and dissociation of the 3F3A-labeled SER domain from mitochondria, the fragmented 3F3A labeling remains associated, but does not overlap, with the calnexin-labeled ER (Figure 2.6C-D). SERCA colocalises with 3F3A labeling even following ATP-mediated dissociation from mitochondria (Figure 2.6E-H). Upon changes in $[Ca^{2+}]_{cyt}$, 3F3A-labeled ER elements therefore retain SERCA but do not mix with the calnexin-labeled ER.

Labeling for the IP3R exhibited extensive overlap with mitochondria-associated 3F3A-labeled SER tubules (Figure 2.7), consistent with the previously reported distribution of IP3R to the SER and its presence in a mitochondria-associated ER domain (Rizzuto et al., 1993; Ross et al., 1989; Sharp et al., 1992; Takei et al., 1992). Quantification of the extent of overlap between the two ER domains by using the Pearson coefficient confirmed that the 3F3A- and IP3R-labeled ER domains colocalise with mitochondria (Figure 2.7C). After 2 minutes ATP treatment, or 1 μM ionomycin and 1 mM $[Ca^{2+}]_{ex}$ (data not shown), the 3F3A- and the IP3R-labeled SER exhibited reduced overlap with mitochondria, which was restored after 5 minutes of treatment (Figure 2.7A,C). Dissociation of those two SER domains from mitochondria was also associated with reduced colocalization between 3F3A and IP3R (Figure 2.7B,C).

2.2.4 Regulation of SER-mitochondria interaction by $[Ca^{2+}]_{cyt}$ in NIH-3T3 and RAS-transformed NIH-3T3 cells

Expression of both AMF and AMFR is generally upregulated in tumour cells, resulting in autocrine activation of this motility factor receptor (Yanagawa et al., 2004). By western blot,

AMFR expression is increased in RAS-transformed NIH-3T3 cells relative to untransformed NIH-3T3 cells (Figure 2.8A). Similarly, quantitative immunofluorescence shows a significant increase in 3F3A labeling of AMFR in RAS-transformed NIH-3T3 cells (Figure 2.8A). By immunofluorescence, 3F3A labeling in RAS-transformed NIH-3T3 cells no longer presents a tubular mitochondrial-associated morphology and is dispersed throughout the cytoplasm, extending to the pseudopodia of these cells (Figure 2.8B). Dissociation of the 3F3A-labeled ER domain from mitochondria corresponds to an increase in $[Ca^{2+}]_{cyt}$ from 40 nM to 100 nM, similar to the $[Ca^{2+}]_{cyt}$ ranges associated with changes in SER tubule-mitochondria association in MDCK cells (Figure 2.8B,C). In the presence of ionomycin and 1 mM $[Ca^{2+}]_{ex}$, 3F3A-labeled SER tubule-mitochondria dissociation was observed in NIH-3T3 cells in a fashion similar to that of MDCK cells. Depletion of $[Ca^{2+}]_{cyt}$ by incubation of RAS-transformed NIH-3T3 cells with ionomycin and EGTA buffer resulted in increased overlap of the 3F3A-labeled ER domain and mitochondria (Figure 2.8D).

As observed for MDCK cells, both 3F3A labeling and IP3R labeling colocalised extensively with mitochondria in NIH-3T3 cells (Figure 2.9). In RAS-transformed NIH-3T3 cells, the IP3R-labeled ER remained associated with mitochondria and showed reduced dissociation from mitochondria relative to the 3F3A-labeled ER, and these two ER domains showed limited overlap. This suggests that 3F3A and IP3R labeling might define ER domains that differentially associate with mitochondria.
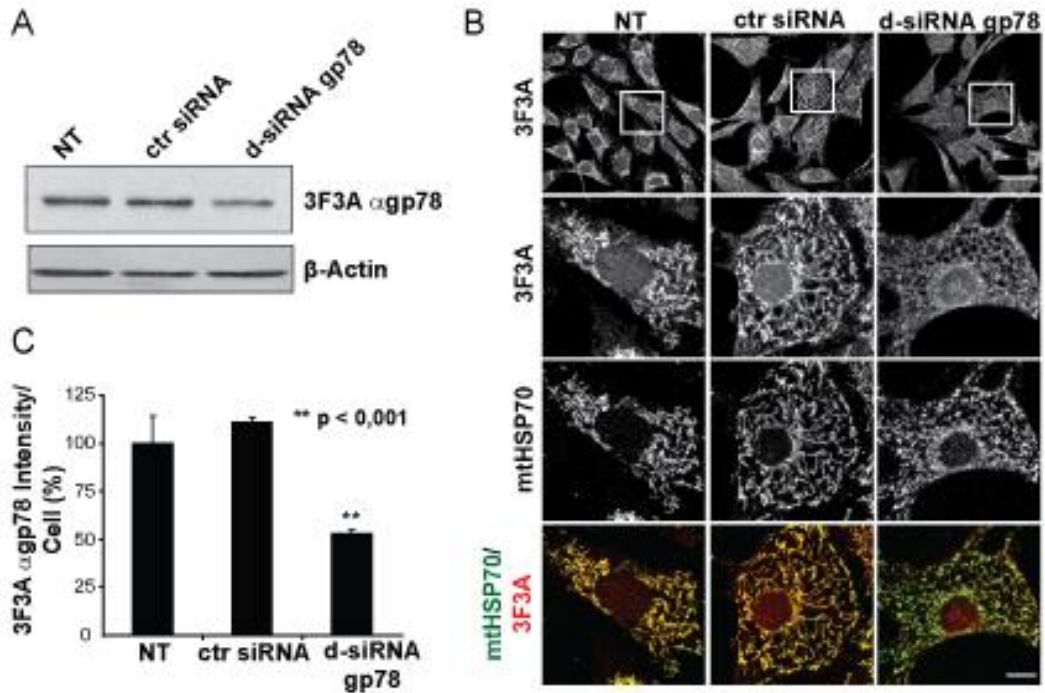
Figure 2.1 siRNA knockdown of expression of gp78.

(A) NIH-3T3 cells untransfected (NT) or transfected with Dicer gp78 siRNA (d-siRNA gp78) or control siRNA (ctl siRNA) were western blotted with the 3F3A antibody against gp78 and antibody against β-actin, as indicated. (B) NIH-3T3 cells untransfected (NT) or transfected with d-siRNA gp78 or control siRNA were fixed and immunofluorescently labeled with the 3F3A mAb and antibody against mtHSP70. Images were acquired with the same confocal settings (using a wide-open pinhole), and the bottom panels show digitally zoomed images of the inset (white box, first row), with the merge presenting 3F3A labeling in red and mitochondrial mtHSP70 labeling in green. (C) 3F3A labeling intensity was quantified from confocal images acquired with an open pinhole (see top row, panel B) of NIH-3T3 cells untransfected (NT) or transfected with d-siRNA gp78 or control siRNA. Total intensity per field was divided by the number of cells in the field (excluding cells touching the edges), determined by Hoechst nuclear labeling (data not shown). $^{**}P<0.001$. Bar, 50 μm (top row); 10 μm (zoom, bottom row).
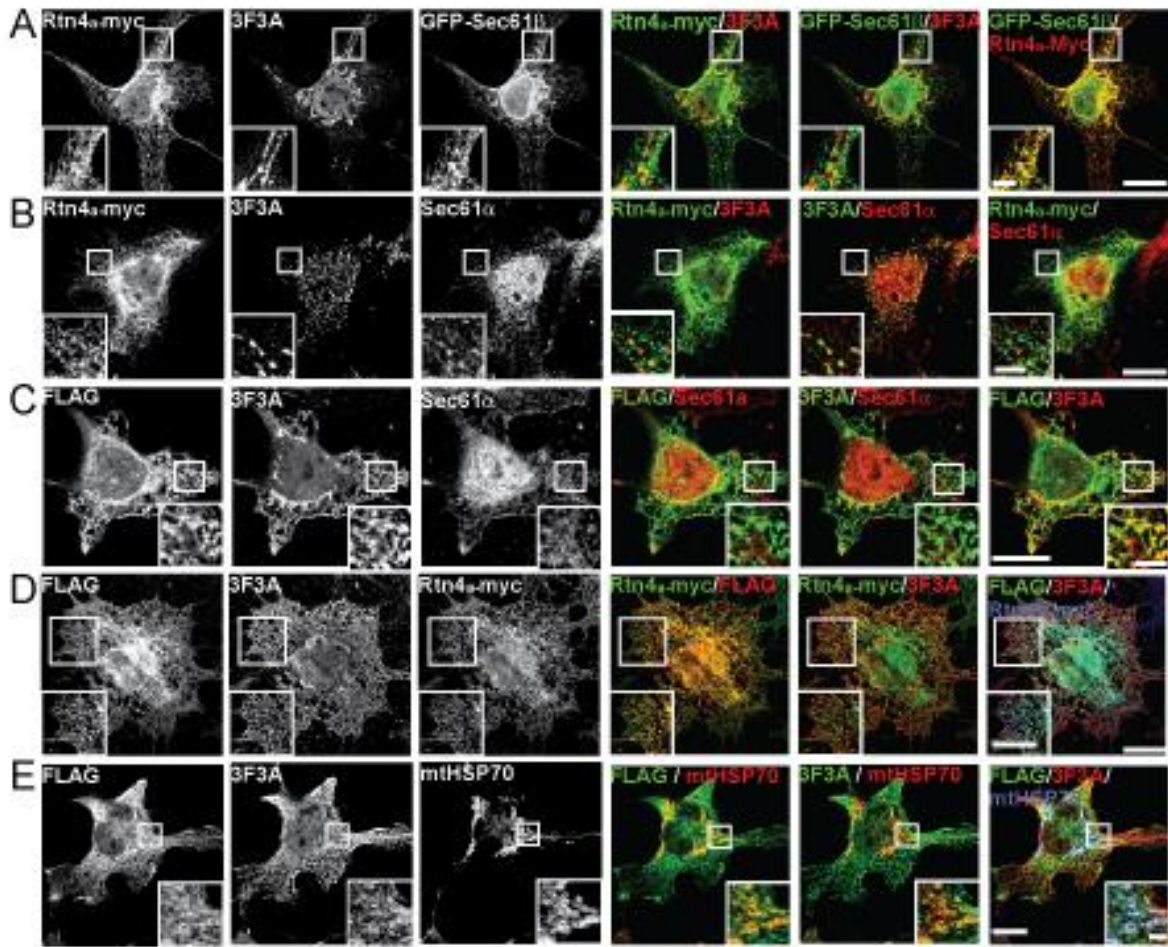
Figure 2.2 Characterization of the 3F3A-labeled ER domain.

(A) Cos-7 cells were co-transfected with GFP-Sec61β and Rtn4a-MYC and visualised using the GFP tag and anti-MYC and 3F3A antibodies. Inset shows that 3F3A labeling does not overlap with the Rtn4a-labeled ER tubules or the perinuclear ER labeled for GFP-Sec61β. (B) Cos-7 cells transfected with Rtn4a-MYC were labeled with anti-MYC, 3F3A and anti-Sec61α antibodies. Rtn4a distribution is distinct from both 3F3A and Sec61α, and 3F3A shows only partial colocalisation with Sec61α. Alternatively, FLAG-gp78-transfected cells were immunofluorescently labeled for FLAG, 3F3A and either Sec61α (C) or mtHSP70 (E) or co-transfected with vector encoding Rtn4a-MYC and labeled for FLAG, 3F3A and MYC (D). Insets highlight colocalisation of 3F3A labeling with anti-FLAG (C), Rtn4a (D) and mtHSP70 (E). Cells labeled for Sec61α were pre-treated with RNAse. Bars, 20 μm; inset bars, 5 μm.
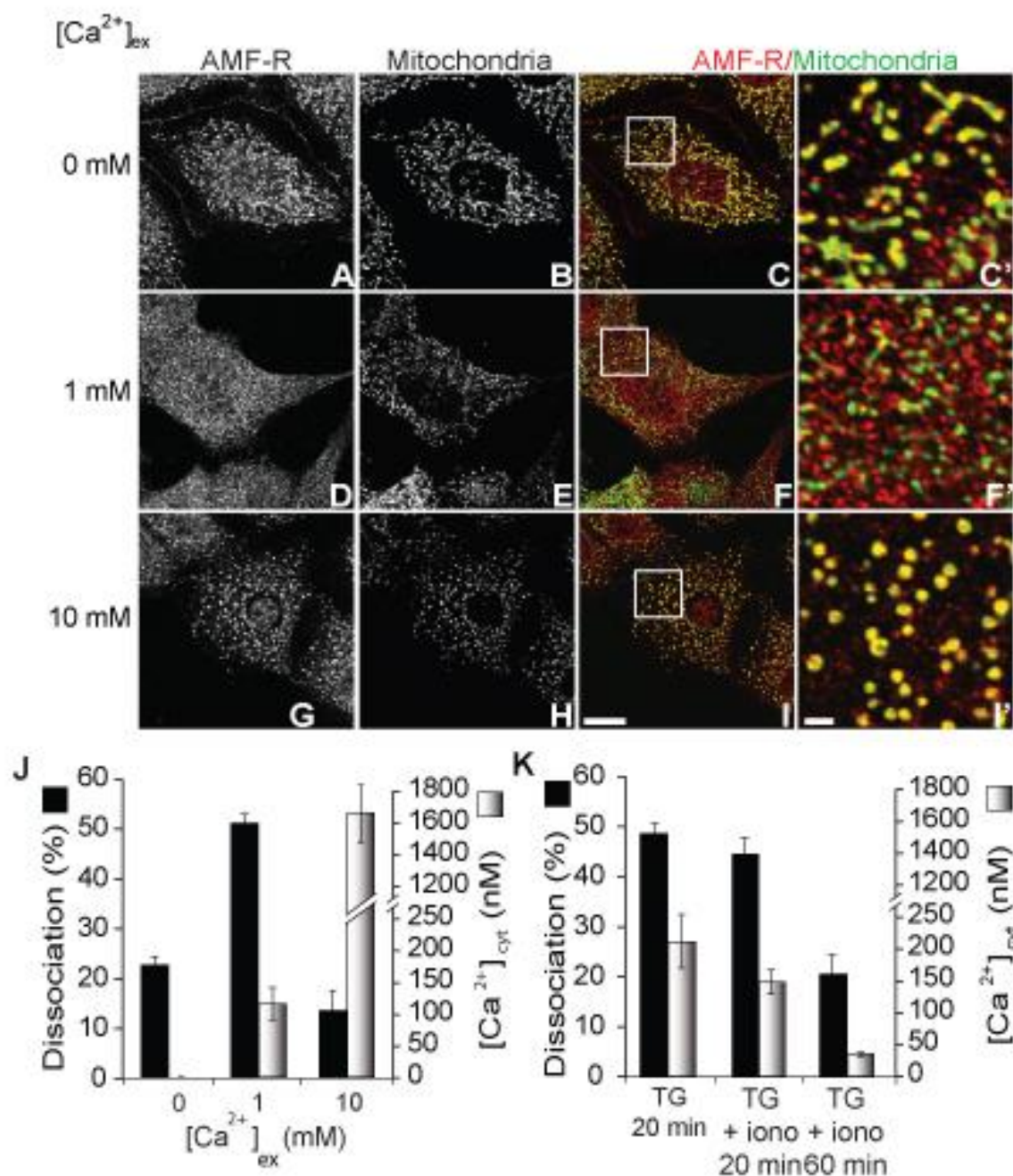
Figure 2.3 Ca²⁺ sensitivity of the mitochondria-interaction of 3F3A-labeled SER tubules in ionomycin-treated cells.

MDCK cells were treated with 1 μM ionomycin and either 200 μM EGTA (A,B,C,C′), 1 mM $[Ca^{2+}]_{ex}$ (D,E,F,F′) or 10 mM $[Ca^{2+}]_{ex}$ (G,H,I,I′) for 20 minutes and double immunofluorescently labeled with the 3F3A mAb and antibody against mtHSP70. Merged images (C,C′,F,F′,I,I′) show 3F3A labeling in red and mtHSP70 in green and overlap in yellow. C′,F′ and I′ show details of a zoomed region from images C,F and I, respectively. (J) The extent of dissociation of 3F3A-labeled SER tubules from mitochondria was quantified

46

by mask overlay (black bars, left Y-axis) for cells treated with 1 µM ionomycin and 0, 1 and 10 mM $[Ca^{2+}]_{ex}$, as indicated. For the same conditions, the corresponding average $[Ca^{2+}]_{cyt}$ determined using Fura-2-AM ratiometric labeling is shown (white bars, right Y-axis). (K) MDCK cells were treated with 10 µM thapsigargin for 20 minutes (TG 20 min) or with 1 µM ionomycin and 10 µM thapsigargin for 20 (TG+Iono 20 min) or 60 (TG+Iono 60 min) minutes. Cells were double immunofluorescently labeled for 3F3A and mtHSP70 and dissociation of 3F3A-labeled SER tubules from mitochondria quantified (black bars, left Y-axis). The corresponding average $[Ca^{2+}]_{cyt}$ (white bars, right Y-axis) is shown. The mask overlay data represent the average (±s.e.m.) of three independent experiments and the $[Ca^{2+}]_{cyt}$ values the average of at least ten Fura-2-AM experiments. Bars, 20 µm (I); 2 µm (I′).
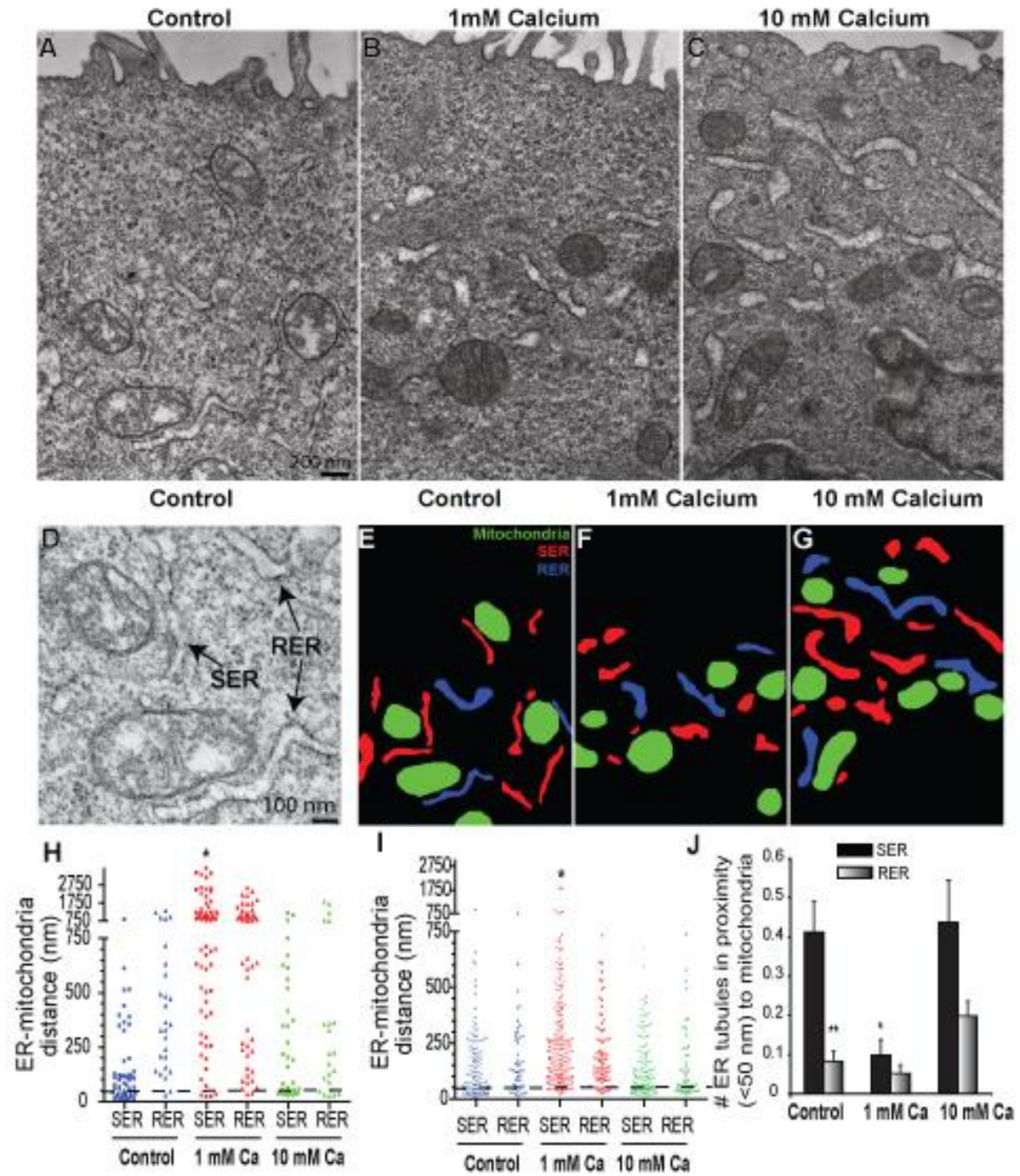
Figure 2.4 Electron microscopy analysis of the Ca^{2+} sensitivity of the ER-mitochondria interaction.

MDCK cells grown on filters were treated with 1 μM ionomycin and either 200 μM EGTA (A,D,E), 1 mM [Ca^{2+}]$_{ex}$ (B,F) or 10 mM [Ca^{2+}]$_{ex}$ (C,G) for 20 minutes and then processed for electron microscopy. D shows details of a zoomed region from A, with examples of smooth ER tubules and rough ER tubules indicated by arrows (rough arrays point to linear arrays of membrane-bound ribosomes). E, F and G represent masks of images A, B and C, respectively, outlining mitochondria (green), smooth ER tubules (red) and rough ER tubules (blue). The shortest distance of ER tubules from the nearest mitochondria was measured from

cells plated on plastic, fixed, scraped and embedded as a cell pellet (H) and from cells grown on filters and fixed and embedded in situ (I) ($^*P<0.001$ for smooth tubules, 1 mM $[Ca^{2+}]_{ex}$ relative to EGTA and 10 mM $[Ca^{2+}]_{ex}$). J presents the average number of ER tubules found within 50 nm of individual mitochondria ($n=5$; $^*P<0.01$ for smooth tubules, 1 mM $[Ca^{2+}]_{ex}$ relative to EGTA and 10 mM $[Ca^{2+}]_{ex}$; $^{**}P<0.01$ smooth tubules relative to rough tubules). Bars, 200 nm (A-C); 100 nm (D).
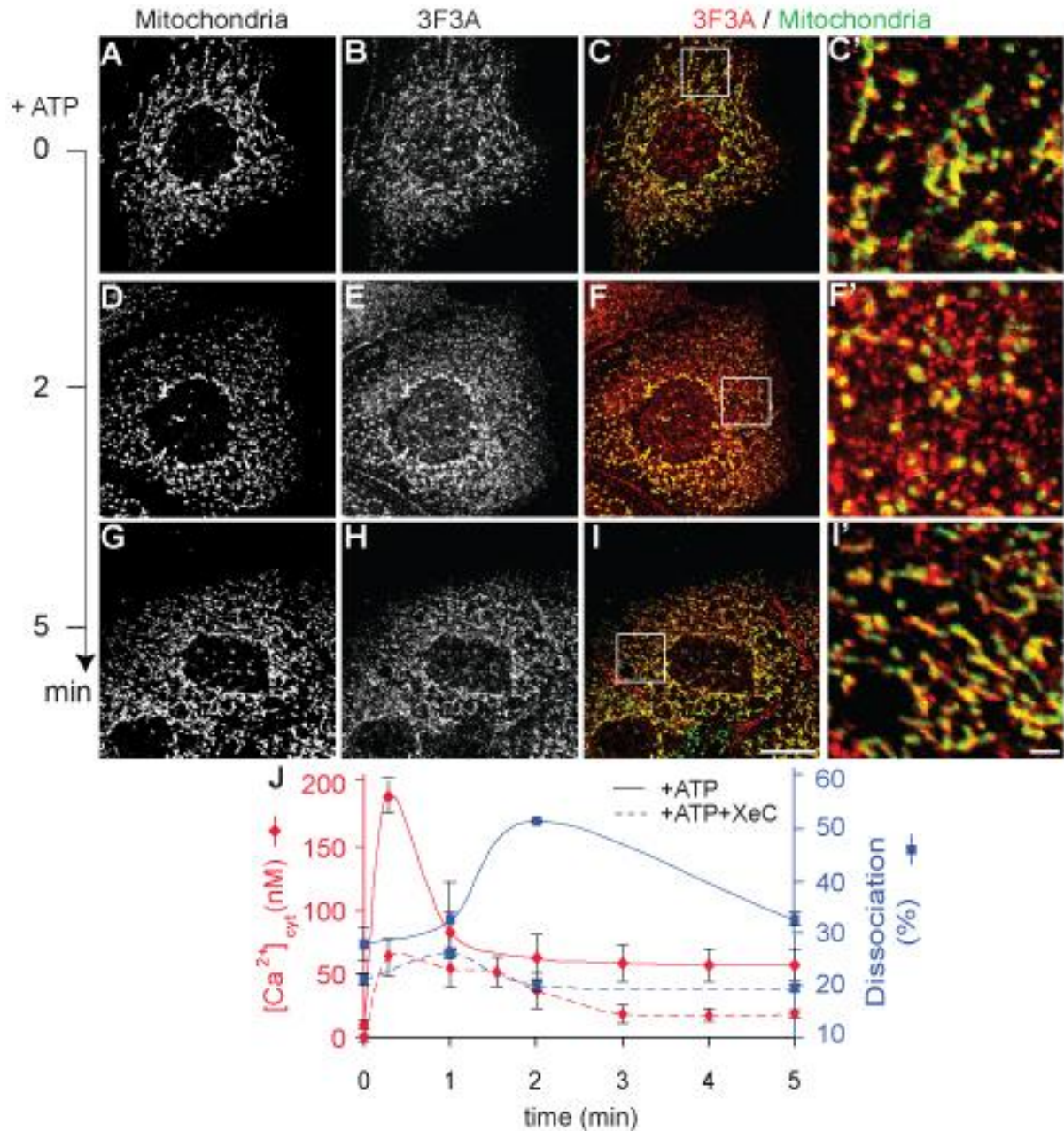
Figure 2.5 IP3R-mediated ER Ca^{2+} release induces transient SER tubule-mitochondria dissociation.
MDCK cells were treated with 10 μM ATP for up to 5 minutes. Treated MDCK cells were fixed at time 0 (A-C′), 2 (D-F′) or 5 (G-I′) minutes and then double immunofluorescently labeled for 3F3A and mtHSP70. Merged images (C,C′,F,F′,I,I′) show 3F3A (red) and mitochondria (green), co-distribution in yellow. C′, F′ and I′ show details of the boxed regions from images C, F and I, respectively. (J) At various times of ATP treatment without (solid lines) or with xestospongin C (XeC) pre-treatment (dashed lines), the extent of dissociation of 3F3A-labeled SER tubules from mitochondria was quantified (blue, right Y-axis) and the corresponding average [Ca^{2+}]$_{cyt}$ determined (red, left Y-axis). The data represent the average (±s.e.m.) of three independent experiments and [Ca^{2+}]$_{cyt}$ values the average of five Fura-2-AM experiments. Bars, 20 μm (H); 2 μm (I).

50
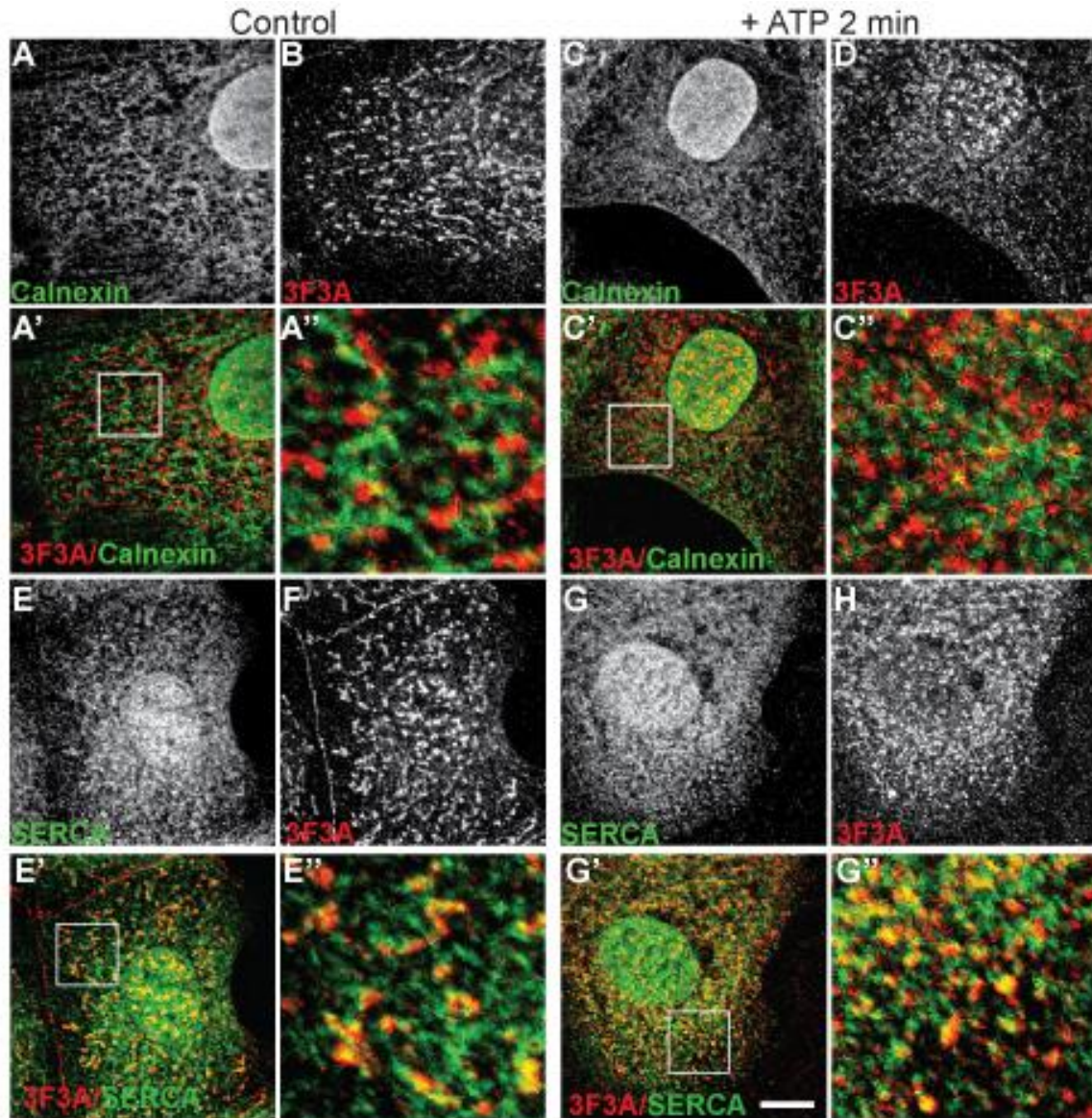
Figure 2.6 Relationship of 3F3A-labeled SER tubules to other ER markers upon ATP-induced mitochondrial dissociation.

MDCK cells untreated (A,B,E,F) or treated for 2 minutes with 10 µM ATP (C,D,G,H) were fixed and double immunofluorescently labeled for 3F3A and calnexin (A-D) or for 3F3A and SERCA (E-H). Merged images show 3F3A (red) and calnexin (green) co-distribution (A′-C′) or 3F3A (red) and SERCA (green) co-distribution (E′-G′) in yellow. A″, C″, E″ and G″ show details of the boxed regions from images A′, C′, E′ and G′, respectively. Bars, 20 µm (G′); 4 µm (G″).
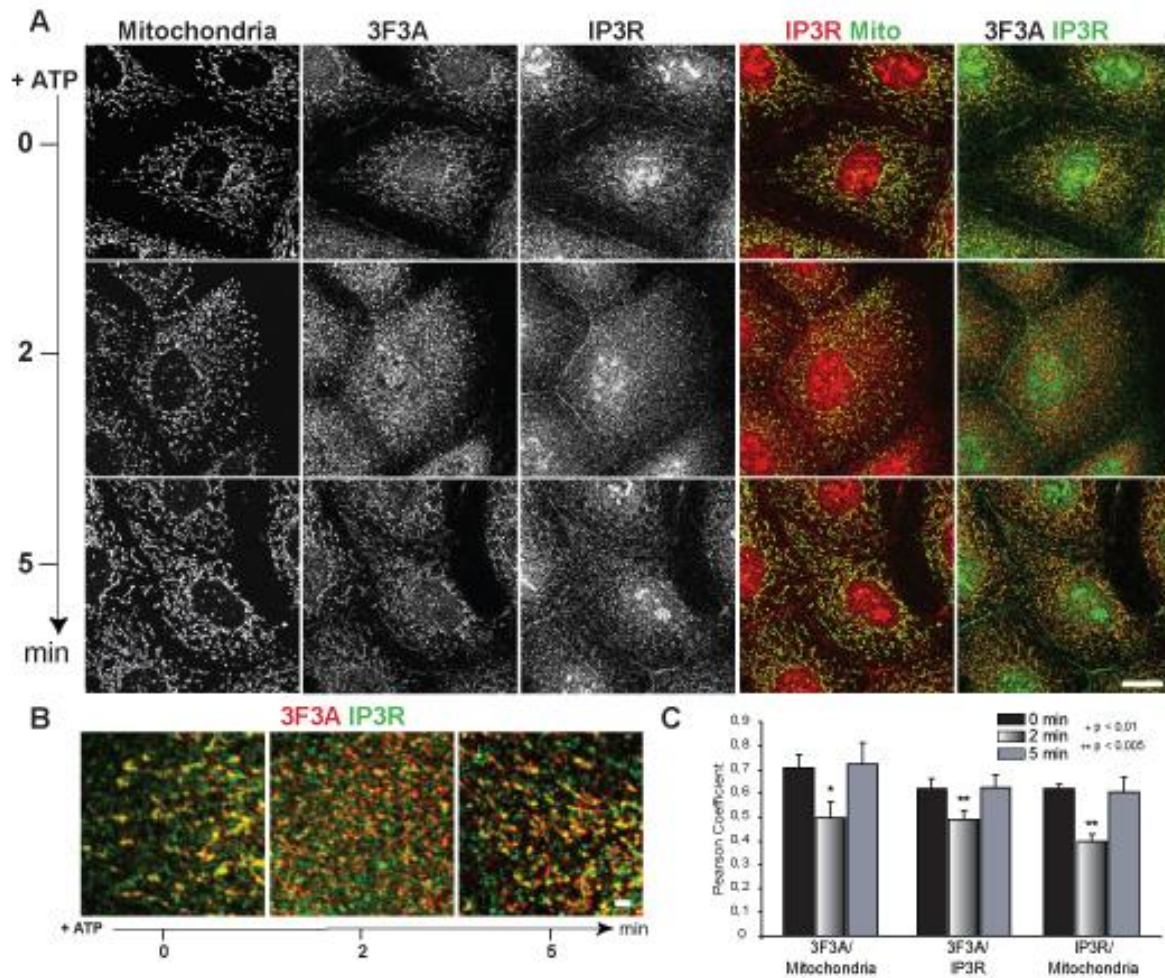
Figure 2.7 IP3R and 3F3A colocalise to mitochondria-associated ER but segregate upon ATP treatment.

(A) MDCK cells either untreated or treated with 10 μM ATP for 2 or 5 minutes were fixed and immunofluorescently labeled for IP3R, 3F3A and mitochondrial ATP-synthase (subunit α). (B) Details of zoomed regions from merges of 3F3A (red) and IP3R (green). (C) The extent of colocalisation of 3F3A and IP3R-labeled ER domains with mitochondria and between the 3F3A and IP3R-labeled ER domains at various times of ATP treatment was quantified using the Pearson coefficient. $^{*}P<0.01$; $^{**}P<0.005$ relative to 0 min. Bars, 20 μm (A); 2 μm (B).
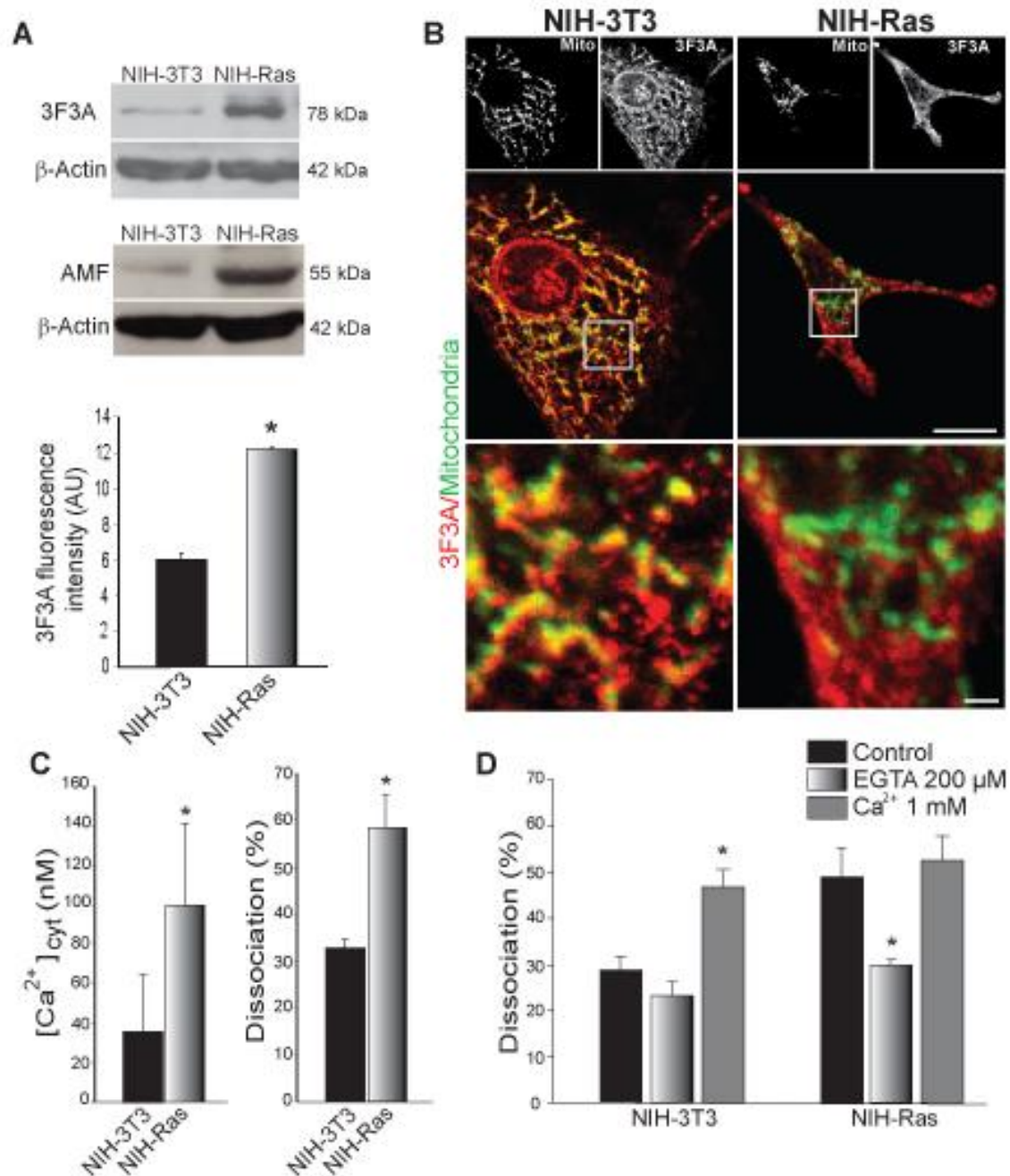
Figure 2.8 Distribution of 3F3A-labeled SER tubules in RAS-transformed NIH-3T3 cells is regulated by $[Ca^{2+}]_{cyt}$.

(A) Expression of AMFR and AMF was assessed in NIH-3T3 and RAS-transformed NIH-3T3 (NIH-Ras) cells by western blot using β-actin as a loading control. The bar graph shows quantitative immunofluorescence analysis of 3F3A labeling intensity from confocal images of NIH-3T3 and NIH-Ras cells acquired with an open pinhole ($^*P<0.005$). (B) NIH-3T3 and NIH-Ras cells were immunofluorescently labeled for 3F3A (red) and mtHSP70 (mito; green) and zooms of boxed regions of the merged images presented in the bottom row. Bars, 20 μm; 2 μm (zoom). (C) Average $[Ca^{2+}]_{cyt}$ using Fura-2-AM ratiometric labeling and 3F3A-labeled

SER tubule dissociation from mitochondria quantified by the mask overlay approach for NIH-3T3 and NIH-Ras cells. (D) Dissociation of 3F3A-labeled SER tubules from mitochondria was quantified by mask overlay in NIH-3T3 and NIH-Ras cells either left untreated (Control) or treated with 1 μM ionomycin in the presence of 200 μM EGTA or 1 mM $[Ca^{2+}]_{ex}$, as indicated. $^{*}P<0.01$; $^{**}P<0.005$.
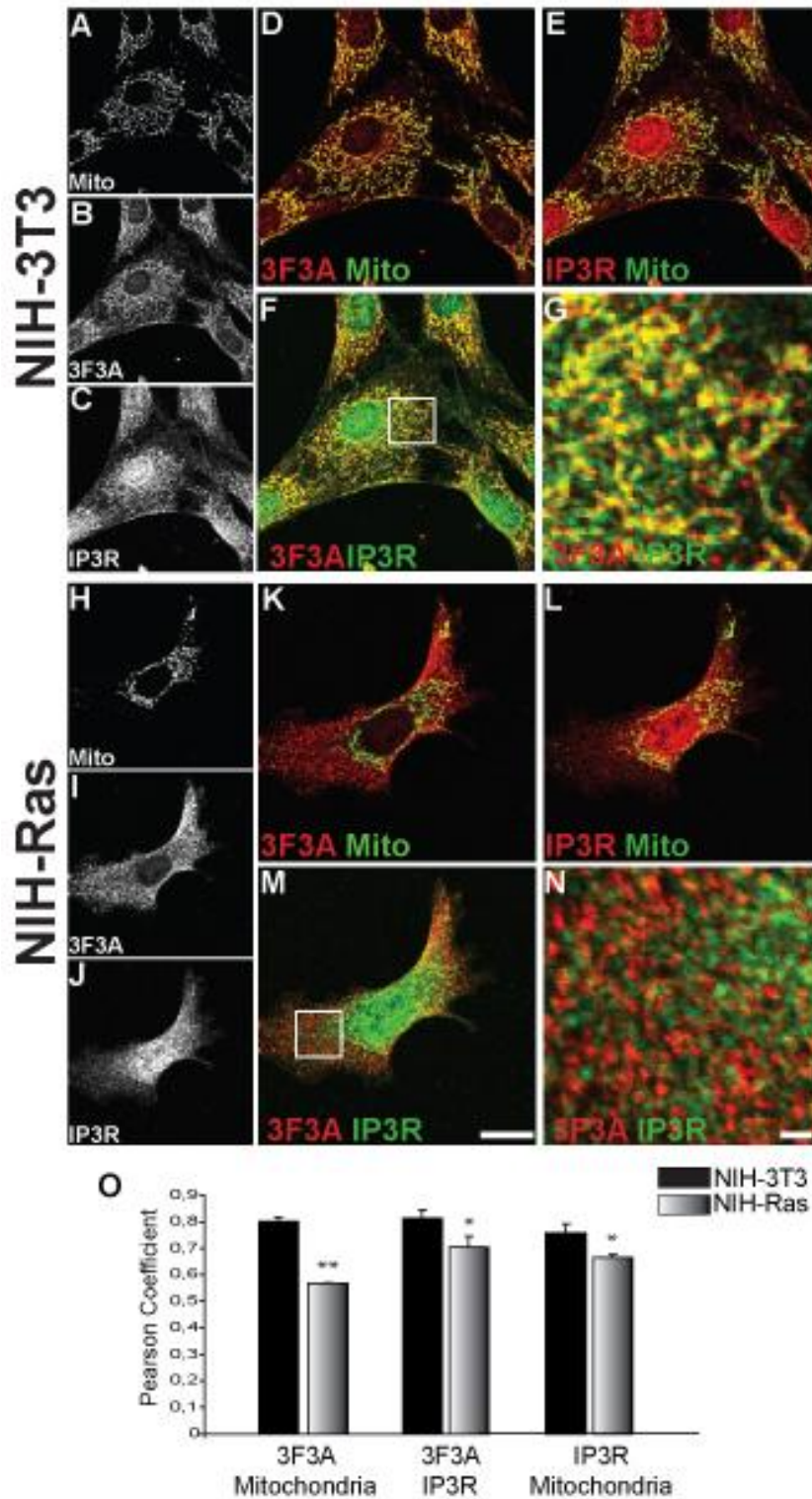
Figure 2.9 Segregation of 3F3A and IP3R-labeled ER domains in RAS-transformed NIH-3T3 cells.

NIH-3T3 (A-G) and RAS-transformed NIH-3T3 (NIH-Ras; H-N) cells were immunofluorescently labeled for mtHSP70 (mito; A,H), 3F3A (B,I) and IP3R (C,J). Merged images show 3F3A (red) and mtHSP70 (mito; green) (D,K), IP3R (red) and mtHSP70 (mito; green) (E,L), or 3F3A (red) and IP3R (green) (F,M). G and N show details of the boxed regions from images F and M, respectively. Bars, 20 μm (M); 2 μm (N). $^{*}P<0.01$; $^{**}P<0.005$.

2.3 Discussion

2.3.1 The 3F3A mAb against gp78 defines a distinct ER domain

The ER is a continuum of multiple domains, including the morphologically distinct SER and ribosome-studded RER. Recent work identified a group of integral membrane proteins, the reticulon and DP1 protein families, responsible for the high membrane curvature observed in ER tubules (Voeltz et al., 2006). Reticulon and DP1 do not label the nuclear membrane and segregate from the perinuclear ER, containing translocon components such as Sec61. The 3F3A mAb against gp78 has been characterised as a marker for a mitochondria-associated SER domain (Benlimame et al., 1998a; Benlimame et al., 1995a; Wang et al., 1997b; Wang et al., 2000). Here, we show that 3F3A labeling of SER tubules diminishes upon gp78 siRNA treatment, does not overlap with perinuclear ER markers, such as GFP-Sec61β or calnexin, does not label the nuclear envelope and does not colocalise with reticulon-labeled ER tubules. Interestingly, partial colocalisation of 3F3A with endogenous Sec61α is observed, consistent with immunoelectron microscopy 3F3A labeling of part-rough part-smooth ER tubules and smooth extensions of the rough ER (Benlimame et al., 1998a; Benlimame et al., 1995a; Wang et al., 1997b). Drug treatment and overexpression of select ER resident proteins, such as GFP-Sec61β, can induce the formation of organised SER domains connected to the RER (Snapp et al., 2003; Sprocati et al., 2006; Wang et al., 1997b). Interestingly, 3F3A does not overlap with overexpressed GFP-Sec61, suggesting that the 3F3A-labeled SER domain is distinct from the stacked smooth ER structures induced by overexpression of GFP-Sec61 (Snapp et al., 2003). However, upon overexpression of FLAG-gp78, the 3F3A mAb labels the peripheral, reticulon-expressing tubular ER network in addition to the mitochondria-associated ER domain (Figure 3.2), indicative of a relationship between these two ER domains.

The 3F3A antibody against gp78 therefore appears to recognize a gp78 conformation distinct from that of newly synthesized gp78 protein retained in the ER, thereby explaining the distinct ER distribution of 3F3A labeling and transfected gp78 (Fang et al., 2001a; Registre

et al., 2004). Gp78 is an E3 ubiquitin ligase that interacts with components of the ER-associated degradation (ERAD) complex such as the p97 ATPase and derlin and is implicated in the degradation of various substrates, including CD3-delta, the T-cell receptor, ApoB lipoprotein and HMG CoA reductase (Fang et al., 2001a; Liang et al., 2003; Song et al., 2005; Ye et al., 2005b; Zhong et al., 2004). The structural and functional specialization of the gp78 conformation within the mitochondria-associated SER might be related to its function in ERAD. In this study, we define the Ca^{2+}-sensitive interaction of the 3F3A-labeled ER domain with mitochondria.

2.3.2   Reversible, Ca^{2+}-sensitive association of the SER and mitochondria

As reported previously, in digitonin-permeabilised cells (Wang et al., 2000), intermediate (100-200 nM) $[Ca^{2+}]_{cyt}$ levels obtained by cell treatment with ionomycin under various $[Ca^{2+}]_{ex}$ conditions were found to disrupt the SER tubule-mitochondria complex, whereas high (>1500 nM) levels tended to favour complex formation in intact cells. By electron microscopy, SER tubules were found preferentially located within 50 nm of mitochondria in single sections (Figure 3.4), consistent with the existence of direct linkages between the two organelles (Csordas et al., 2006) and with our previous report of the close association of mitochondria with 3F3A-labeled SER tubules (Wang et al., 2000). Electron microscopy of ionomycin-treated MDCK cells paralleled the results obtained by 3F3A immunofluorescence, showing reduced SER tubule-mitochondria association at intermediate levels of $[Ca^{2+}]_{cyt}$. We also observed an increase in the number of RER tubules in proximity to mitochondria at high $[Ca^{2+}]_{cyt}$, consistent with previously reported effects of elevated $[Ca^{2+}]_{cyt}$ on general ER morphology (Ribeiro et al., 2000; Subramanian and Meyer, 1997). It is important to note that SER and RER in cultured cells do not present the dramatic morphological differences observed in tissue. Indeed, we define ER tubules as rough based on the presence of a linear array of more than three membrane-bound ribosomes (Benlimame et al., 1998a; Benlimame et al., 1995a). Using this approach, our data argue that smooth ER tubules lacking ribosomes, unlike ribosome-studded rough ER tubules, show a preferential Ca^{2+}-dependent association with mitochondria. Whether SER and RER in tissues present differential mitochondria association remains to be determined.

Levels of $[Ca^{2+}]_{cyt}$ between 110 and 210 nM were associated consistently with SER tubule-mitochondria dissociation, whereas levels of $[Ca^{2+}]_{cyt}$ below 60 nM were found to correlate with SER tubule-mitochondria association. The two organelles were observed to reassociate when $[Ca^{2+}]_{cyt}$ was decreased in MDCK cells treated with ionomycin and thapsigargin or following the ATP-induced Ca^{2+} transient or in RAS-transformed NIH-3T3 cells treated with ionomycin-EGTA. The SER tubule-mitochondria interaction is therefore a reversible process closely tied to $[Ca^{2+}]_{cyt}$. Reduced $[Ca^{2+}]_{cyt}$ was not associated with SER tubule-mitochondria association in digitonin-permeabilised cells (Wang et al., 2000), suggesting that the mechanisms underlying SER tubule-mitochondria association under conditions of high or low $[Ca^{2+}]_{cyt}$ are distinct. Those prevailing at low $[Ca^{2+}]_{cyt}$ might not be functional in cytosol-replenished digitonin-permeabilised cells as a result of disruption of the cytoskeletal network and because of the overall cellular architecture (Wang et al., 2000).

The temporal dissociation of SER tubules and mitochondria following ATP-induced release of Ca^{2+} from $Ins(1,4,5)P_3$-sensitive Ca^{2+} pools clearly demonstrates that dissociation of the two organelles is a physiological response to changes in $[Ca^{2+}]_{cyt}$. The specific role of Ca^{2+} release from ER stores was shown by the ability of xestospongin C, a specific inhibitor of $Ins(1,4,5)P_3$ activation (Gafni et al., 1997), to prevent SER tubule-mitochondria dissociation. The SER tubule-mitochondria reassociation observed following extended incubation with thapsigargin and ionomycin (Figure 3.3) indicates that depletion of free Ca^{2+} from the ER does not modify the response of 3F3A-labeled SER tubules to changes in $[Ca^{2+}]_{cyt}$. The interaction of this SER domain with mitochondria can therefore respond to changes in $[Ca^{2+}]_{cyt}$ independently of the replenishment state of ER Ca^{2+} stores.

2.3.3   Regulation of SER tubule-mitochondria interaction

Both the 3F3A- and IP3R-labeled ER domains dissociated from mitochondria upon stimulation with ATP (Figure 3.7). This is consistent with the overall reduction in SER tubule-mitochondria association observed upon elevation of $[Ca^{2+}]_{cyt}$ by electron microscopy (Figure 3.4). Compared with the IP3R-labeled ER domain, the 3F3A ER domain shows

increased dissociation from mitochondria in RAS-transformed NIH-3T3 cells relative to nontransformed NIH-3T3 cells. IP3R gating occurs at a $[Ca^{2+}]_{cyt}$ of 200-300 nM (Bezprozvanny et al., 1991; Hirata et al., 1984; Iino, 1990). This is slightly higher than reported here for mitochondrial dissociation of the 3F3A SER domain (100-200 nM) but sufficient for increased clustering of IP3R in the ER adjacent to mitochondria (Shuai and Jung, 2003; Wilson et al., 1998). Mitochondrial and ER mobility are controlled by physiological $[Ca^{2+}]_{cyt}$, with an IC_{50} of ~400 nM, that might recruit these organelles to cell regions of elevated $[Ca^{2+}]_{cyt}$ (Brough et al., 2005; Yi et al., 2004). While comparison of absolute $[Ca^{2+}]_{cyt}$ based on Fura-2 measurements must be done with caution, local, physiological changes in $[Ca^{2+}]_{cyt}$ would appear to have variable effects on the integrity and mitochondrial interaction of SER domains. Together with the segregation of the IP3R- and 3F3A-labeled ER domains upon elevation of $[Ca^{2+}]_{cyt}$, this suggests that multiple mechanisms regulate the association of SER tubules with mitochondria.

PACS-2 is a sorting protein that regulates the amount of mitochondria-associated membrane (MAM)-localized lipid-synthesizing enzymes, ER homeostasis, Ca^{2+} signaling and the translocation to mitochondria of the pro-apoptotic factor Bid following an apoptotic stimulus (Simmen et al., 2005). The voltage-dependent anion channel (VDAC) has been proposed as the mitochondrial partner for IP3R-mediated Ca^{2+} transport from ER to mitochondria; VDAC expression has been localized to both ER and mitochondrial outer membranes and is enriched in the zone of apposition, where it enhances Ca^{2+} transfer to mitochondria (Hajnoczky et al., 2002; Rapizzi et al., 2002; Shoshan-Barmatz et al., 2004; Szabadkai et al., 2006). Gp78-dependent recruitment of the p97 ATPase and its p47 cofactor, implicated in ER membrane fusion (Kano et al., 2005; Roy et al., 2000), might impact on the integrity and morphology of mitochondria-associated SER domains. Whether [Ca2+]cyt impacts on specific mechanisms of ER-mitochondria interaction or generally affects the interaction between ER and mitochondria by impacting on ER domain morphology remains to be determined.

2.4 Materials and methods

2.4.1 Antibodies, plasmids and chemicals

The 3F3A rat IgM mAb against gp78 was as described (Nabi et al., 1990b). Antibodies to mitochondrial heat shock protein 70 (mtHSP70; clone JG1) and SERCA-2 were purchased from Affinity Bioreagents, to calnexin from Sigma, to IP3R from Calbiochem, to the mitochondrial ATP-synthase (Complex V, Subunit α) from Molecular Probes and to Sec61α from Upstate. Cross-absorbed secondary antibodies conjugated to FITC (Rat IgM) were purchased from Jackson ImmunoResearch Laboratories and to Alexa (568, 647) from Molecular Probes. Plasmid for expression of FLAG-gp78 was as previously described (Registre et al., 2004) and for expression of Rtn4a-MYC and GFP-Sec61β (Voeltz et al., 2006) were kindly provided by G. Voeltz and T. Rapoport (Harvard University, MA). Xestospongin C was from Calbiochem and ionomycin, thapsigargin, ATP, Fura-2-AM and other chemical reagents from Sigma.

2.4.2 Cell culture and treatments

MDCK (Wang et al., 2000), Cos-7 (Registre et al., 2004), NIH-3T3 and RAS-transformed NIH-3T3 cells (Le et al., 2002) were grown as previously described. Cos-7 cells were transfected using Effectene transfection reagent (Qiagen) and fixed 24 hours after transfection (Registre et al., 2004). Ionomycin and thapsigargin were used at 1 μM and 10 μM, respectively, in a 125 mM NaCl, 20 mM HEPES, 5 mM KCl, 1.5 mM $MgCl_2$ and 10 mM glucose buffer adjusted to pH 7.4 (normal buffer). Normal buffer was supplemented with 1 or 10 mM Ca^{2+}, or 200 μM EGTA as indicated. For ATP treatments, cells were incubated with normal buffer containing 10 μM ATP and, where indicated, pretreated with 2 μM xestospongin C in culture medium for 15 minutes at 37°C.

2.4.3 d-siRNA gp78 preparation and transfection

About 815 bp of C-terminal AMFR was amplified by PCR using the following set of primers, AMFR-C-For (5′ AGA CAC CTC CTG TCC AAC 3′), AMFR-C-Rev (5′ GGA GGT CTG CTG CTT CTG 3′), and TA cloned. Positive clones were screened for the cis and

trans orientation of fragments. Using T7 RNA polymerase (Invitrogen) and linearised cis and trans positive clones, complementary mRNAs were synthesized in vitro. These mRNA molecules were annealed, diced and the resulting 19-21-bp d-siRNA gp78 molecules were purified using Block-it RNAi kit (Invitrogen). Transfection of NIH-3T3 with d-siRNA gp78 or control siRNA was performed using Lipofectamine 2000 (Invitrogen).

2.4.4 Electron microscopy

Two methods were used to process cells for ultrastructural analysis. Cells grown on Petri dishes were washed rapidly twice with 0.1 M sodium cacodylate (pH 7.3) before fixing in the same solution containing 2% glutaraldehyde for 60 minutes at room temperature. The fixed cells were rinsed in 0.1 M sodium cacodylate, scraped from the Petri dish and collected by centrifugation. The cell pellet was post-fixed for 1 hour with 2% osmium tetroxide in sodium cacodylate buffer, dehydrated and embedded in LR-White resin. The sections were stained with 2% uranyl acetate and visualised in a Hitachi H7600 transmission electron microscope. Alternatively, cells were grown on polycarbonate filters, fixed in 0.1 M sodium cacodylate, 1.5% paraformaldehyde and 1.5% glutaraldehyde (pH 7.3), post-fixed for 1 hour on ice in 1% osmium tetroxide in 0.1 M sodium cacodylate (pH 7.3), stained for 1 hour with 0.1% uranyl acetate and then dehydrated. The filters were left in a 1:1 solution of propylene oxide:Polybed overnight and then embedded in 100% Polybed. Sections were viewed and photographed on a Philips 300 electron microscope operating at 60 kV.

2.4.5 Immunofluorescence

MDCK cells plated for 2 days were fixed by the direct addition of pre-cooled (–80°C) methanol-acetone (80-20%, vol-vol) and labeled as described previously (Wang et al., 1997). Endogenous Sec61α labeling was performed following treatment with 0.1 mg/ml RNAse A for 30 minutes at room temperature. No labeling was observed in the absence of RNAse treatment. Confocal images were obtained using 488, 568 and 633 laser line excitation with 63× (NA 1.4) and 100× (NA 1.3) or 60× (NA 1.4) and 100× (NA 1.35) planapochromat objectives of Leica TCS SP1 and Olympus FV1000 confocal microscopes, respectively.

Mask overlay quantification of 3F3A labeling with mitochondria was determined from 15 8-bit confocal images of mtHSP70 and 3F3A labeling acquired just below saturation with the 100× objective at zoom 2 and quantified with Northern Eclipse software (Empix Imaging, Mississauga, Ontario, Canada), as described previously (Wang et al., 2000). Complete cells within the field were selected and non-specific nuclear 3F3A labeling (Benlimame et al., 1995a) cut from both images. The mtHSP70 image was saturated (0-155 grey levels) to ensure that mitochondria-associated 3F3A labeling was covered by the mitochondrial mask and the 3F3A image thresholded (50-255 grey levels) to eliminate background pixels. The ratio of 3F3A pixel intensity after mask subtraction relative to total cytoplasmic 3F3A pixel intensity provides a relative measure of dissociation of the SER from mitochondria for samples for which cell treatment, labeling and image acquisition were performed in parallel. For IP3R labeling, 12-bit confocal images were acquired with an Olympus FV1000 confocal microscope using the same acquisition parameters, determined using the Hi-Lo function, for all samples and Pearson's coefficients determined using ImagePro image analysis software (Media Cybernetics).

2.4.6 Ca^{2+} measurements

$[Ca^{2+}]_{cyt}$ was estimated at pH 7.4 at room temperature using the Ca^{2+}-sensitive fluorophore Fura-2-AM (2 µM potassium salt) and a dual-excitation spectrofluorometer (Spex Industries) with excitation at 350 and 380 nm and emission at 505 nm, and $[Ca^{2+}]_{cyt}$ was calculated as described previously (Grynkiewicz et al., 1985). The maximum fluorescence ratio (R_{MAX}) was determined using a 10 mM $CaCl_2$, 10 µM ionomycin (pH 8) solution to saturate Fura-2, and R_{MIN} with a Ca^{2+}-free solution containing 2.5 mM EGTA and 10 µM ionomycin (pH 8).

Chapter 3: Peripheral ER localization of Gp78 ubiquitin ligase activity

2.5 Introduction

The ER is composed of multiple domains implicated in various cellular functions including lipid synthesis and metabolism, calcium homeostasis, and protein synthesis and degradation (Voeltz et al., 2002). Structurally, the ER consists of central, juxtanuclear rough ER sheets, the site of protein biosynthesis, as well as peripheral, smooth membrane tubules, whose expression is defined by the reticulons and DP1, proteins that form homo-oligomers that drive membrane curvature (Shibata et al., 2010). Endoplasmic reticulum-associated degradation (ERAD) is a quality control pathway in which misfolded and misassembled proteins are ubiquitylated and targeted for proteasomal degradation (Meusser et al., 2005; Vembar and Brodsky, 2008). A juxtanuclear, ER quality control (ERQC) compartment where ERAD substrates accumulate upon proteasomal inhibition has been described (Kamhi-Nesher et al., 2001b; Spiliotis et al., 2002a), however a role for other ER domains in ERAD remains poorly characterized.

Gp78 (also called autocrine motility factor receptor, AMFR) is an E3 ubiquitin ligase involved in ERAD. The gp78 C-terminal tail contains a RING finger motif, responsible for its ubiquitin ligase catalytic activity, as well as an ubiquitin binding CUE motif (Fang et al., 2001b; Shimizu et al., 1999b). The CUE motif is essential for gp78 E4 ubiquitin ligase activity targeting mutant CFTR (ΔF508) for degradation (Morito et al., 2008b). The C-terminal extremity of gp78 is the site of interaction with the AAA ATPase p97 that provides the driving force to dislocate polyubiquitylated substrates from the membrane into the cytoplasm (Ballar et al., 2006; Lilley and Ploegh, 2005; Ye et al., 2001; Ye et al., 2003; Zhong et al., 2004). P97 also serves as an adaptor protein that links gp78 to components of the retro-translocation complex, including derlin-1, VIMP and PNGase (Ballar et al., 2007; Li et al., 2006; Ye et al., 2005a). Gp78 substrates include unassembled subunits of the T-cell receptors CD3δ and TCRα (Chen et al., 2006a; Fang et al., 2001b). Gp78 substrate regulation

has been linked to pathological processes in the case of α1-antitrypsin, CFTRΔF508 and KAI-1, a tumor metastasis suppressor protein (Joshi et al., 2010; Morito et al., 2008b; Shen et al., 2006; Tsai et al., 2007). Gp78-mediated ERAD is also associated with physiological processes, such as the sterol-dependent ubiquitylation and degradation of HMG-CoA reductase and insig-1 (Cao et al., 2007; Lee et al., 2006b; Song et al., 2005).

Immunoelectron microscopy has localized gp78 to a smooth ER domain (Benlimame et al., 1998b; Benlimame et al., 1995b; Goetz and Nabi, 2006a; Wang et al., 1997a). Overexpression of FLAG-tagged gp78 results in the distribution of 3F3A labeling to the tubular, peripheral ER but not to the juxtanuclear, central ER (Goetz et al., 2007b). We show here that the peripheral ER is the site of ubiquitin ligase activity of gp78 where Cue domain interaction with ubiquitylated substrate restricts gp78 mobility. Polyubiquitylation and gp78 recruitment of p97 are required for translocation of ubiquitylated substrate to the central ER for proteasomal degradation.

2.6 Results

2.6.1 ER domain distribution of ERAD components

To study gp78 function in ERAD we generated the following N-terminal Flag-tagged constructs (Fig. 3.1A): 1) RING finger mutant (FLAG-RINGmut) containing an inhibitory point mutation of the third cysteine (C356S) in the RING-H2 domain (Freemont, 2000); 2) CUE domain mutant (FLAG-CUEmut) containing inhibitory point mutations of the MFP motif (M467F, F468S, P469S) responsible for CUE domain affinity for ubiquitin (Shih et al., 2003b); and 3) a deletion mutant (FLAG-Δp97) lacking the C-terminal p97 binding domain (Ballar et al., 2006; Zhong et al., 2004). Anti-Flag immunoprecipitates of the gp78 constructs expressed in Cos7 cells were recognized by the gp78-specific 3F3A monoclonal antibody (mAB)(Fig. 3.1B) (Goetz et al., 2007b; Nabi et al., 1990a; Registre et al., 2004) and, except for FLAG-Δp97, coimmunoprecipitated with p97 (Fig. 3.1C).

In Cos7 cells, the 3F3A labeled smooth ER domain and the extended 3F3A-labeled peripheral ER network formed upon transient transfection of FLAG-gp78wt (Goetz et al., 2007b) show limited overlap with central ER localized retrotranslocon proteins derlin-1 and derlin-2. Transfected Sec61β-GFP colocalizes extensively with the derlins and therefore serves as an excellent central ER marker (Fig. 3.2A, B). p97 shows limited association with the 3F3A-labeled ER in untransfected cells but colocalizes extensively with FLAG-gp78wt labeling and is recruited to the peripheral 3F3A-labeled ER in Flag-gp78wt but not Flag-Δp97 transfected cells (Fig. 3.2C). Gp78 overexpression therefore results in an expanded 3F3A-labeled peripheral ER that contains p97 and is spatially distinct from the central ER that includes derlin-1 and derlin-2, involved in retrotranslocation of ubiquitylated substrates and found in complex with gp78 (Ballar et al., 2007; Ye et al., 2005a). This suggests ER domain-specific functions for this ERAD-associated E3 ubiquitin ligase.

2.6.2 Gp78 ubiquitylation is initiated in the peripheral ER

To assess whether exogenous gp78 can ubiquitylate substrate, we co-transfected gp78 with HA-tagged ubiquitin (HA-Ubwt). In the presence of FLAG-gp78wt, the ubiquitylated protein smear was elevated relative to cells transfected with HA-Ubwt alone (Fig. 3.3A). Gp78 is targeted for degradation via the proteasome (Chen et al., 2006a) however the ubiquitylated smear detected extends below 78 kDa, suggesting that it includes not only ubiquitylated gp78 but also ubiquitylated gp78 substrates. The ubiquitylated smear shows increased intensity upon transfection with Flag-Δp97, suggesting that inability to recruit p97 does not limit gp78 ubiquitin ligase activity but, rather, by reducing translocation across the ER membrane, results in accumulation of ubiquitylated substrate (Jarosch et al., 2002; Ye et al., 2001). The minimal levels of HA-Ubwt labeled protein detected in pcDNA transfected control cells indicate that the ubiquitylated proteins detected upon transfection of FLAG-gp78wt are predominantly substrates of gp78 ubiquitin ligase activity. Overexpressed gp78 therefore appears to dominate the ERAD machinery in transfected Cos7 cells such that co-transfected HA-Ubwt represents a faithful reporter for gp78 ubiquitin ligase substrate activity.

In the presence of HA-tagged ubiquitin mutated at three critical lysine residues (K29, 48, 63R) involved in polyubiquitin chain elongation (HA-Ubmono), FLAG-gp78wt or FLAG-Δp97 ubiquitylated protein smears were significantly decreased. Similarly, HA-Ubmono reduced protein polyubiquitylation in pcDNA-transfected cells treated with the proteasome inhibitor MG132 (Fig. 3A). While K11 linkages have also been reported in ERAD (Xu et al., 2009), the ability of the triple lysine (K29, 48 and 63R) ubiquitin mutant to significantly reduce gp78 ubiquitylated smears argues that it is not a major linkage in these experiments. The ubiquitylated protein smear was reduced by RING finger and CUE domain mutation, consistent with a role for these domains in gp78 ubiquitin ligase activity (Fig. 3.2B).

In contrast to the predominantly nuclear labeling of HA-Ubwt in empty vector transfected cells, in FLAG-gp78wt and HA-Ubwt cotransfected cells, ubiquitylated substrate colocalizes extensively with and is restricted to the 3F3A-labeled peripheral ER (Fig. 3.3C). The

dramatic redistribution of HA-Ubwt labeling from a predominant nuclear localization in pcDNA transfected control cells to the ER upon transfection of FLAG-gp78wt and mutants suggests that the ER-associated ubiquitylated proteins detected are substrates of gp78 ERAD activity. Upon cotransfection of HA-Ubwt with FLAG-CUEmut, polyubiquitylated proteins are present not only in the peripheral but also the central ER, as evidenced by HA-Ubwt labeling of the nuclear envelope. In FLAG-gp78wt or Flag-CUEmut transfected cells, prevention of polyubiquitylation by cotransfection with HA-Ubmono restricts ubiquitylated substrates to the peripheral ER increasing colocalization with the 3F3A-labeled peripheral ER (Fig. 3.3C). In the peripheral ER of Flag-gp78wt transfected cells, HA-Ubwt shows extensive colocalization with both 3F3A and the reticulon (myc-Rtn4a)-labeled peripheral ER (Fig. 3.3D). This suggests that initiation of gp78 mediated ubiquitylation occurs in the peripheral ER.

2.6.3   CUE domain-polyubiquitylated substrate interaction reduces gp78 mobility in the peripheral ER

The central ER accumulation of polyubiquitylated substrate upon mutation of the gp78 Cue domain led us to determine the role of Cue domain integrity and ubiquitylated substrate interaction on gp78 mobility in the ER. Mobility of gp78 and mutants in the peripheral and central ER was measured using fluorescent recovery after photobleaching (FRAP). Gp78 tagged with GFP, either N- or C-terminally, accumulates in the central ER, exhibits reduced ubiquitin ligase activity and, when tagged C-terminally, interferes with p97 recruitment (unpublished data). To visualize gp78 by live cell imaging, we added an eight amino acid tetracysteine (4c) tag between the N-terminal FLAG tag and gp78 cDNA. The 4c tag binds selectively to FlAsH and ReAsH, arsenic-based compounds that fluoresce when bound to the 4c tag (Adams et al., 2002; Martin et al., 2005b). Transfected FLAG-4c-gp78wt labeled with FlAsH distributes to peripheral and central ER elements best visualized in live cells by maximum projections over time (Fig. 3.4A). Compared to GFP-Sec61β, that diffuses freely throughout the ER (Shibata et al., 2008), and shows 75-80% recovery after bleaching, Flag-4c-gp78wt shows a highly restricted recovery of less than 20% in both the peripheral and central ER (Fig. 3.4B). This suggests that the bulk of gp78 exists within stable complexes

68

that do not freely diffuse within the ER. Flag-4c-CUEmut exhibits a significantly increased mobile fraction (~40%) in both the peripheral and juxtanuclear ER, suggesting that Cue domain dependent interaction with ubiquitylated substrate stabilizes the gp78 complex motility. Loss of the p97-binding domain did not affect the gp78 mobile fraction. However, Flag-4c-RINGmut, assessed only in the central ER where it concentrates (Fig. 3.2A), exhibits a highly restricted diffusion rate, significantly reduced relative to FLAG-4c-gp78wt (Fig. 3.4B, Table 3.1). While cotransfection with HA-Ubwt did not affect FLAG-4c-gp78wt mobility, cotransfection with HA-Ubmono increased FLAG-4c-gp78wt motility to levels similar to FLAG-4c-CUEmut, but only in the peripheral ER (Fig. 3.4C, Sup. Table 3.1). These data indicate that mobility of gp78 requires active ubiquitin ligase activity. The ability of both Cue domain mutation and co-expression of HA-Ubmono to enhance gp78 mobility in the peripheral ER argues that gp78 mobility is regulated, at least in part, by interaction with polyubiquitylated substrate.

2.6.4   Transfer of gp78 polyubiquitylated substrate to the central ER

Initiation of ubiquitylation and interaction with polyubiquitylated substrate therefore appear to be peripheral ER events. However, derlins are concentrated in the central ER where they colocalize with GFP-Sec61β and are depleted from the 3F3A-labeled peripheral ER in gp78 overexpressing cells (Fig. 3.2A,B). To identify the site of proteasomal targeting, we treated cells with the proteasome inhibitor MG132, resulting in accumulation of ubiquitylated protein. As observed previously (Fig. 3.3C), HA-Ubwt labeled protein is excluded from the GFP-Sec61β labeled central ER when cotransfected with FLAG-gp78wt. However, upon treatment with MG132, ubiquitylated proteins accumulate in the central ER (Fig. 3.5A,B), as previously reported for the ERQC (Kamhi-Nesher et al., 2001b; Spiliotis et al., 2002a). This suggests that proteasomal targeting occurs in the central ER but, in the absence of proteasome inhibition, ubiquitylated substrates do not accumulate and are rapidly degraded.

In cells cotransfected with HA-Ubwt and FLAG-Δp97, ubiquitylated substrates are restricted to the peripheral ER, even in cells treated with MG132 (Fig. 3.5A,B). P97 recruitment by gp78 to the peripheral ER where polyubiquitylation is initiated therefore appears to be

required for subsequent transfer of the complex to the central ER. To verify this, we deleted the p97 binding site from Flag-CUEmut (Flag-CUEmut-Δp97). In the absence of p97 binding, expression of the CUE mutant no longer resulted in central ER accumulation of polyubiquitylated substrate (Fig. 3.5A,B). Furthermore, central ER accumulation of ubiquitylated substrate in Flag-CUEmut transfected cells and in MG132-treated Flag-gp78wt transfected cells is prevented by expression of mutant HA-Ubmono (Fig. 3.5A,B). This suggests that Cue domain interaction with polyubiquitin chains promotes stabilization of a gp78 complex that restricts, and potentially regulates, its exit from the peripheral ER. Substrate polyubiquitylation and p97 recruitment to gp78 appear to be required for central ER distribution of ubiquitylated substrates, irrespective of CUE domain integrity.

To directly demonstrate the transfer of ERAD substrates from their site of ubiquitylation in the peripheral ER to their site of proteasome targeting in the central ER, we performed a MG132 washout experiment. We measured the intensity of the HA-Ubwt signal in the GFP-Sec61β-defined central ER after MG132 treatment and over time after transfer to inhibitor-free media. In MG132-treated FLAG-gp78wt transfected cells, up to ~50% of the polyubiquitylated protein was localized in the central ER. After subsequent washout of the proteasome inhibitor, the amount of ubiquitylated protein in the central ER dropped rapidly reaching the level of untreated cells (~10%) after 90 minutes (Fig. 3.5C). In FLAG-CUEmut transfected cells, MG132 only slightly increased ubiquitylated protein accumulation in the juxtanuclear ER. MG132 treatment did not induce the accumulation of ubiquitylated protein in the central ER in cells co-transfected with either wild-type or CUE mutant gp78 and HA-Ubmono, indicating that central ER ubiquitylated substrates are polyubiquitylated. While the precise hierarchy of events remains to be more clearly defined, the fact that levels of polyubiquitylated proteins in the central ER remains essentially unchanged after MG132 washout (Fig. 3.5C) argues that CUE domain integrity is important for the efficient delivery of substrates to the proteasome.

2.6.5 Gp78 ubiquitin ligase activity localizes to the peripheral ER of HT-1080 fibrosarcoma cells

HT-1080 cells express elevated gp78 levels and concomitant reduced expression of the gp78 substrate, KAI1 (Fig. 3.6A). Consistent with elevated functional gp78 levels in HT-1080 cells, transfected HA-Ubwt shows a more peripheral distribution of ubiquitylated substrate in HT-1080 relative to HEK293t cells (Fig. 3.6B). Although HA-Ubwt was closely associated with the peripheral, tubular ER network defined by reticulon (myc-Rtn4a) (Voeltz et al., 2006) in both cell lines, increased colocalization of 3F3A with both reticulon and HA-Ubwt was observed in HT-1080 cells compared to HEK293t cells (Fig. 3.6C).

Upon proteasome inhibition with MG132, HA-Ubwt, but not HA-Ubmono, redistributed to the central ER of HT-1080 cells (Fig. 3.7A). As observed in gp78-overexpressing Cos7 cells (Figs. 3.3, 3.5), polyubiquitylation therefore appears to be required for central ER delivery of ubiquitylated substrate in HT-1080 cells. To determine the role of gp78, we generated stable gp78 knockdown HT-1080 cells that present reduced gp78 mRNA transcript levels, ~50% reduced gp78 expression and increased KAI1 expression by Western blot (Fig. 3.7B). In these cells, ubiquitylated substrate remains localized to the peripheral ER and MG132 treatment does not induce the central ER redistribution of ubiquitylated substrate (Fig. 3.7C). These data in HT-1080 fibrosarcoma cells therefore support the peripheral ER as the site of gp78-dependent ubiquitylation and suggest that transfer of ubiquitylated substrate to the central ER for targeting to the proteasome may occur in response to elevated gp78 ERAD activity.
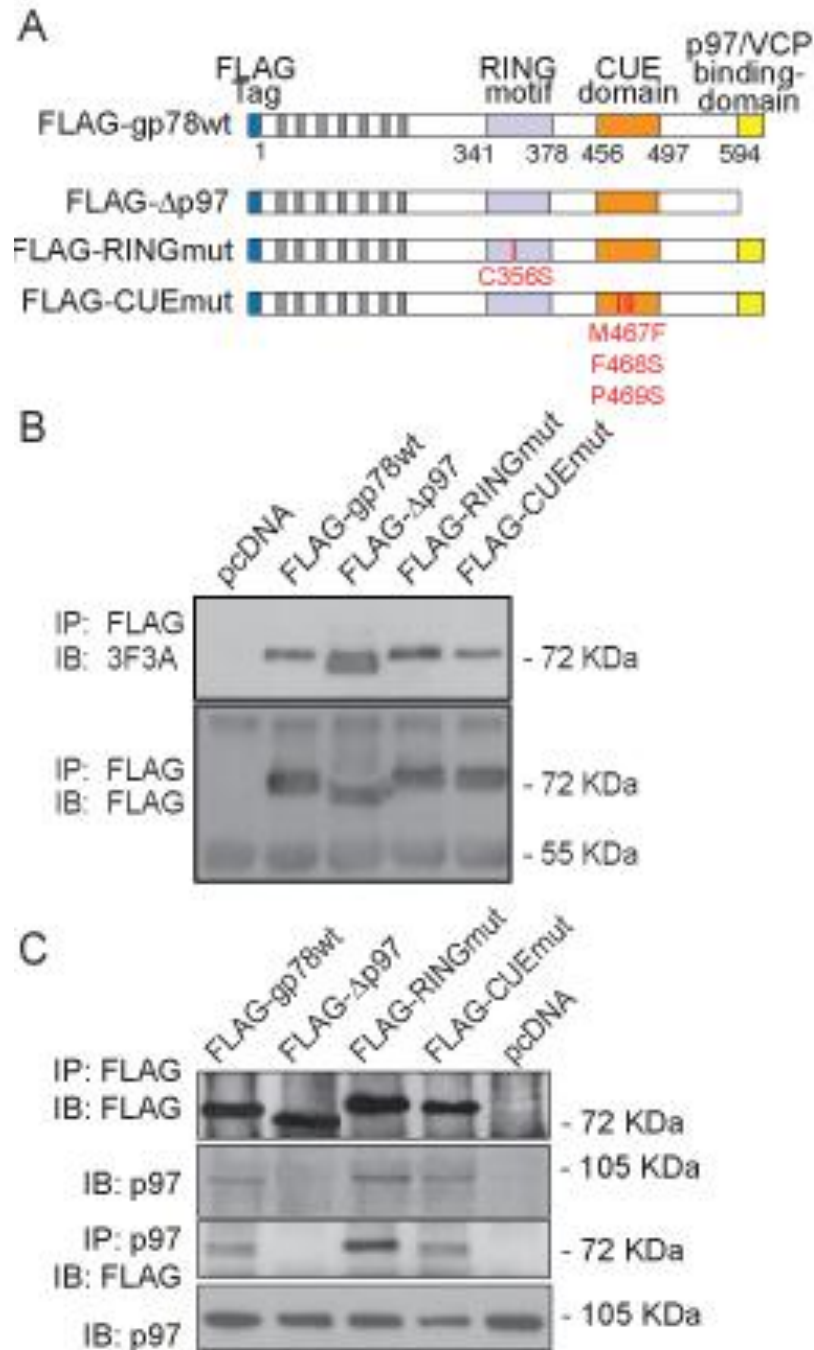
Figure 3.1 Gp78 construct validation.

A) N-terminal FLAG-tagged gp78 constructs: wild type (FLAG-gp78wt); p97-binding domain deletion (FLAG-Δp97); RING finger domain mutation (C356S; FLAG-RINGmut); CUE domain mutation (M467F, F468S, P469S; FLAG-CUEmut. B) Lysates of Cos7 cells transfected with empty vector (pcDNA) or the indicated FLAG-gp78 constructs were immunoprecipitated (IP) with anti-Flag antibody and immunoblotted (IB) with 3F3A or anti-FLAG antibodies. C) Lysates of Cos7 cells transiently transfected as in A were

immunoprecipitated with anti-FLAG or anti-p97 antibodies and immunoblotted with either anti-FLAG or anti-p97 antibodies, as indicated. Deletion of the p97-binding domain prevents p97 co-immunoprecipitation with FLAG-tagged constructs.
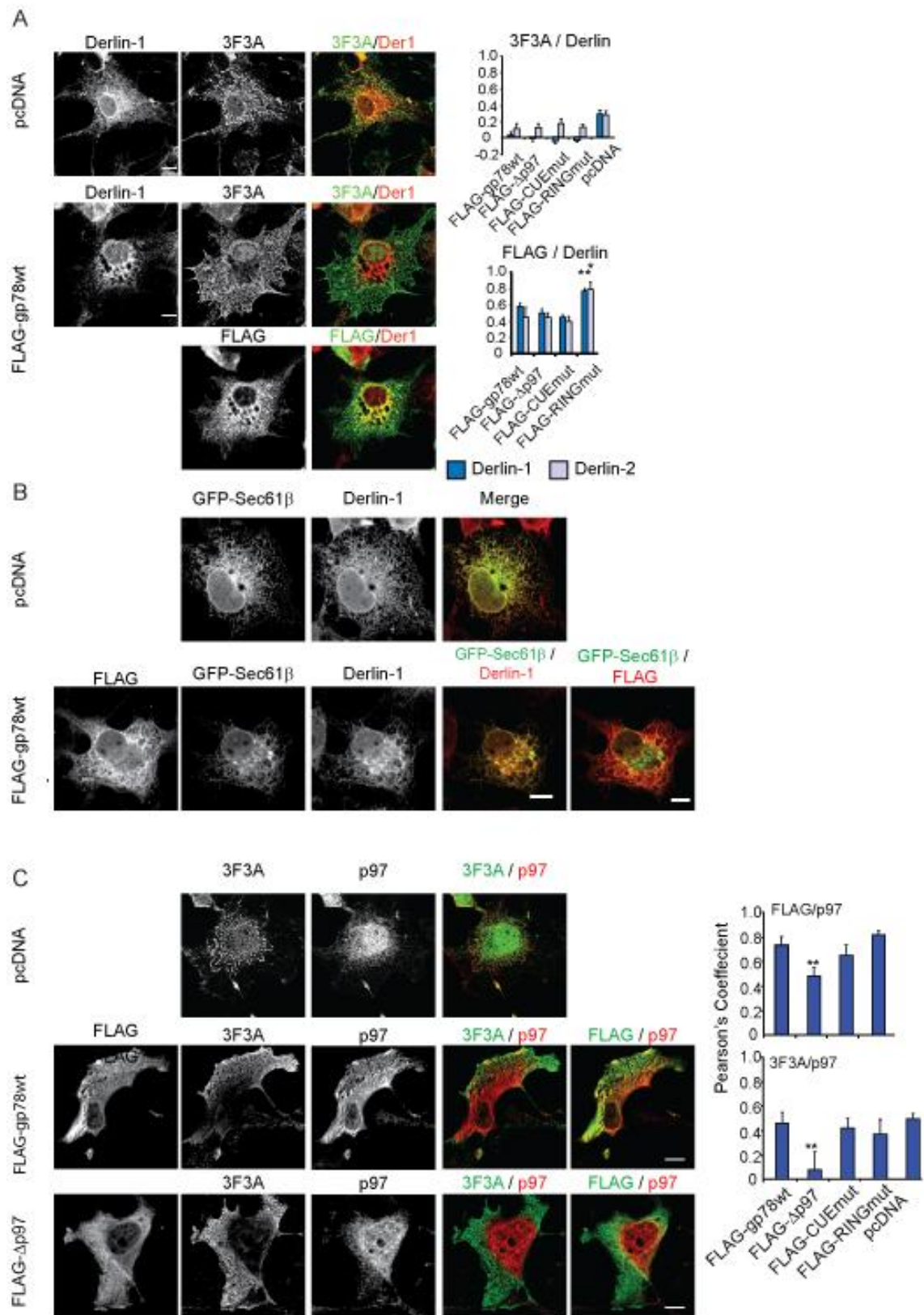
Figure 3.2 ER domain distribution of gp78 and ERAD proteins.

A) Cos7 cells transfected with the indicated Flag-gp78 constructs or empty vector (pcDNA) were immunofluorescently labeled with anti-FLAG, 3F3A antibody and either anti-derlin-1 or anti-derlin-2. Representative images of pcDNA and FLAG-gp78wt transfected cells labeled for derlin-1 and 3F3A are shown. Bar graphs present Pearson's colocalization coefficients between 3F3A (top) or FLAG (bottom) and derlin-1 or derlin-2 labeling (24 cells per condition from 3 distinct experiments, mean±SEM, *p< 0.05, **p<0.001; Bar = 10 µm). B) Cos7 cells were transfected with GFP-Sec61β alone or with FLAG-gp78wt, as indicated, then fixed and labeled with anti-FLAG and anti-derlin-1 antibodies and appropriate species-specific secondary antibodies. GFP was visualized as is. FLAG-gp78wt labeling extends to the peripheral ER but its overexpression induces concentration of GFP-Sec61β and derlin-1 to the central ER. Error Bar: 10 µm. C) Cells were transfected as in (A), then fixed and immunofluorescently labeled with anti-FLAG, 3F3A mAB and anti-p97, as indicated and followed by the appropriate species-specific secondary antibodies. Representative images of FLAG-gp78wt and FLAG-Δp97 transfected cells are shown. Bar graphs present Pearson's coefficients of p97 and FLAG or 3F3A colocalization, as indicated (24 cells per condition from 3 distinct experiments, mean±SEM, **p<0.001; Bar = 10 µm).
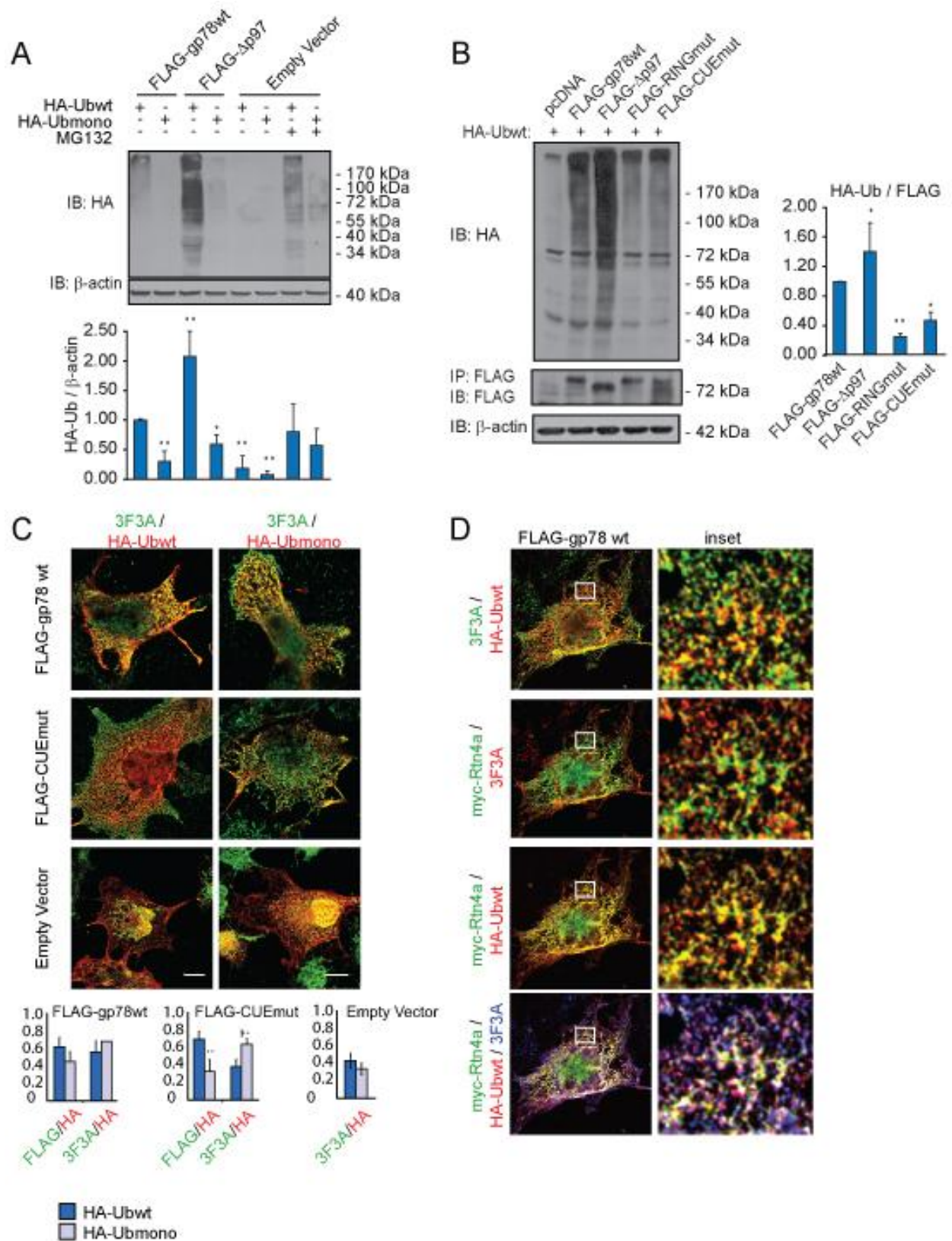
Figure 3.3 Ubiquitin ligase activity of gp78 is initiated in the peripheral ER.

A) Cos7 cells were cotransfected with FLAG-gp78wt, FLAG-Δp97 or empty vector (pcDNA) and either HA-Ubwt or HA-Ubmono. pcDNA transfected cells were also treated with MG132 (30 μg/ml) for 8 hours (*p<0.05, **p< 0.001 relative to Flag-gp78wt/HA-Ubwt). B) TX-100 soluble cell lysates of Cos7 cells cotransfected with pcDNA or the indicated Flag-gp78 constructs and HA-tagged ubiquitin (HA-Ubwt) were immunoblotted with anti-HA antibodies (top) or immunoprecipitated and immunoblotted with anti-FLAG antibody. The bar graph represents the density of the ubiquitin smears relative to anti-FLAG signal (*p<0.05, **p< 0.001 relative to Flag-gp78wt) C) Cos7 cells were cotransfected with FLAG-gp78wt, FLAG-CUEmut or empty vector and either HA-Ubwt or HA-Ubmono and immunofluorescently labeled with anti-HA, 3F3A and anti-FLAG antibodies. Bar graphs present Pearson's colocalization coefficients between HA and either Flag or 3F3A labeling (n=24, mean±SEM, **p<0.001). D) Peripheral regions of Cos7 cells transfected with FLAG-gp78wt, myc-Rtn4a and HA-Ubwt were labeled with anti-HA, 3F3A and anti-myc antibodies, as indicated. Bar = 2μm.
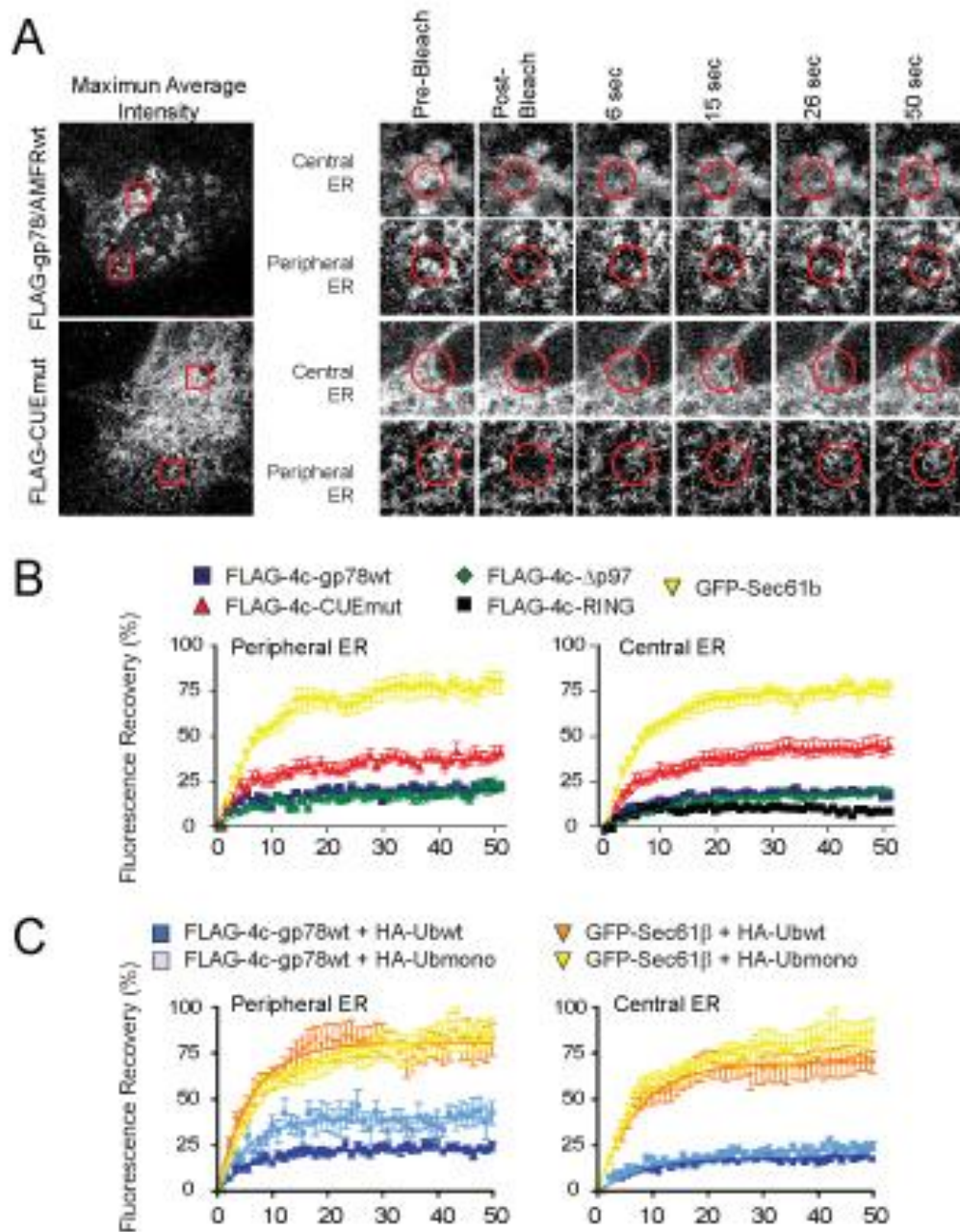
Figure 3.4 Polyubiquitylated substrate-CUE motif interaction stabilizes gp78 in the peripheral ER.

A) Cos7 cells were transfected with FLAG-4c-gp78wt, FLAG-4c-Δp97, FLAG-4c-RINGmut or FLAG-4c-CUEmut constructs and visualized in live cells with FlAsH reagent. Representative maximum projections (50 images over 52 seconds) of FLAG-4c-gp78wt and Flag-4c-CUEmut are shown. Peripheral and central ER regions (boxes) are shown pre-bleach, immediately after bleach and 6, 15, 26 and 50 s after bleach (circles). (n=12, Bar: 10 μm; inset: 2 μm). B) Graphs show normalized recovery after photobleaching of indicated FLAG-4c-gp78 constructs as well as GFP-Sec61β (yellow), as a control, in the peripheral (left) and central

(right) ER. D) Graphs show recovery after photobleaching of FLAG-4c-gp78wt or GFP-Sec61β cotransfected with HA-Ubwt or HA-Ubmono, as indicated.
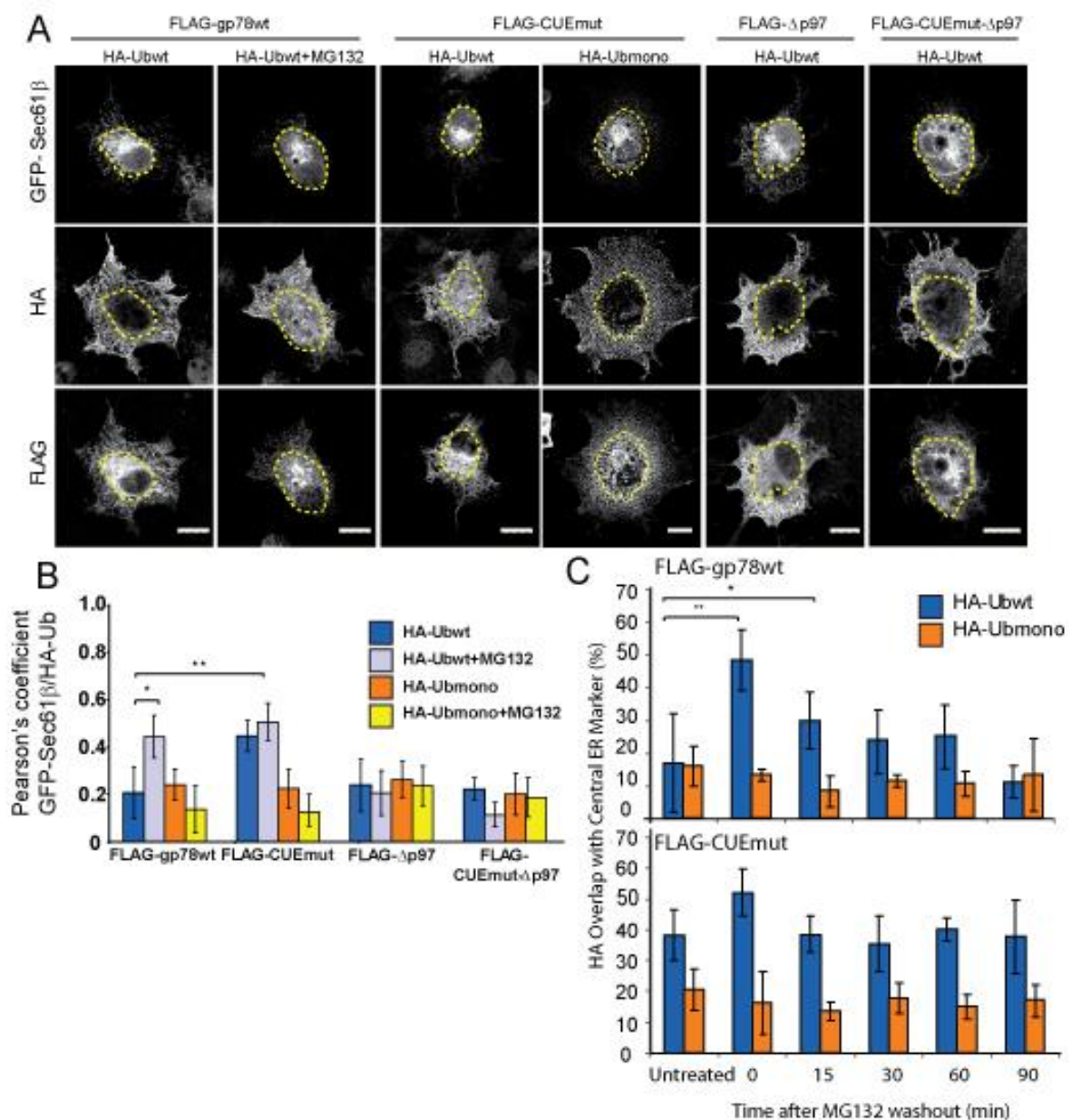
Figure 3.5 Proteasomal delivery of gp78 ERAD substrates in the central ER

(A) Cos-7 cells transfected with the indicated FLAG-gp78 constructs, either HA-Ubwt or HA-Ubmono and the central ER marker GFP-Sec61β (yellow line) were treated with or without MG132 for 8 hours, then labeled for HA and Flag. Bar: 20 μM. (B) Colocalization between GFP-Sec61β and HA-Ub labeling was determined for the indicated Flag-gp78 constructs in the presence of HA-Ubwt or HA-Ubmono with or without MG132 treatment. (C) Cos-7 cells transfected as in (A) were treated with MG132 for 8 hours then incubated in MG132-free media for the indicated times. Using GFP-Sec61β to define the central ER, the intensity of HA labeling in the peripheral ER was determined relative to total HA intensity (24 cells per condition from 3 distinct experiments, mean±SEM, *p< 0.05, **p<0.001).
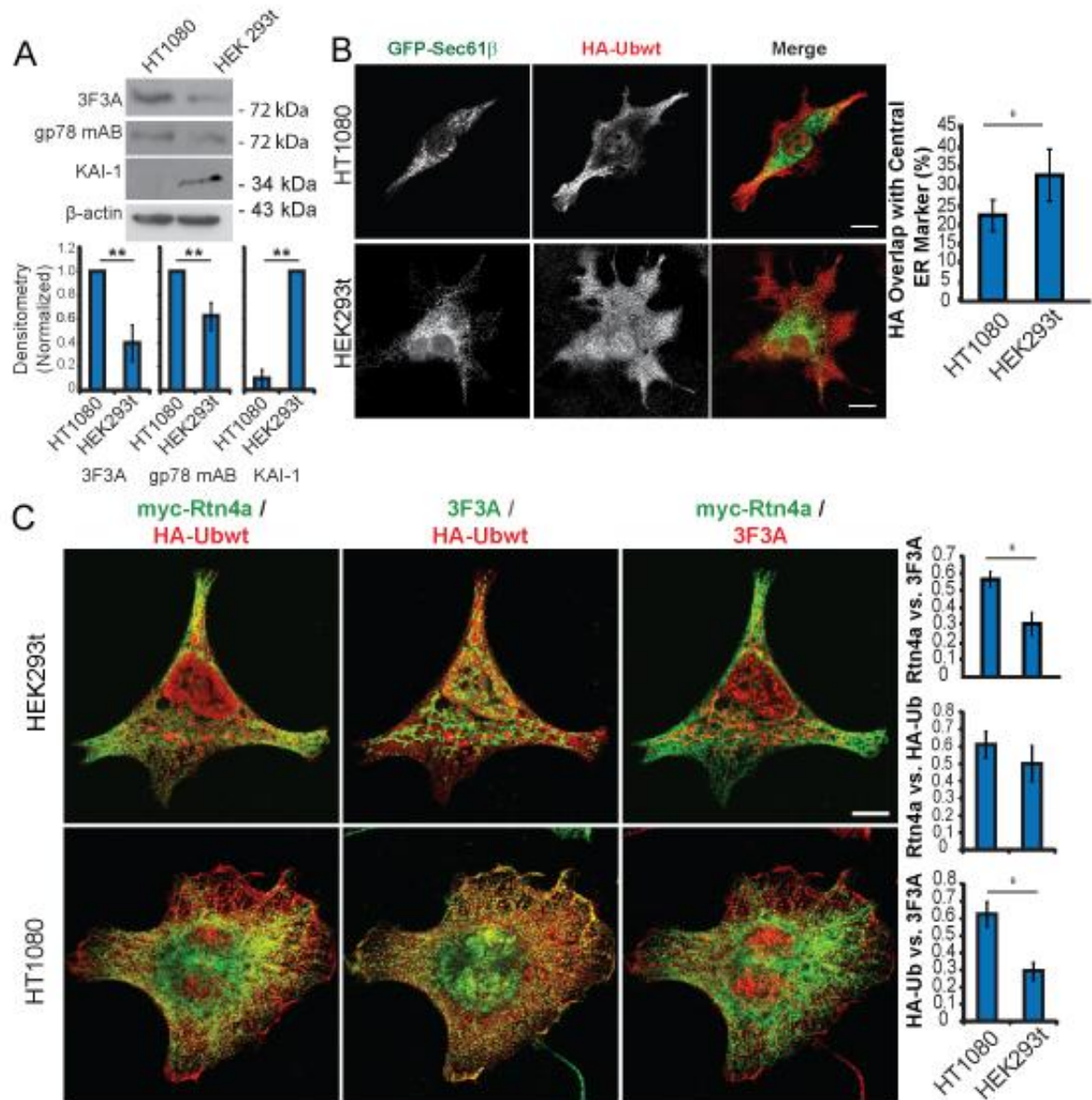
Figure 3.6 Elevated gp78-mediated ERAD in HT-1080 fibrosarcoma cells

(A) HT-1080 and HEK293t cell lysates were western blotted with 3F3A and mouse monoclonal anti-gp78 (gp78 mAb), KAI1 and β-actin and 3F3A and KAI1 band intensity quantified relative to β-actin. (B) HT-1080 and HEK293t cells were transiently transfected with GFP-Sec61β and HA-Ubwt and HA-Ub labeling overlap with the central ER marker GFP-Sec61β quantified (18 cells per condition, Bar: 10 μm). (C) HT-1080 and HEK293t cells were cotransfected with myc-Rtn4a and HA-Ubwt in and labeled for myc, HA and 3F3A. Representative images of peripheral cellular regions are presented and Pearson's colocalization coefficients determined (12 cells per condition, mean±SEM, *p< 0.05, **p<0.001, Bar: 10 μm).
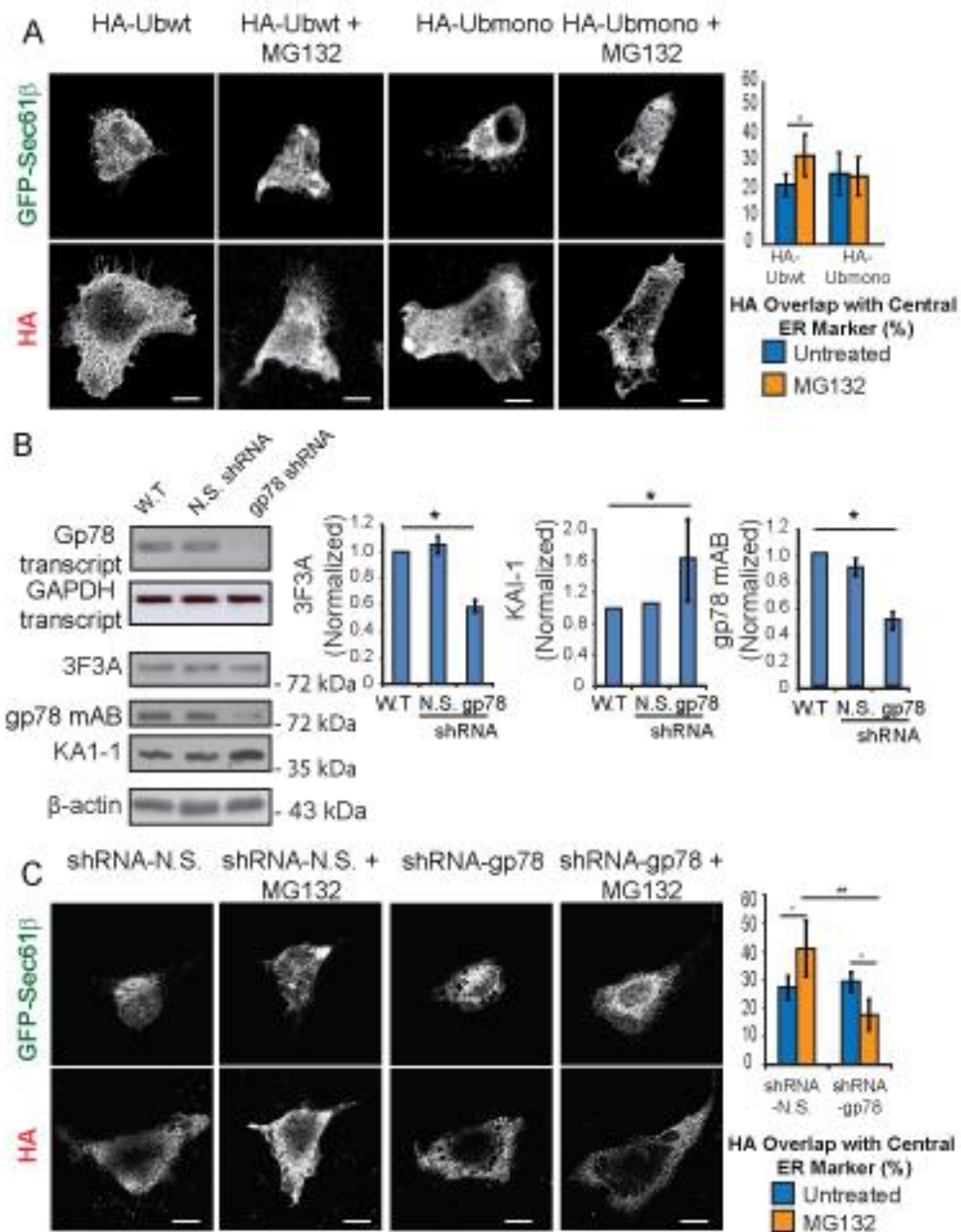
Figure 3.7 ERAD domain segregation is gp78-dependent in HT-1080 fibrosarcoma cells.

(A) HT-1080 cells cotransfected with GFP-Sec61β and either HA-Ubwt or HA-Ubmono were treated with or without MG132 for 8 hours and overlap of HA-Ub labeling with the central ER marker GFP-Sec61β quantified. (B) Stable gp78-shRNA expressing HT-1080 cells show reduced gp78 mRNA by RT-PCR and reduced 3F3A and mouse anti-gp78 mAb and increased KAI1 by immunoblot relative to wild-type or non-silencing (N.S.) shRNA

transfected cells. Densitometric quantification of 3F3A, gp78 mAb and KAI1 band intensity were determined relative to β-actin. n= 3gels(C) Gp78- or NS-shRNA expressing HT-1080 cells were transiently transfected with GFP-Sec61β and HA-Ubwt and treated with or without MG132 for 8 hours. HA-Ub labeling overlap with the central ER marker GFP-Sec61β was quantified. Bar: 10 μm. (24 cells per condition, mean±SEM, *p< 0.05, **p<0.001).

Table 3-1 Average mobile fraction of 4c-tagged gp78 construct in peripheral and central ER as determined by FRAP.

Gp78/AMFR const.	Cotransfection	n	Average mobile fraction %
FLAG-4c-gp78wt			
Peripheral ER	NC	5	22.1 ± 5.12
	+HA-Ubwt	3	23.6 ± 3.5
	+HA-Ubmono	5	43.6 ± 10.5[a]
Central ER	NC	3	19.4 ± 2.3
	+HA-Ubwt	3	18.5 ± 2.7
	+HA-Ubmono	3	24.6 ± 4.7
FLAG-4c-CUEmut			
Peripheral ER	NC	5	40.6 ± 9.3[a]
Central ER	NC	3	48.3 ± 14.2[b]
FLAG-4c-Δp97			
Peripheral ER	NC	3	19.5 ± 2.6
Central ER	NT	3	23.3 ± 6.5
FLAG-4c-RING			
Central ER	NC	3	10.1 ± 1.1[c]

Data are presented as average ± SEM.

NC = Not cotransfected with HA tagged ubiquitin constructs.
[a] $p < 0.001$ compared with FLAG-4c-gp78wt NC in the peripheral ER.
[b] $p < 0.0001$ compared with FLAG-4c-gp78wt NC in the central ER.
[c] $p < 0.0001$ compared with FLAG-4c-gp78wt NC in central ER.

2.7   Discussion

Taken together, these data show that gp78 ERAD activity occurs in the peripheral ER where CUE domain mediates interaction of gp78 with ubiquitylated substrate. Indeed, in mice deficient for TAP, required for assembly of the MHC complex, ubiquitin-associated heavy chain (HC) and β_2-microglobulin (β_2m) subunits accumulate in ER tubules morphologically similar to 3F3A-labeled smooth ER suggesting the presence of a subcompartment of the ER where misassembled proteins are recognized and ubiquitylated for degradation (Benlimame et al., 1995b; Raposo et al., 1995a). A role for ubiquitin chain elongation and Cue domain interaction in restricting ubiquitylated substrate to the peripheral ER suggest that gp78 ubiquitylation of and interaction with its substrates in this domain is a highly regulated process. It has been proposed that monoubiquitylation acts as an ER retention signal to allow folding of newly synthesized membrane proteins functioning as a quality control mechanism in ERAD (Feldman and van der Goot, 2009). Correct protein folding would result in deubiquitylation while protein misfolding would lead to polyubiquitin chain extension and degradation. Our demonstration that monoubiquitylated gp78 substrates are restricted to the peripheral ER support monoubiquitylation as an ER retention signal and identify the peripheral ER as the putative site of this ERAD quality control mechanism.

Prolonged proteasomal inhibition results in retention of unassembled subunits of the class I major histocompatibility complex in the juxtanuclear ERQC (Kamhi-Nesher et al., 2001b; Spiliotis et al., 2002a). Similarly, we observe the accumulation of ubiquitylated substrate in the central ER of gp78 expressing cells upon proteasome inhibition. The fact that ERAD substrate accumulation in the central ERQC is predominantly observed upon proteasome inhibition argues that central ER proteasomal targeting is a highly efficient process. Gp78-dependent recruitment of ubiquitylated substrate to the central ER requires polyubiquitylation and p97 recruitment. Consistently, juxtanuclear, ubiquitin-associated aggregates that accumulate after MG132 treatment were dispersed throughout the ER upon p97 silencing (Wojcik et al., 2004). Moreover, expression of a dominant negative mutant of p97 ATPase function was sufficient to induce accumulation of p97 itself, derlin-1 and polyubiquitylated

substrates in the ERQC, identifying this site as the potential retro-translocation site in the ER (Wakana et al., 2008).

A role for central ER translocation of polyubiquitylated substrate in proteasomal targeting is consistent with the previously reported interaction of gp78 not only with p97 (Ballar et al., 2007; Li et al., 2005; Zhong et al., 2004) but also with various components of the retrotranslocation machinery, including the derlins, Sec61 and JAMP1, that recruit proteasomes to the ER (Li et al., 2005; Tcherpakov et al., 2009; Ye et al., 2005a). Localization of CLIMP-63, a transmembrane protein involved in maintaining the architecture of ER sheets, is stabilized via interaction with ribosomes (Shibata et al., 2010). The basis for differential protein localization in the ER may be due to complex domain-specific interactions. For instance, while CUE domain mutation enhances gp78 mobility in both the central and peripheral ER, expression of HA-Ubmono selectively enhances gp78 mobility in the peripheral but not the central ER. We are therefore only beginning to understand the mechanisms that regulate the mobility and distribution of gp78.

The inefficient removal of ubiquitylated substrate from the central ER in Flag-Cue mutant transfected cells suggests that Cue-dependent retention and processing of substrate in the peripheral ER may impact on efficient proteasome delivery of gp78 ERAD substrates. CUE domains exhibit preferential binding to monoubiquitin and structural studies show that the contact surface of the CUE domain with monoubiquitin encompasses K48, potentially inhibiting polyubiquitin chain elongation (Kang et al., 2003; Shih et al., 2003a). In contrast, polyubiquitin is a p97 recognition signal and p97 restricts polyubiquitin chain length to that required for efficient proteasomal targeting and degradation (Flierman et al., 2003; Richly et al., 2005; Ye et al., 2003). It is tempting to speculate that the differential specificity of CUE domain for monoubiquitin and p97 for polyubiquitin may underlie their opposing roles as regulators of the peripheral-central distribution of ubiquitylated substrates. By retaining substrates carrying mono- or short ubiquitin chains in the peripheral ER, Cue domain interactions might ensure that only proteins with extended polyubiquitin chains are delivered to the central ER for proteasomal delivery. Such a mechanism would enhance the efficiency

of proteasomal delivery and explain the accumulation of ubiquitylated substrate in the central ER upon mutation of the gp78 CUE domain.

Gp78 knockdown in HT-1080 cells increases KAI1 levels and while ubiquitylated substrate is still distributed to the peripheral ER, it no longer redistributes to the central ER upon proteasome inhibition. This supports the peripheral ER as the site of gp78-mediated ERAD and suggests that central ER accumulation of ubiquitylated substrate may be related to gp78 expression levels and overall ERAD activity. Gp78 overexpression upon transfection results in the clear separation of peripheral, smooth and central, rough ER. However, previous EM studies have shown that gp78-positive smooth ER structures are interspersed with and connected to ribosome studded rough ER (Benlimame et al., 1998b; Benlimame et al., 1995b; Wang et al., 1997a). Domain segregation of gp78 ubiquitylation and proteasomal targeting may therefore occur on a much more intimate scale within ER tubules and cisternae. Indeed, synthetic and degradatory machineries can function in parallel within the same ER structures, a process named cotranslational degradation, allowing for tight regulation of protein synthesis (Fisher and Ginsberg, 2002; Oyadomari et al., 2006). By regulating delivery of ubiquitylated substrate to the central ER, spatial segregation of ERAD functions may limit access by unwanted ER proteins to common ER translocation machinery and thereby ensure efficient production of essential, newly synthesized proteins. Sequestration of gp78 ubiquitin ligase activity to an expanded peripheral ER may occur selectively in response to enhanced ERAD activity. Finally, multiple E3 ligases contribute to ERAD (Vembar and Brodsky, 2008) and how differential, and potentially competitive, interactions between ligases, substrates, and ubiquitin supply impact on gp78 function in ERAD remains to be determined.

2.8 Materials and methods

2.8.1 Antibodies

Anti-FLAG, anti-β-actin, anti-Derlin-1 and anti-Derlin-2 antibodies were purchased from Sigma, anti-p97 from Abcam and anti-HA from Neomarker. The 3F3A monoclonal antibody was as described (Nabi et al., 1990b) and mouse monoclonal anti-gp78 antibody purchased from Abcam. The anti-KAI1 antibody was purchased from Santa-Cruz Biotechnology. All fluorescent secondary antibodies were purchased from Invitrogen and HRP conjugated secondary antibodies from Jackson Immunoresearch.

2.8.2 Plasmids and constructs

HA-Ubwt and HA-Ubmono expression plasmids were obtained from Tony Morielli (University of Vermont) and Myc-Rtn4a and GFP-Sec61β from Gia Voeltz (University of Colorado). FLAG-gp78wt was inserted into pcDNA3.1 (+) as described (Registre et al., 2004). FLAG-CUEmut (M467F, F468S, P469S) and FLAG-RINGmut (C356S) were generated by point mutation using the Quickchange mutagenesis kit (Stratagene). FLAG-Δp97 was generated by deletion of the 49 amino-acid C-terminal region and re-cloned in pcDNA 3.1 (+). For live cell visualization, a tetracysteine tag (4c) was added in frame (FLNCCPGCCMEP) by PCR extension to the N-terminal extremity and in a second step, a FLAG tag was added N-terminal of the 4c tag to prevent palmitoylation of the 4c tag (Martin et al., 2005a).

2.8.3 Cell culture and transfection

Cos-7and HEK293t, cells were maintained in DMEM containing 10% fetal bovine serum (FBS, Medicorp), and supplemented with 0.2 mM L-Glutamine, 10 μg/ml Penicillin, 10 μg/ml Streptomycin, vitamins and non-essential amino acids. HT-1080 cells were maintained in RPMI containing the same supplements (all supplements and media from Invitrogen).

Cells were transfected using Effectene (Qiagen). Where indicated, cells were treated with MG132 (Sigma) for 8 hours at a concentration of 30 μM.

2.8.4   Fluorescence recovery after photobleaching (FRAP)

Cos-7 cells were transfected 24 hrs after plating in chamber slides (Ibidi) and stained with FlAsH dye (Invitrogen) according to the manufacturer's instructions. Briefly, cells were rinsed twice with Opti-MEM media (Invitrogen) and incubated for 30 minutes with FlAsH diluted in Opti-MEM media (1/800) and then rinsed twice with Opti-MEM + 1X BAL buffer (0.25 mM 2,3-Dimercapto-1-propanol, Invitrogen). FRAP measurements were conducted immediately after staining at 37oC with a Fluoview 1000 laser scanning confocal microscope (Olympus). After the first frame was taken, a small region in the central or peripheral ER was bleached with the 405 nm laser of a SIM scanner (Olympus).

2.8.5   Immunofluorescence labeling

Cells grown on glass cover slips were fixed 24 hours post-transfection with pre-cooled (-80°C) methanol:acetone (80:20) for 15 minutes at -20°C, a fixation procedure that liberates free cytosolic proteins, such as GFP and ubiquitin, and then washed with PBS supplemented with 1 mM $CaCl_2$ and 10 mM $MgCl_2$ (PBS-CM). Cells were blocked with PBS-CM containing 1% BSA blocking solution for 15 minutes. The cells were then incubated with primary antibodies for 30 minutes, rinsed three times with blocking solution, and then further incubated with the appropriate secondary antibody for an additional 30 minutes. The cells were rinsed three times for 10 minutes with blocking solution. Cover slips were mounted and imaged with the 100x Planapochromatic objective of a Fluoview 1000 confocal laser scanning microscope (Olympus). Quantification of the percentage of ubiquitylated substrates localized to the central ER was obtained by measure the HA-Ub labeling intensity colocalizing with a mask of GFP-Sec61β (threshold 5000-65535) over the total ubiquitin intensity signal. All fluorescence quantification experiments, including Pearson's coefficient's, were determined from three independent experiments.

2.8.6   shRNA Silencing of gp78

shRNA-gp78 plasmids were purchased from Molecular Biosystem and transfected with a third generation viral encapsidation in HEK239t following the manufacturer guideline. The viruses were harvested and used to infect HT-1080 cells. Infected cells were selected with 2μgml puromycin and FACS sorted after 2 weeks in selection media. We used semi-quantitative RT-PCR to assess gp78 knock-down at the transcript level, as previously described (Joshi et al., 2010). Briefly, total RNA was extracted by the TRIzol method, total cDNAs generated using SuperScript III reverse transcriptase (Invitrogen) and transcript levels determined from total cDNAs by PCR using primer sets for gp78 (5'-cca tgc cgc tgc tct tcc tc-3'; 5'-gct gag gcc cgt gta ggt gcg-3') and GAPDH (5'-ggt cgg agt caa cgg att tgg tcg-3';5'-cct ccg acg cct gct tca cca c-3') (25 cycles each).

2.8.7   Western blot and immunoprecipitation

For western blot analysis, cells were manually collected in cold PBS, pelleted and re-suspended in lysis buffer (25 mM Tris-HCl pH 8.0, 20 mM N-ethylmaleimide, 2 mM EDTA, 0.5 mM PMSF, 140 mM NaCl, 1% TX-100 and protease inhibitor cocktail (Roche)). Lysates were clarified at 15,000 rpm and supernatant and insoluble fractions run on 8% SDS-PAGE gels and transferred onto PVDF membranes (Millipore) using a semi-dry system (0.8 mA/cm^2). Membranes were blocked overnight in 5% milk and then probed with the indicated antibodies. For anti-FLAG and anti-HA immunoprecipitation, cells were rinsed and harvested in PBS and cell pellets resuspended in lysis buffer (25 mM Tris, ph 8.0, 20 mM N-ethylmaleimide, 2 mM EDTA, 1% Triton X-100, 0.5 mM PMSF and protease inhibitor tablet (Roche)), passed through a 25G syringe 5 times and incubated 30 min on ice. Supernatants were incubated with anti-FLAG or anti-HA coupled agar beads (Sigma) pre-blocked with 1% BSA, then washed once with lysis buffer, three times with rinsing buffer A (Tris-HCl pH 8.0, 150 mM NaCl, 5 mM EDTA, 0.5% TX-100, 0.1% SDS and 0.2% BSA), three times with rinsing buffer B (500 mM Nacl, 20 mM Tris-HCl pH8.0, 0.5% TX-100 and 0.2% BSA) and once with 50 mM Tris-HCl pH 8.0. Proteins were eluted from beads by boiling in sample buffer prior to analysis by western blot.

Chapter 4: Ubiquitin ligase regulation of endoplasmic reticulum-mitochondria interaction

3.1   Introduction

Close contacts between endoplasmic reticulum (ER) and mitochondria enables transfer between these organelles of lipids, promoting phospholipid and glycosphingolipid biosynthesis, and of calcium, regulating calcium homeostasis, mitochondrial enzyme activity and apoptosis. ER-mitochondria interactions are regulated by multiple mechanisms. The mitochondrial fusion protein mitofusin2 is enriched at contact sites and directly tethers ER and mitochondria (de Brito and Scorrano, 2008). Depletion of PACS-2 results in mitochondrial fragmentation and uncoupling from the ER (Simmen et al., 2005). IP$_3$R interacts with the voltage-dependent anion-selective channel (VDAC) to form an ER-mitochondria Ca^{2+} tunnel (Rapizzi et al., 2002; Szabadkai et al., 2006). In yeast, ubiquitination and the yeast MET30 component of the SCF ubiquitin ligase complex have been shown to regulate phosphatidyl transport from the ER to mitochondria (Schumacher et al., 2002). However, a role for ER-associated degradation (ERAD)-associated proteins in ER-mitochondria interaction has yet to be reported. Here, we describe a novel mechanism linking extracellular regulation of an ER localized ubiquitin ligase to ER-mitochondria interaction.

Autocrine motility factor (AMF), a secreted cytokine equivalent to the glycolytic enzyme phosphoglucose isomerase (PGI), promotes cancer cell motility and metastasis via its 78 kDa receptor, gp78/AMFR. Gp78/AMFR is also a key E3 ubiquitin ligase in the ERAD machinery (Fairbank et al., 2009) and electron microscopy studies have localized gp78/AMFR to both the plasma membrane and mitochondria-associated smooth ER (SER) tubules (Goetz and Nabi, 2006b; Wang et al., 2000). Here we show that extracellular AMF

regulates ER-mitochondria coupling via gp78/AMFR ubiquitin ligase activity and polyubiquitylation.

3.2   Results

3.2.1   AMF regulates ER-mitochondria calcium coupling

By immunoelectron and confocal microscopy, the 3F3A anti-gp78/AMFR mAb is a specific marker of a mitochondria-associated SER domain (Goetz and Nabi, 2006b). As previously reported (Goetz et al., 2007b; Wang et al., 2000), 3F3A-labeled SER colocalizes extensively with OxphosV-labeled mitochondria in 2D confocal images. 3D blind deconvolution of confocal stacks and 3D reconstruction show that the 3F3A and OxphosV labels do not overlap (Figure 4.1A,). AMF treatment disperses 3F3A labeling reducing overlap with mitochondria in 2D confocal sections and apposition between the 3F3A-labeled SER and mitochondria in deconvolved, 3D reconstructed images (Figure 4.1A). By electron microscopy (Figure 4.1B), AMF treatment significantly increased the shortest distance from individual ER tubules to the nearest mitochondria and the number of ER tubules within 50 nm of a mitochondrion decreased from almost half to less than 10% (Figure 4.1B).

To specifically study ER-mitochondrial Ca^{2+} coupling, cells were loaded with both Fura-2 AM and Rhod-2 AM and ATP-induced increase of cytosolic ($[Ca^{2+}]_{cyt}$) and mitochondrial ($[Ca^{2+}]_m$) calcium measured simultaneously in the same cell (Figure 4.1C). In the vast majority of untreated cells, ATP stimulation induced a steep rise in $[Ca^{2+}]_{cyt}$ closely followed by a fast rise in $[Ca^{2+}]_m$ synchronized to the rising phase of the $[Ca^{2+}]_{cyt}$ signal, indicative of the rapid and efficient delivery of Ca^{2+} from ER to mitochondria. In AMF pretreated cells, there was a considerable delay of $[Ca^{2+}]_m$ but not of $[Ca^{2+}]_{cyt}$ after ATP stimulation. Calculation of coupling times (peak $[Ca^{2+}]_m$ minus peak $[Ca^{2+}]_{cyt}$) showed that AMF delayed propagation of the ATP-evoked $[Ca^{2+}]_{cyt}$ rise to mitochondria (Figure 4.1C). These data confirm that AMF induces functional dissociation of ER from mitochondria.

The dissociation of SER and mitochondria is regulated by $[Ca^{2+}]_{cyt}$ (Goetz et al., 2007b; Wang et al., 2000). Increasing $[Ca^{2+}]_{cyt}$ with either ATP, the sarco/endoplasmic reticulum Ca^{2+}-ATPase (SERCA) inhibitor thapsigargin (TG) or ionomycin plus 1 mM extracellular Ca^{2+} ($[Ca^{2+}]_{ext}$) or depleting $[Ca^{2+}]_{cyt}$ with EGTA or BAPTAs (Goetz et al., 2007b) did not impact on AMF-induced SER-mitochondria dissociation (Figure 4.2A and B). In particular, while dimethyl BAPTA and BAPTA could reverse SER-mitochondria dissociation induced by ionomycin plus 1 mM $[Ca^{2+}]_{ext}$, they did not affect SER-mitochondria dissociation induced by AMF (Figure 4.2C and D). AMF therefore regulates SER-mitochondria interaction independently of $[Ca^{2+}]_{cyt}$.

3.2.2 AMF regulates ER-mitochondria coupling via gp78/AMFR ubiquitin ligase activity

To determine whether AMF treatment affects gp78/AMFR ubiquitin ligase activity, Cos-7 cells were co-transfected with Flag-tagged gp78 wild-type (Flag-gp78wt) and HA-tagged ubiquitin (HA-Ub). A smear of HA-Ub tagged proteins in gp78/AMFR transfected cells was significantly elevated relative to control cells (Figure 4.3A). A polyubiquitylated protein smear was not detected in cells transfected with a Flag-gp78 Ring Finger mutant deficient in ubiquitin ligase activity (Flag-RINGmut) or in cells co-transfected with Flag-gp78wt and a HA-Ub mutant lacking three lysines critical for Ub conjugation that cannot form polyubiquitin chains (HA-UbMono). Interestingly, AMF significantly decreased accumulation of polyubiquitylated substrate upon overexpression of gp78 (Figure 4.3A).

Insertion of a tetracysteine motif (4c) after the Flag tag allowed fluorescent detection of gp78/AMFR transfected cells with the FlAsH reagent (Adams et al., 2002). In cells loaded with both Fura-2 AM and Rhod-2 AM, propagation of the ATP-evoked $[Ca^{2+}]_{cyt}$ rise to mitochondria (lag time of $[Ca^{2+}]_m$) in Flag-4c-gp78wt transfected cells was delayed relative to untransfected cells and further reduced upon AMF treatment (Figure 4.3B). In Flag-4c-RINGmut transfected cells, the lag time of $[Ca^{2+}]_m$ and ER-mitochondria coupling times were significantly prolonged and no longer impacted by AMF treatment. Similarly, co-transfection with Flag-4c-gp78wt and HA-Ubmono resulted in longer ER-mitochondria

coupling times insensitive to AMF treatment (Figure 4.3B). Gp78 ubiquitin ligase activity and associated polyubiquitylation therefore promote ER-mitochondria coupling.

3.2.3 Gp78/AMFR-mediated ER-mitochondria association reduces mitochondrial mobility and dynamics

In FLAG-gp78wt transfected cells, the 3F3A label extends beyond mitochondria-associated ER domains to a peripheral, tubular ER network (Goetz et al., 2007b) resulting in reduced colocalization of the 3F3A-labeled ER with OxphosV labeled mitochondria (M2) in 3D stacks (Figure 4.4). As in untransfected cells, AMF treatment significantly decreased 3F3A-OxPhosV colocalization in FLAG-gp78wt transfected cells. Upon expression of Flag-RINGmut, 3F3A labeling shows minimal association with mitochondria that is not affected by AMF treatment (Figure 4.4). Reduced ER colocalization with mitochondria parallels the reduced calcium coupling observed in Flag-gp78wt and Flag-RINGmut transfected cells (Figure 4.2B). However, mitochondria colocalization with the 3F3A-labeled ER (M1) was increased in FLAG-gp78wt but not Flag-RINGmut transfected cells and this was prevented by AMF treatment (Figure 4.4). This suggests that gp78 overexpression and expansion of the 3F3A-labeled ER reduces the proportion of ER in contact with mitochondria but enhances the extent of mitochondrial interaction with ER.

In 4D movies of pOCT-DsRed labeled mitochondria, gp78 overexpression significantly reduced mitochondrial size, length and mobility (Figure 4.5). Ring finger mutation or AMF treatment prevented gp78/AMFR impact on mitochondrial morphology and mobility (Figure 4.6). While elevated $[Ca^{2+}]_{cyt}$ limits mitochondrial movement (Yi et al., 2004), gp78 transfection does not affect basal $[Ca^{2+}]_{cyt}$ (Figure 4.3) suggesting that other mechanisms mediate reduced mitochondrial motility upon gp78 overexpression.

FRAP analysis showed that FLAG-gp78wt reduced and Flag-RINGmut increased the mobile fraction of pOct-dsRed, an indict of mitochondrial fusion (Figure 4.6). AMF treatment or cotransfection with HA-Ubmono increased the pOct-dsRed mobile fraction to levels observed in Flag-RINGmut transfected cells. These data define a role for regulation of ER-

mitochondria interaction by AMF-gp78 and polyubiquitylation in the regulation of mitochondrial mobility and fusion. Similarly, mitofusin, a mitochondrial fusion protein, regulates ER-mitochondria contact (de Brito and Scorrano, 2008) suggesting the existence of a close relationship between ER-mitochondria interaction and mitchondrial fusion and dynamics.
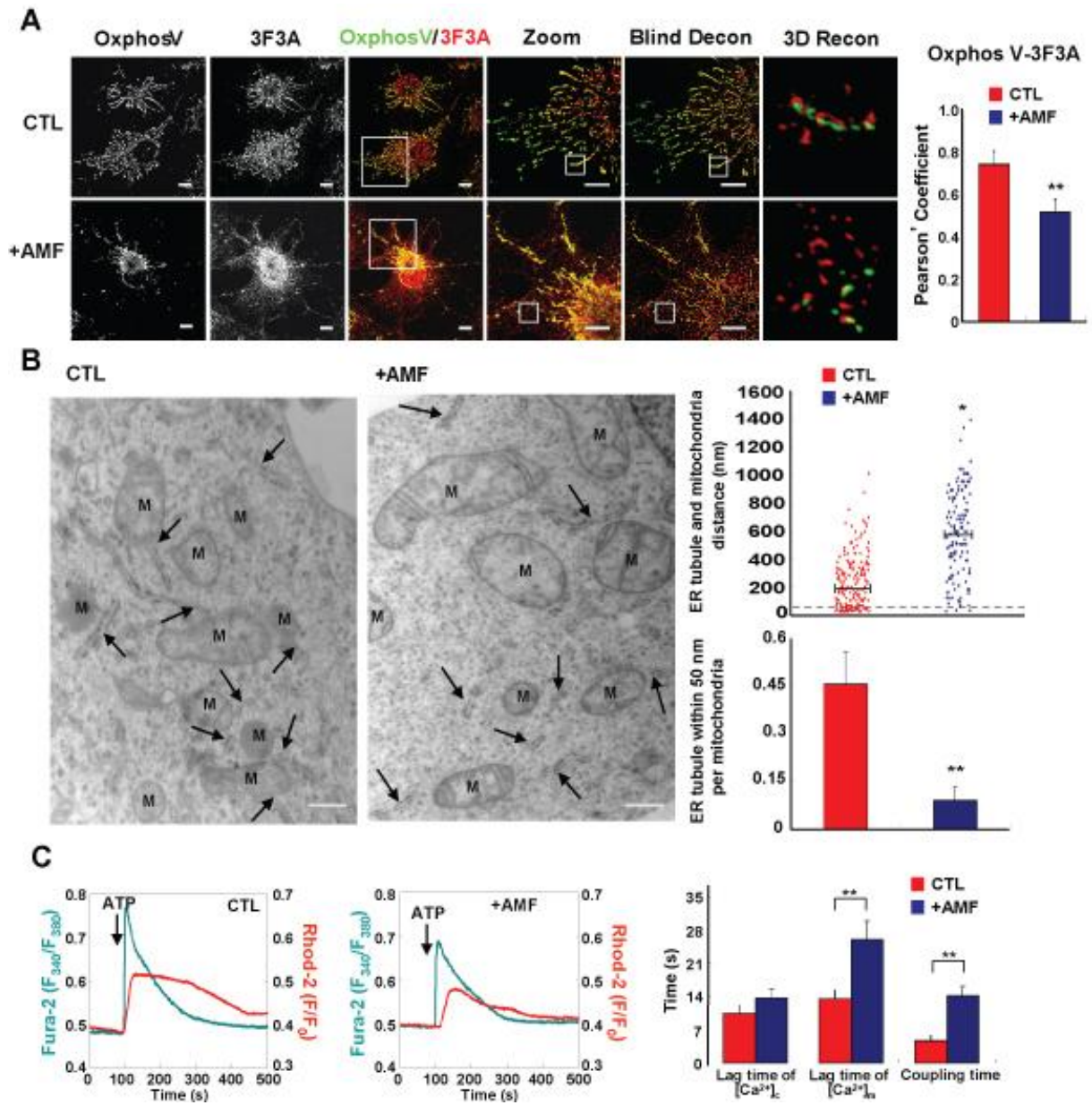
Figure 4.1 AMF disrupts ER-mitochondria interaction

(A) Cos-7 cells untreated (CTL) or treated with 24 μg/ml AMF (+AMF) for 8 hours were immunofluorescently labeled with 3F3A anti-gp78/AMFR (red) and mitochondrial OxphosV (green) mAbs. Boxed regions were deconvolved (Blind Decon) and 3D reconstructed (3D Recon). Pearson's coefficients of 3F3A/OxPhosV colocalization were quantified from untreated and AMF treated cells (left) (Mean±SEM; **$p<0.01$; Bar: 5 μm; Zoom: 3.2 μm). (B) Electron microscopy of untreated and AMF treated Cos-7 cells. Arrows indicate ER tubules and graphs show the minimal distance of individual ER tubules from nearest mitochondria and percentage of ER tubules within 50 nm of a mitochondrion (Mean; *$p<0.05$; Bar: 0.5 μm). (C) Simultaneous recording of ATP-evoked $[Ca^{2+}]_{cyt}$ (Fura-2 AM; blue) and $[Ca^{2+}]_m$ (Rhod-2 AM; red) in Cos-7 cells with (right) or without (left) AMF

treatment. Bar graph shows lag times of $[Ca^{2+}]_{cyt}$ or $[Ca^{2+}]_m$ after ATP stimulation and ER-mitochondria coupling times (Mean±SEM; n=60-90, *p<0.05, **p<0.01).
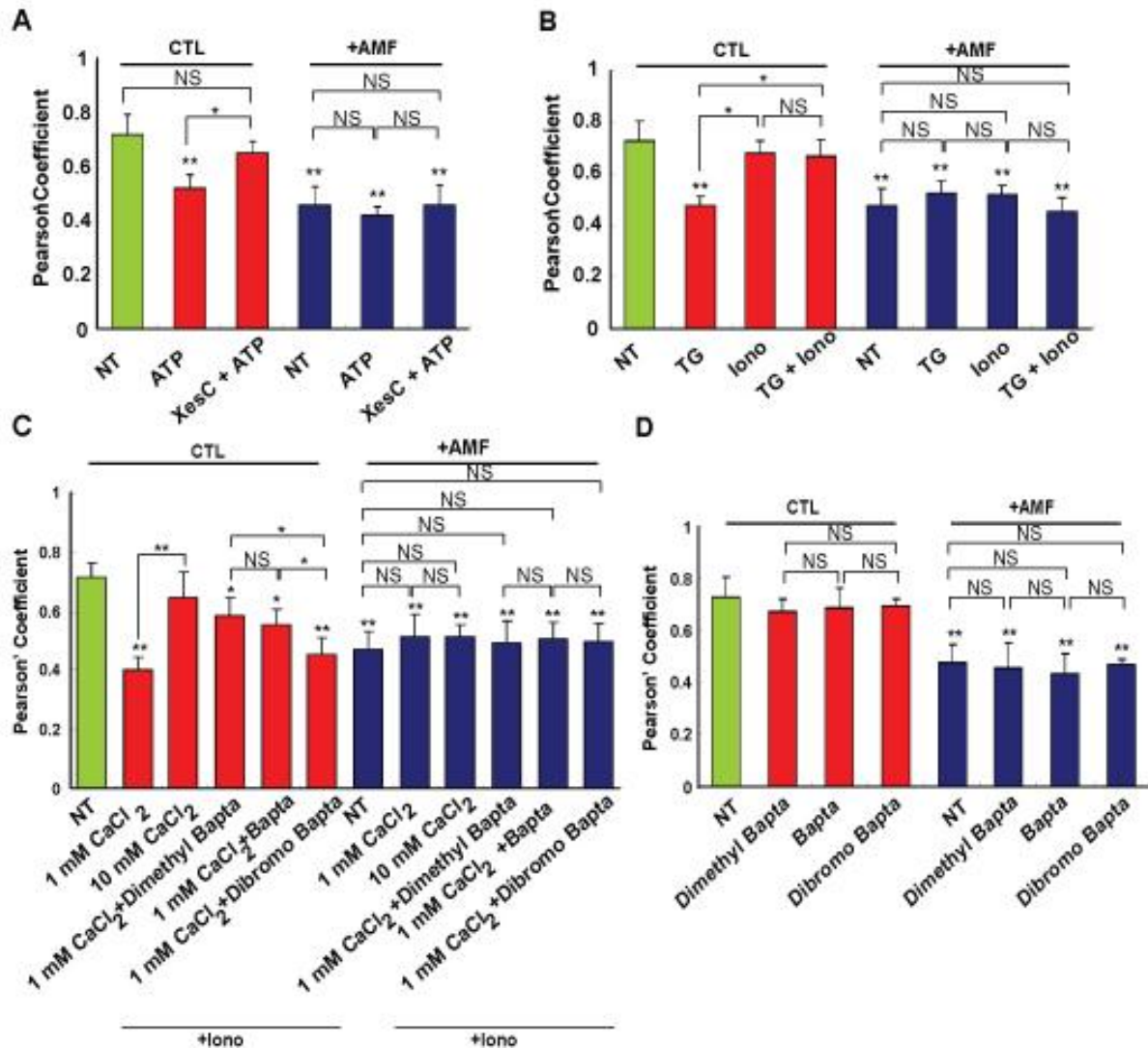
Figure 4.2 AMF-induced ER-mitochondria dissociation is calcium-independent

For all panels, Cos-7 cells treated with or without AMF were incubated with the indicated compounds, fixed and labeled with 3F3A and OxphosV mAbs and ER-mitochondria colocalization quantified. (A) Cos-7 cells were treated with 10 μM ATP for 2 min in the presence or absence of the IP$_3$R inhibitor xestospongin C. (B) Cos-7 cells were treated with 10 μM TG and/or 10 μM ionomycin for 60 min (C) Cos-7 cells were treated with ionomycin plus either 1 mM CaCl$_2$ or 10 mM CaCl$_2$ in the presence of 20 μM dimethyl BAPTA (Kd=40 nM), BAPTA (Kd=160 nM) or dibromo BAPTA (Kd=1.6 μM) for 30 min. Bar graphs present Pearson's coloclaization coefficients for the indicated conditions (Mean±SEM from 60-90 cells; *p<0.05, **p<0.01 relative to untreated cells; NS: no significance, NT: unstimulated cells; XesC: xestospongin C, iono: ionomycin; Green: untreated, Red: treated with indicated compounds, Blue: treated with AMF and indicated compounds).
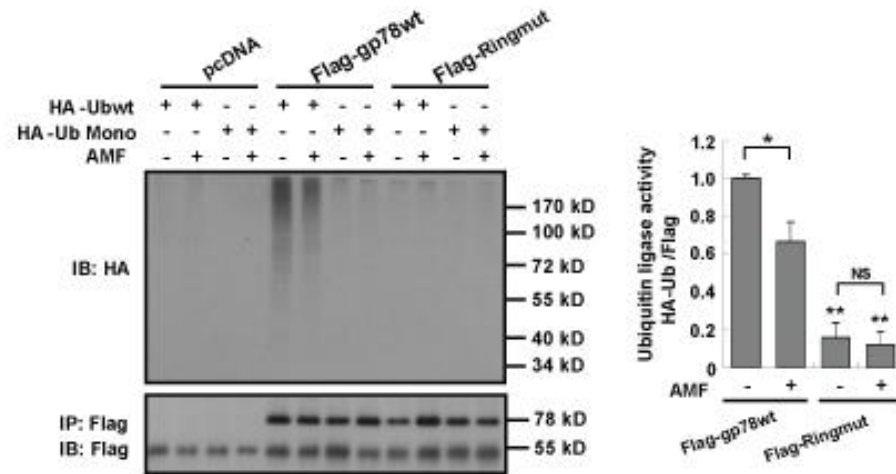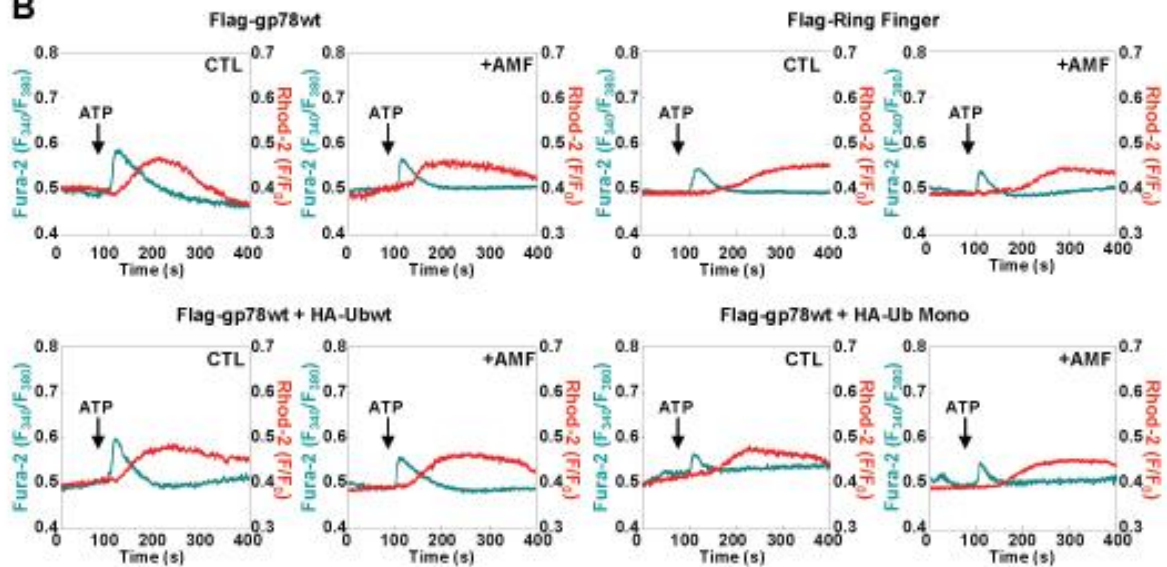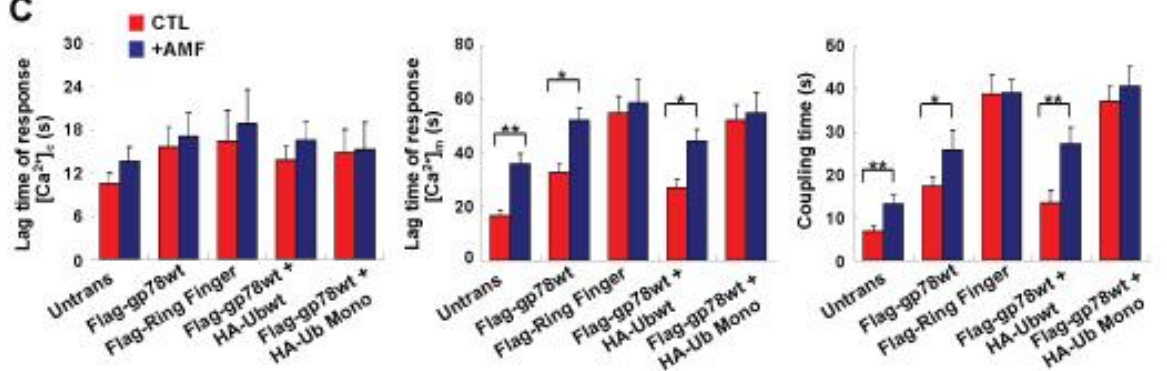
Figure 4.3 Gp78 ubiquitin ligase activity regulates ER-mitochondria calcium coupling

(A) Cos-7 cells were co-transfected with pcDNA, FLAG-gp78wt or Flag-RINGmut and either HA-Ub or HA-UbMono and treated or not with AMF. HA-Ub tagged proteins were

detected by western blot and FLAG-gp78wt and Flag-RINGmut expression determined by immunoprecipitation. HA-Ub smears were quantified by densitometry relative to anti-Flag immunoprecipitates (n=3, ±SEM; *p<0.05, **p<0.01). B) Cos-7 cells were transfected with Flag-4c-gp78/AMFR or Flag-4c-RINGmut or co-transfected with Flag-4c-gp78/AMFR and HA-Ub or HA-UbMono, as indicated. Simultaneous recording of ATP-evoked $[Ca^{2+}]_{cyt}$ (Fura-2 AM; blue) and $[Ca^{2+}]_m$ (Rhod-2 AM; red) were recorded simultaneously with (right) or without (left) AMF treatment. Bar graphs show lag time of ATP-induced $[Ca^{2+}]_{cyt}$ (left) and $[Ca^{2+}]_m$ (middle) as well as ER-mitochondria coupling time (right) with (blue) or without (red) AMF treatment (Mean±SEM; 20-30 transfected cells, *p<0.05, **p<0.01 relative to untreated cells).
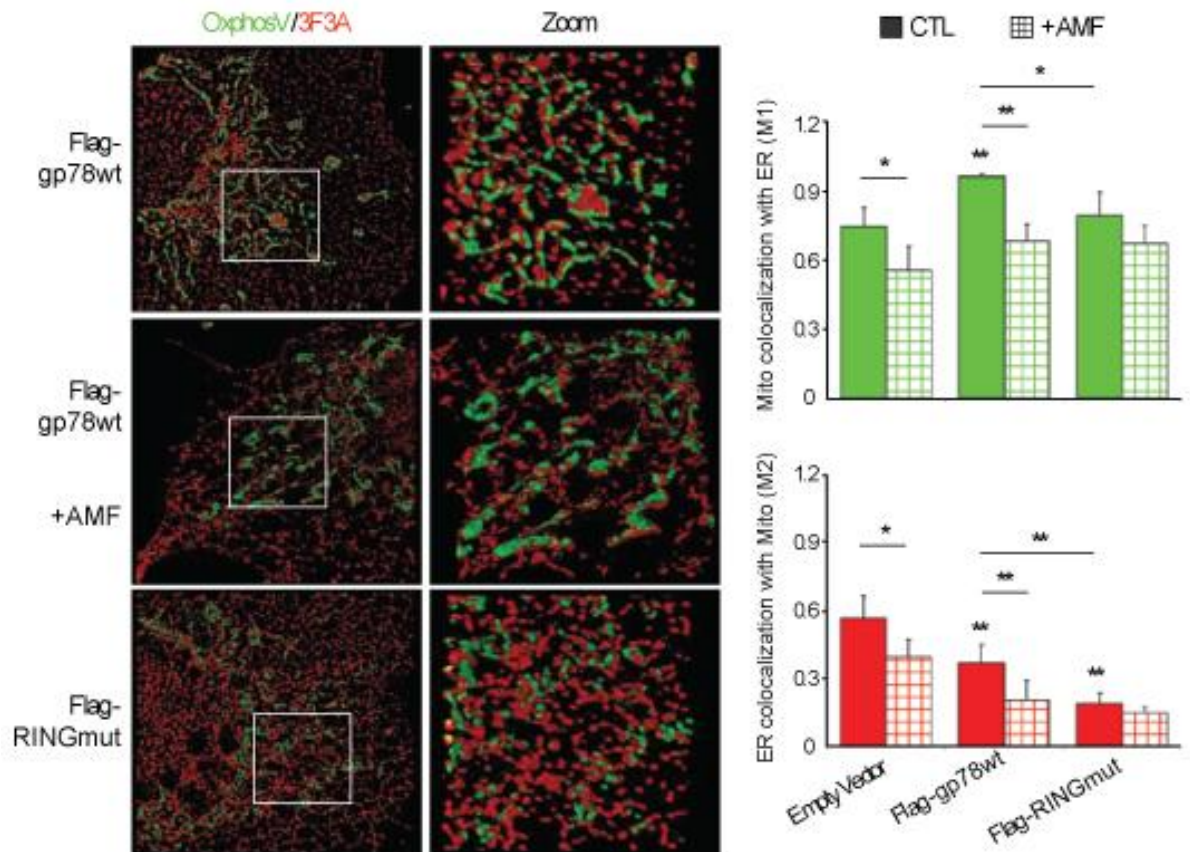
Figure 4.4 Gp78 promotion of ER association with mitochondria is AMF-dependent

3D reconstructions of deconvolved confocal stacks of untreated or AMF treated Cos-7 cells transfected with FLAG-gp78wt or Flag-RINGmut constructs and labeled for 3F3A and OxphosV. Bar graphs show colocalization of OxphosV labeled mitochondria with 3F3A-labeled ER (M1; green) and of 3F3A-labeled ER with mitochondria (M2; red) in deconvolved 3D confocal stacks. Colocalization coefficients are shown with (hatched bars) or without (solid bars) AMF treatment (Mean±SEM; n=10, *p<0.05, **p<0.01; Bar: 10 μm;).
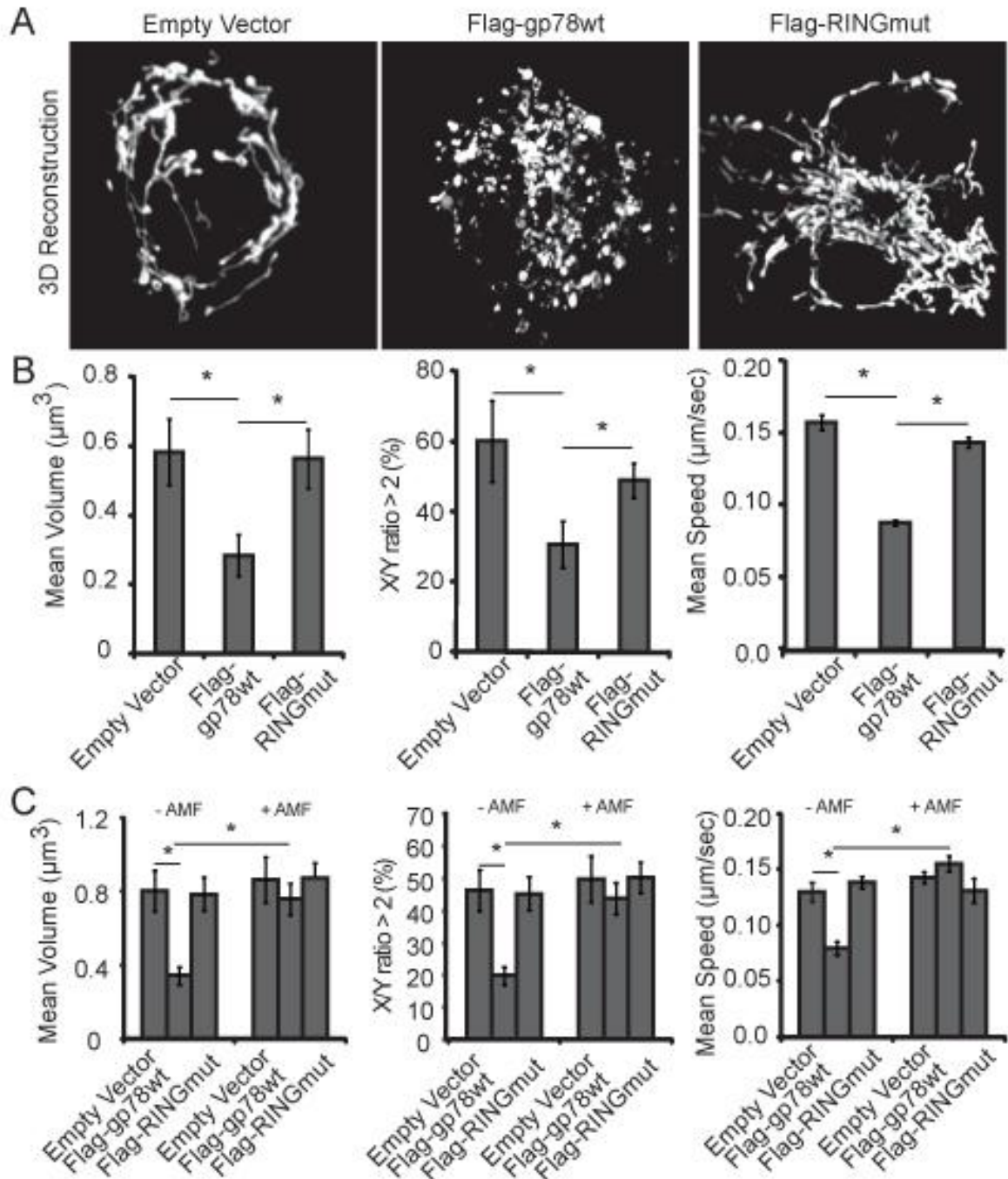
Figure 4.5 Gp78 regulation of mitochondrial volume, shape and mobility

(A) 3D projection of Cos-7 cells cotransfected with pOCT-DsRed and empty vector, Flag-gpo78/AMFR or Flag-RINGmut. (B) Bar graphs show the quantification of the 4D movies. Volume (micron^3) and X/Y axis ratio (% with X/Y axis ratio > 2) of mitochondria were quantified from individual 3D projections and speed (μm/sec) of individual mitochondria (tracked for at least 5 time points/25 sec). (C) Quantification of mitochondrial volume, X/Y axis and mobility from cells treated with and without AMF in serum-free media (Mean±SEM, n=15-20 cells (3 expts); *p< 0.01, **p<0.0001).
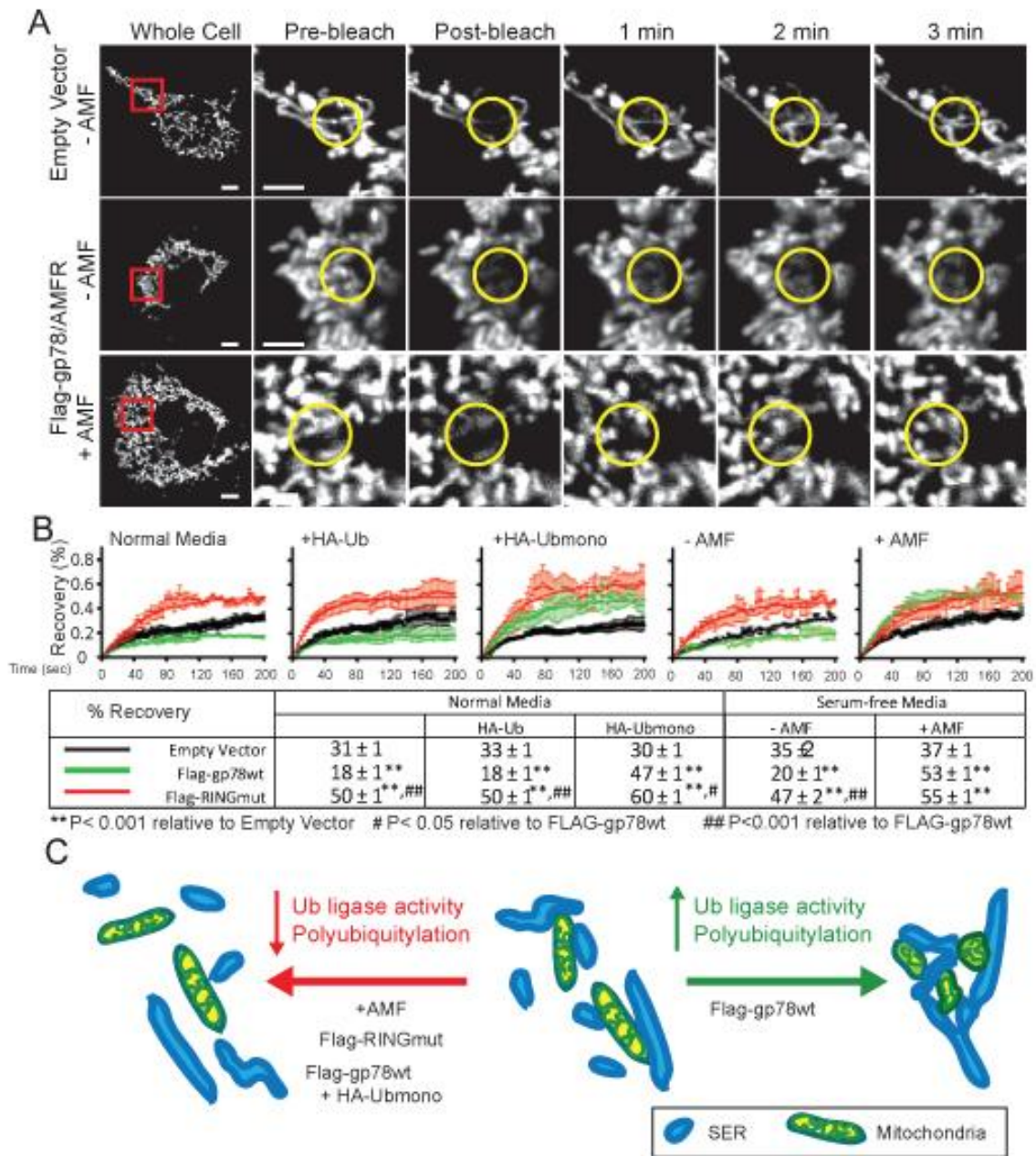
Figure 4.6 Gp78 regulation of mitochondria fusion

(A) FRAP on Cos-7 cells were cotransfected with pOCT-DsRed and FLAG-gp78wt or Flag-RING,mut and pOCT-DsRed mitochondria photobleached and recovery followed over 3 minutes. Insets (red squares) show a magnification of the bleach area (yellow circles). (B) Recovery of pOCT-DsRed fluorescence in bleached region in Cos-7 cells in normal media or serum-free media +/-AMF or cotransfected with HA-Ubwt or HA-Ubmono as indicated (% recovery ± SEM). (C) Our data suggests that increased gp78/AMFR ubiquitin ligase activity and polyubiquitylation upon FLAG-gp78wt overexpression induces ER-mitochondria interaction and mitochondrial rounding and fragmentation and that AMF disrupts ER-

mitochondria association, possibly through regulation of gp78/AMFR ubiquitin ligase activity.

3.3   Discussion

3.3.1   Novel mechanism of ER-mitochondria interaction

Regulation of ER-mitochondria association via the ubiquitin ligase activity of gp78/AMFR and polyubiquitylation defines a novel mechanism of association between these two organelles and supports the previously described role of ubiquitylation in ER-mitochondria interaction in yeast (Schumacher et al., 2002). Regulation by AMF defines a novel role for an extracellular cytokine in ER-mitochondria association and Ca^{2+} coupling. TGF-β treatment reduces the rate, but not the amplitude, of the $[Ca^{2+}]_{cyt}$ response and depresses $[Ca^{2+}]_m$ uptake due to downregulation of IP_3R, not ER-mitochondria uncoupling (Pacher et al., 2008). Gp78/AMFR associates with polyubiquitinated IP_3Rs (Pearce et al., 2007), however Cos-7 cells express low levels of IP_3R1 (Szado et al. 2008) and AMF regulation of the ER-mitochondria Ca^{2+} coupling is not associated with downregulation of IP_3R3 expression (not shown).

AMF and HA-Ubmono induce mitochondrial fusion selectively in gp78 overexpressing but not vector control cells. Furthermore, AMF and HA-Ubmono treatment of FLAG-gp78wt transfected cells and expression of Flag-RINGmut promote mitochondrial fusion above that seen in vector control cells. The fact that AMF regulates ER-mitochondria association, but not mitochondrial dynamics, independently of gp78 overexpression suggests that AMF-gp78 is one of many mechanisms regulating ER-mitochondria interaction. Only upon gp78 overexpression does this become a dominant mechanism regulating not only ER-mitochondria Ca^{2+} coupling but also mitochondrial fusion and mobility.

AMF is internalized via a raft-dependent pathway to the 3F3A labeled SER that is upregulated in metastatic tumor cells (Kojic et al., 2007; Le et al., 2002). Whether interaction of AMF with gp78 at the cell surface or in the SER regulates gp78/AMFR ubiquitin ligase activity and ER-mitochondria interaction remains to be determined. AMF has established pro-survival functions (Tsutsumi et al., 2003a) and control of ER calcium release by AMF

prevents the ER stress response (Fu et al. 2011). AMF regulation of ER-mitochondria interaction via gp78 ubiquitin ligase activity therefore represents a novel mechanism for regulation of ER-mitochondrial interaction and mitochondrial fusion that may have important implications for their role in cancer progression.

3.4   Materials and methods

3.4.1   Antibodies and chemicals

3F3A anti-gp78/AMFR mAb is as described (Nabi et al., 1990b). Anti-OxphosV was from Molecular Probes, anti-IP$_3$R3 from BD Transduction, anti-HA from NeoMarker and M2 anti-Flag mAb from Sigma. Anti-rat IgM was from Jackson ImmunoResearch Laboratories and anti-mouse and rabbit IgG from Molecular Probes. BAPTAs and xestospongin C were from Calbiochem, Rhod-2 AM and pluronic F-127 (PAc) from Invitrogen and PGI, ionomycin, thapsigargin, ATP, Fura-2 AM and others from Sigma.

3.4.2   Cell culture, constructs and treatments

Cos-7 cells were grown in complete DMEM and transfected using Effectene (Qiagen). HA-Ubwt and HA-Ubmono (K29,48,63R) expression plasmids were obtained from Tony Morielli (Univ. Vermont) and pOCT-DsRed from Heidi McBride (Univ. Ottawa). FLAG-gp78wt in pcDNA3.1(+) was as described (Goetz et al., 2007b) and FLAG-RINGmut (C356S) generated by point mutation using the Quickchange mutagenesis kit (Stratagene). A tetracysteine tag (4c) (FLNCCPGCCMEP) and FLAG tag N-terminal to the 4c tag were added sequentially by PCR extension (Martin et al., 2005a). Flag-4c transfected cells were labeled with FlAsH (Invitrogen) that is not excited at the excitation wavelengths for Fura-2 and Rhod-2. For AMF treatment, cells were serum starved overnight and incubated with fresh media containing AMF. Cells were treated with ATP, TG, ionomycin and CaCl$_2$ and BAPTAs in normal buffer (125 mM NaCl, 20 mM HEPES, 5 mM KCl, 1.5 mM MgCl$_2$ and 10 mM glucose, pH 7.4) (Goetz et al., 2007b). For 4D and FRAP analysis, FLAG-gp78wt

and FLAG-RINGmut were cloned in pIRES2-EGFP and GFP used to identify transfected cells.

3.4.3   Immunofluorescence

Cells were fixed by pre-cooled methanol-acetone (80-20%, v-v, -80°C) and labeled with 3F3A, OxphosV or Flag Abs as described previously (Goetz et al., 2007b). Confocal images were obtained with the 100× (NA 1.4) UPlanApo objective of an Olympus FV1000 confocal microscope and Z-series deconvolved using Sharpstack 3D blind deconvolution and the deblurred 3D volume created using 3D Constructor. Colocalization was analyzed using ImagePro image analysis software (Media Cybernetics). FRAP analysis was performed with the 60X (NA 1.35) UPlanApo objective on the Olympus FV1000 with open pinhole (800nm). Images were acquired every 3.3 seconds over 200 seconds and bleaching done with a 500 msec pulse of a 543nm laser at 50%. 4D analysis of dsRed-pOct mitochondria was performed using a III-Zeiss spinning disk confocal and Sharpstack image analysis software (Intelligent Imaging Innovations). Stacks were acquired every 5 seconds over 2 minutes.

3.4.4   Electron microscopy

Cos-7 cells grown on Aclar film (Pelco) were washed with 0.1 M sodium cacodylate buffer, fixed with 2% glutaraldehyde (pH 7.4) in cacodylate buffer (1 h), post-fixed with 1% osmium tetroxide in cacodylate buffer (1 h) and the samples then progressively dehydrated through an ethanol series, then 100% acetone and embedded in Epon 812 (Fluka). 50-60 nm thick sections (Leica Ultramicrotome) were stained with 2% uranyl acetate and 2% lead citrate, and photographed on a Hitachi H7600 transmission electron microscope.

3.4.5 Ca^{2+} imaging

To monitor $[Ca^{2+}]_{cyt}$ and $[Ca^{2+}]_{m}$, cells were loaded with 5 µM Fura-2 AM or Rhod-2 AM in fresh media containing 0.02% PAc for 45 or 30 min, respectively. To simultaneously measure both $[Ca^{2+}]_{cyt}$ and $[Ca^{2+}]_{m}$, cells were loaded sequentially with Rhod-2 AM and

Fura-2 AM. Cells were perfused with normal buffer and images acquired with the 40× UApo objective of an inverted Olympus IX71 microscope. Fura-2 was excited at 340 and 380 nm with a PTI high speed random access monochromator (Photon Technology International) and emission detected at 510 nm. Rhod-2 was excited at 545 nm and emission detected at 575 nm. Images were analyzed using InVivo Analyzer V3.0 software (Media Cybernetics).

3.4.6   Western blots and immunoprecipitation

To assess gp78/AMFR-dependent ubiquitylation, pcDNA, FLAG-gp78wt or Flag-RINGmut mutant were co-transfected with HA-Ubwt or HA-Ubmono for 24 hours. Cell lysate supernatants were probed directly for HA by immunoblotting (30 μg protein) or immunoprecipitated with anti-Flag M2 agarose beads (300 μg protein) and then blotted with anti-Flag mAb and detected with ECL (GE Healthcare Bio-Sciences). Densitometry was performed using Quantity One V4.62 software (Bio-Rad).

Chapter 5: Conclusion

4.1   3F3A-labeled ER defined a new peripheral ER subdomain

Gp78 has been extensively studied using the 3F3A antibodies (Chiu et al., 2008). The 3F3A labeling was first described as a distinct tubular organelle marker related to the smooth ER in close contact to mitochondria (Benlimame et al., 1995a; Wang et al., 2000). We assessed the specificity of 3F3A for gp78 using a Dicer siRNA approach, confirming that 3F3A labeling is representative of gp78 expression level and localization (Chapter 2). Since the mitochondria association of 3F3A-labeled ER was known to be regulated by calcium, we studied the dynamics the 3F3A-labeled ER association to mitochondria in relation to other ER domains.

Immunoelectron microscopy showed previously that 3F3A labeled mainly the SER in close association with mitochondria and partially the cell surface (Benlimame et al., 1998a; Benlimame et al., 1995a). This was the case by immunofluorescence as well, where 3F3A was found to label almost exclusively mitochondria associated ER. 3F3A-labeled domain showed minimal overlap with other ER markers such as calnexin, sec61α and the peripheral ER markers reticulon 4a, but belong to the same continuous structure. This defined the 3F3A antibody as a specific ER marker for a mitochondrial-associated ER domain.

Overexpression of gp78 induces the expansion of the 3F3A labeled ER to the peripheral, reticulon labeled ER, indicating continuity between the two domains. The reticulons are a family of proteins that induces curvature of the ER and maintained the tubular network, preventing the membranes from adopting an energy neutral spherical shape (Voeltz and Prinz, 2007; Voeltz et al., 2006). The tubular structure has a higher surface to volume ratio by nature, perhaps allowing more efficient contact with other organelles and sensitivity to cytosolic changes. The impact of ER structure on calcium homeostasis and its functional

109

association with mitochondria remains to be tested. It is unknown if ER calcium release is faster or greater in cells with extended tubular peripheral ER compared to cells with mostly ER sheets. Similarly, the effect of ER structure on its coupling time with mitochondria hasn't been tested. The continuity between mitochondria-associated ER and the reticulon-labeled ER suggests that the structure of these two domains is important for calcium homeostasis.

The 3F3A-labeled ER association with mitochondria is highly dynamic and regulated by ER calcium release. Upon ATP stimulation of purinergic receptor, mitochondria dissociation occurs after two minutes to be re-established after five minutes. The dissociation of 3F3A labeled ER from mitochondria also segregates 3F3A from the ER marker calnexin but retained the SERCA labeled ER, showing that the 3F3A domain composition also varied depending on mitochondria association. The opposite was observed for the IPR3-labeled ER. At resting stage, 3F3A and IP3R are localized to the same mitochondria associated ER but dissociated in distinct domains after ER calcium released. This indicates that multiple SER domains are associated with mitochondria. Interestingly, the IP3R has been shown to be ubiquitylated five minutes after ER calcium released through stimulation of gonadotropin-releasing hormone (GnRH) receptor, which is consistent with reassociation of 3F3A with the IP3R-labeled ER. Moreover, gp78 co-immunoprecipitates with IP3R 5 minutes after stimulation of ER calcium release, paralleling IP3R polyubiquitylation (Pearce et al., 2007). This suggests that gp78 ubiquitin ligase activity is linked to ER-mitochondria dynamic association.

4.2 Gp78 ubiquitin ligase is localized in the peripheral ER.

Interestingly, 3F3A does not label the FLAG-gp78wt protein localized in the juxtanuclear ER, indicating that the 3F3A antibody specifically recognized a sub-population of gp78 localized to the peripheral ER. The motif recognized by the 3F3A antibody is unknown. The 3F3A labeled gp78 colocalized with the peripheral ER marker myc-reticulon 4a. Moreover, gp78 overexpression induces re-distribution of calnexin, derlin-1 and 2 and GFP-Sec61β to the juxtanuclear ER. This redistribution is intriguing because derlin-1, -2 and the Sec61

translocon have been shown to be involved in retro-translocation of ERAD substrates. Ubiquitylated substrates in gp78 overexpressing cells were found in peripheral 3F3A-labeled ER. This peripheral colocalization was dependent on the CUE motif. Mutation of the CUE motif leads to accumulation of ubiquitylated substrates in the juxtanuclear ER and high mobility of gp78 in the ER, as seen by FRAP measurement.

Using this FLAG-tagged gp78, we identified the 3F3A positive peripheral ER as the site of ubiquitylation of gp78. Transfection with HA-tagged ubiquitin together with a methanol/acetone fixation method that does not preserved most cytosolic protein showed that the central ER does not contained ubiquitylated substrates in normal conditions. Proteasomal inhibition showed accumulation of ubiquitylated proteins in the central ER, suggesting that this is the site of proteasome delivery. This is consistent with previous identification of a quality-control compartment in the ER (ERQC) upon proteasome inhibition. Interestingly, substrate accumulation of ubiquitylated protein is dependent on p97 recruitment to the peripheral ER and ubiquitin chain elongation. Polyubiquitylated substrates were found in the juxtanuclear ER only after proteasome inhibition. Wash-out experiments have shown that the juxtanuclear ER is the site of proteasome delivery, as suspected by the derlins and GFP-Sec61β redistribution. P97 recruitment to the expanded 3F3A labeled ER was gp78-depended, and its recruitment, as well as ubiquitin chain extension, was essential to substrates accumulation in the juxtanuclear ER following proteasome inhibition. This shows that ubiquitylation and proteasome delivery or ERAD-substrates are two spatially distinct processes.

Because the ubiquitin distribution in the peripheral ER and segregation of juxtanuclear ER markers was observed under overexpression condition, we used as a model HEK293t and the fibrosarcoma HT-1080 cell lines. HT-1080 cells expresshigh level of gp78 compared to HEK293t and a lower level of the gp78 substrate KAI1, a transmembrane metastasis suppressor, indicating that gp78 is actively involved in ERAD in these cells (Tsai et al., 2007). Polyubiquitylated substrates were localized to the central ER in HT1080 cells only upon proteasome inhibition, correlating results obtained with Cos-7 overexpressing cells.

This two-step process in which the substrate is first recognized in the peripheral ER, monoubiquitylated and maintained in complex with gp78 via monoubiquitin-CUE motif interaction and then becomes polyubiquitylated, and transfered to the juxtanuclear ER refines our understanding of the ERAD process. It is consistent with previous observation that monoubiquitylation function as an ER retention signal of transmembrane protein folding in the ER (Abrami et al., 2008; Feldman and van der Goot, 2009). This shows that ubiquitylation and proteasome delivery are two spatially distinct processes of ERAD.

4.3   Is the peripheral ER a folding monitoring domain of the ER?

The ER is the biosynthetic site of proteins entering the secretory pathway. Proteins entering the ER have to be folded, assembled and monitored for quality control. An extensive quality control system is present in the ER. Misfolded proteins are recognized by the UPR pathway and send for proteasomal degradation via ERAD. It is unclear if the different steps of protein folding and of quality control monitoring take place in discreet subdomains. It was shown that upon proteasomal inhibition, ERAD substrates accumulated in a juxtanuclear ER subdomain called the ER quality control compartment (ERQCC)(Frenkel et al., 2004; Kamhi-Nesher et al., 2001a; Spiliotis et al., 2002b). However, it remains unclear if the step preceding proteasomal targeting, such as folding, assembly, recognition of misfolded protein and ubiquitylation take place in a distinct domain or at the ERQCC.

The peripheral ER has been shown to be labeled for ERp57, thiol oxidoreductase involved in protein folding. Interaction of a subpopulation of the model substrates asialoglycoprotein receptor H2a and H2b with ERp57 was protected from degradation, another subpopulation of substrates interacting with calnexin was localized to the juxtanuclear ER and sent for degradation (Frenkel et al., 2004). This correlates with my observations and suggests that the peripheral ER is the folding site of the ER and the juxtanuclear ER is the proteasomal delivery site in the ER. Upon proteasome inhibition, calnexin was redistributed to the central ER, but ERp57 remains in the peripheral ER. This suggested that ERp57, a peripheral ER protein, could play a protective role against degradation of newly synthesised polypeptide during the initial folding attempts (Frenkel et al., 2004).

An important limitation of my study of localization of different ERAD step through the ER is the inability to monitor the ERAD substrate trafficking in real time. Misfolded ERAD substrates such as GFP-tagged CFTRΔ508 do not localized in the peripheral ER and rather forms aggregates in the juxtanuclear ER. Such mutated ligands are recognized by the ERAD machinery as they are being insert in the ER. It would be interesting to develop a system in which an ER protein could be visualized a physiological level, since overexpression induce ER stress, and be recognized or not by the ERAD system upon cell stimulation. For example, GFP-tagged HMG-CoA reductase express under endogenous promoter could be monitor in the absence of sterol to prevent its degradation. The addition of sterol to the media would act as a signal for GFP-HMG-CoA reductase degradation and its trafficking to the site of proteasome degradation could be observed.

4.4   The pro-survival role of gp78 ligand, AMF

Gp78 is involved in ERAD, an essential pathway to clear misfolded proteins from the ER, and prevent their accumulation. The UPR pathway also increased expression of chaperones, such as BIP, to assist with protein folding. If the UPR activation is sustained, the cell will enter apoptosis. AMF, the gp78 ligand, is internalized to the ER-mitochondria domain labeled by 3F3A (Benlimame et al., 1998a; Benlimame et al., 1995a; Kojic et al., 2008) and has been shown to have a pro-survival role via activation of the AKT pathway (Kojic et al., 2007; Kojic et al., 2008) and prevent apoptosis induces by ER stress (Fu et al., 2011). AMF treatment protects from ER stress and apoptosis induction by tunicamycin and thapsigargin, observed by reduction of Bip and CHOP expression and cytochrome C release. The effect of AMF treatment was shown to be gp78-dependent and mediated by inhibition of ER calcium release. This shows that the AMF-gp78 role at the ER-mitochondria interface is not limited to the modulation of ubiquitin ligase activity but also to the modulation of calcium homeostasis between these two organelles, protecting against apoptosis.

4.5 Gp78 ligand, AMF, modulates ubiquitin ligase activity and mitochondrial dynamics.

We investigated the response of gp78 ubiquitin ligase activity, ER-mitochondria association and mitochondrial dynamics following AMF stimulation. We found that gp78 deficient in ubiquitin ligase activity or mutant ubiquitin unable to form polyubiquitylated chains disrupt ER-mitochondria coupling. I show that reduced mobility and increased fragmentation of mitochondria upon overexpression of gp78 are prevented by AMF and dependent on gp78/AMFR ubiquitin ligase activity. We therefore describe a novel mechanism linking extracellular regulation of gp78/AMFR ubiquitin ligase activity and polyubiquitylation to ER-mitochondria coupling and mitochondrial dynamics. We recently found that mitofusin 1 and 2 (Mfn1 and Mfn2) were substrates of gp78, preventing their degradation results in interconnected mitochondria.

Mitochondrial fragmentation is usually a step into the apoptosis process (Karbowski, 2011). Gp78 overexpression induces survival on carcinogenic cell, which might seem paradoxical. This might be indication that inhibition of the gp78 ubiquitin ligase activity by its ligand is essential to its pro-survival role in cancer. This would results in AMF internalization and reduce ER calcium released, therefore preventing induction of ER stress (Fu et al., 2011). Our model used overexpressed gp78 in Cos7 cells well above physiological level, inducing mitochondria fragmentation to a greater level than in carcinogenic cells. It would be interesting to measure the effect of AMF treatment on a cellular model that express gp78 to high physiological level such as HT1080.

4.6 Final remarks

The works shown in this thesis have shown that 3F3A defined a specific domain of the ER where gp78 ubiquitin ligase activity takes place. The association with mitochondria of this 3F3A-labeled ER was regulated by calcium concentration but it remains to be tested if ER-mitochondria contacts are playing a role in ubiquitylation and ERAD. The ubiquitin ligase activity of gp78 has an impact on mitochondria dynamics but the reverse hypothesis, the

regulation of ubiquitylation by mitochondria dynamics remains to be tested. Finally, since gp78 is a cell surface receptor of AMF as well, it was shown that AMF treatment would modulates both gp78 ubiquitin ligase activity as well as mitochondrial dynamics. This is a significant step in the understanding of ERAD organization and modulation of mitochondria dynamics.

References

Abe, M., Sugiura, T., Takahashi, M., Ishii, K., Shimoda, M. and Shirasuna, K. (2008). A novel function of CD82/KAI-1 on E-cadherin-mediated homophilic cellular adhesion of cancer cells. *Cancer Lett* **266**, 163-70.

Abrami, L., Kunz, B., Iacovache, I. and van der Goot, F. G. (2008). Palmitoylation and ubiquitination regulate exit of the Wnt signaling protein LRP6 from the endoplasmic reticulum. *Proc Natl Acad Sci U S A* **105**, 5384-9.

Adams, S. R., Campbell, R. E., Gross, L. A., Martin, B. R., Walkup, G. K., Yao, Y., Llopis, J. and Tsien, R. Y. (2002). New biarsenical ligands and tetracysteine motifs for protein labeling in vitro and in vivo: synthesis and biological applications. *J Am Chem Soc* **124**, 6063-76.

Amchenkova, A. A., Bakeeva, L. E., Chentsov, Y. S., Skulachev, V. P. and Zorov, D. B. (1988). Coupling membranes as energy-transmitting cables. I. Filamentous mitochondria in fibroblasts and mitochondrial clusters in cardiomyocytes. *J Cell Biol* **107**, 481-95.

Amiott, E. A., Cohen, M. M., Saint-Georges, Y., Weissman, A. M. and Shaw, J. M. (2009). A mutation associated with CMT2A neuropathy causes defects in Fzo1 GTP hydrolysis, ubiquitylation, and protein turnover. *Mol Biol Cell* **20**, 5026-35.

Balaban, R. S., Nemoto, S. and Finkel, T. (2005). Mitochondria, oxidants, and aging. *Cell* **120**, 483-95.

Ballar, P., Shen, Y., Yang, H. and Fang, S. (2006). The role of a novel p97/valosin-containing protein-interacting motif of gp78 in endoplasmic reticulum-associated degradation. *J Biol Chem* **281**, 35359-68.

Ballar, P., Zhong, Y., Nagahama, M., Tagaya, M., Shen, Y. and Fang, S. (2007). Identification of SVIP as an endogenous inhibitor of endoplasmic reticulum-associated degradation. *J Biol Chem* **282**, 33908-14.

Bays, N. W. and Hampton, R. Y. (2002). Cdc48-Ufd1-Npl4: stuck in the middle with Ub. *Curr Biol* **12**, R366-71.

Bebok, Z., Mazzochi, C., King, S. A., Hong, J. S. and Sorscher, E. J. (1998). The mechanism underlying cystic fibrosis transmembrane conductance regulator transport from the endoplasmic reticulum to the proteasome includes Sec61beta and a cytosolic, deglycosylated intermediary. *J Biol Chem* **273**, 29873-8.

Benlimame, N., Le, P. U. and Nabi, I. R. (1998a). Localization of autocrine motility factor receptor to caveolae and clathrin-independent internalization of its ligand to smooth endoplasmic reticulum. *Mol Biol Cell* **9**, 1773-86.

Benlimame, N., Le, P. U. and Nabi, I. R. (1998b). Localization of autocrine motility factor receptor to caveolae and clathrin-independent internalization of its ligand to smooth endoplasmic reticulum. *Molecular Biology of the Cell* **9**, 1773-1786.

Benlimame, N., Simard, D. and Nabi, I. R. (1995a). Autocrine motility factor receptor is a marker for a distinct membranous tubular organelle. *J Cell Biol* **129**, 459-71.

Benlimame, N., Simard, D. and Nabi, I. R. (1995b). Autocrine motility factor receptor is a marker for a distinct tubular membrane organelle. *Journal of Cell Biology* **129**, 459-471.

Bernales, S., McDonald, K. L. and Walter, P. (2006). Autophagy counterbalances endoplasmic reticulum expansion during the unfolded protein response. *PLoS Biol* **4**, e423.

Bernardi, K. M., Forster, M. L., Lencer, W. I. and Tsai, B. (2008). Derlin-1 facilitates the retro-translocation of cholera toxin. *Mol Biol Cell* **19**, 877-84.

Bernardi, K. M., Williams, J. M., Kikkert, M., van Voorden, S., Wiertz, E. J., Ye, Y. and Tsai, B. (2010). The E3 ubiquitin ligases Hrd1 and gp78 bind to and promote cholera toxin retro-translocation. *Mol Biol Cell* **21**, 140-51.

Berridge, M. J. (2002). The endoplasmic reticulum: a multifunctional signaling organelle. *Cell Calcium* **32**, 235-49.

Bertolotti, A., Zhang, Y., Hendershot, L. M., Harding, H. P. and Ron, D. (2000). Dynamic interaction of BiP and ER stress transducers in the unfolded-protein response. *Nat Cell Biol* **2**, 326-32.

Bezprozvanny, I., Watras, J. and Ehrlich, B. E. (1991). Bell-shaped calcium-response curves of Ins(1,4,5)P3- and calcium-gated channels from endoplasmic reticulum of cerebellum. *Nature* **351**, 751-4.

Biederer, T., Volkwein, C. and Sommer, T. (1997). Role of Cue1p in ubiquitination and degradation at the ER surface. *Science* **278**, 1806-9.

Braschi, E., Zunino, R. and McBride, H. M. (2009). MAPL is a new mitochondrial SUMO E3 ligase that regulates mitochondrial fission. *EMBO Rep* **10**, 748-54.

Breckenridge, D. G., Germain, M., Mathai, J. P., Nguyen, M. and Shore, G. C. (2003). Regulation of apoptosis by endoplasmic reticulum pathways. *Oncogene* **22**, 8608-18.

Briese, J., Schulte, H. M., Sajin, M., Bamberger, C., Redlin, K., Milde-Langosch, K., Loning, T. and Bamberger, A. M. (2008). Correlations between reduced expression of the metastasis suppressor gene KAI-1 and accumulation of p53 in uterine carcinomas and sarcomas. *Virchows Arch* **453**, 89-96.

Brough, D., Schell, M. J. and Irvine, R. F. (2005). Agonist-induced regulation of mitochondrial and endoplasmic reticulum motility. *Biochem J* **392**, 291-7.

Calfon, M., Zeng, H., Urano, F., Till, J. H., Hubbard, S. R., Harding, H. P., Clark, S. G. and Ron, D. (2002). IRE1 couples endoplasmic reticulum load to secretory capacity by processing the XBP-1 mRNA. *Nature* **415**, 92-6.

Cao, J., Wang, J., Qi, W., Miao, H. H., Ge, L., DeBose-Boyd, R. A., Tang, J. J., Li, B. L. and Song, B. L. (2007). Ufd1 is a cofactor of gp78 and plays a key role in cholesterol metabolism by regulating the stability of HMG-CoA reductase. *Cell Metab* **6**, 115-28.

Cao, M. J., Osatomi, K., Matsuda, R., Ohkubo, M., Hara, K. and Ishihara, T. (2000). Purification of a novel serine proteinase inhibitor from the skeletal muscle of white croaker (Argyrosomus argentatus). *Biochem Biophys Res Commun* **272**, 485-9.

Carlson, E. J., Pitonzo, D. and Skach, W. R. (2006). p97 functions as an auxiliary factor to facilitate TM domain extraction during CFTR ER-associated degradation. *Embo J* **25**, 4557-66.

Carvalho, P., Goder, V. and Rapoport, T. A. (2006). Distinct ubiquitin-ligase complexes define convergent pathways for the degradation of ER proteins. *Cell* **126**, 361-73.

Casagrande, R., Stern, P., Diehn, M., Shamu, C., Osario, M., Zuniga, M., Brown, P. O. and Ploegh, H. (2000). Degradation of proteins from the ER of S. cerevisiae requires an intact unfolded protein response pathway. *Mol Cell* **5**, 729-35.

Cereghetti, G. M., Stangherlin, A., Martins de Brito, O., Chang, C. R., Blackstone, C., Bernardi, P. and Scorrano, L. (2008). Dephosphorylation by calcineurin regulates translocation of Drp1 to mitochondria. *Proc Natl Acad Sci U S A* **105**, 15803-8.

Cerqua, C., Anesti, V., Pyakurel, A., Liu, D., Naon, D., Wiche, G., Baffa, R., Dimmer, K. S. and Scorrano, L. (2010). Trichoplein/mitostatin regulates endoplasmic reticulum-mitochondria juxtaposition. *EMBO Rep* **11**, 854-60.

Chao, J. T. and Loewen, J. R. (2010). ER Junctions. In *Cellular Domains*, (ed. I. R. Nabi): Wiley Press.

Chen, B., Mariano, J., Tsai, Y. C., Chan, A. H., Cohen, M. and Weissman, A. M. (2006a). The activity of a human endoplasmic reticulum-associated degradation E3, gp78, requires its Cue domain, RING finger, and an E2-binding site. *PNAS* **103**, 341-346.

Chen, B., Mariano, J., Tsai, Y. C., Chan, A. H., Cohen, M. and Weissman, A. M. (2006b). The activity of a human endoplasmic reticulum-associated degradation E3, gp78, requires its Cue domain, RING finger, and an E2-binding site. *Proc Natl Acad Sci U S A* **103**, 341-6.

Chen, H. and Chan, D. C. (2009). Mitochondrial dynamics--fusion, fission, movement, and mitophagy--in neurodegenerative diseases. *Hum Mol Genet* **18**, R169-76.

Chen, H., Chomyn, A. and Chan, D. C. (2005). Disruption of fusion results in mitochondrial heterogeneity and dysfunction. *J Biol Chem* **280**, 26185-92.

Chen, H., Detmer, S. A., Ewald, A. J., Griffin, E. E., Fraser, S. E. and Chan, D. C. (2003). Mitofusins Mfn1 and Mfn2 coordinately regulate mitochondrial fusion and are essential for embryonic development. *J Cell Biol* **160**, 189-200.

Cheng, E. H., Sheiko, T. V., Fisher, J. K., Craigen, W. J. and Korsmeyer, S. J. (2003). VDAC2 inhibits BAK activation and mitochondrial apoptosis. *Science* **301**, 513-7.

Chin, D. J., Luskey, K. L., Anderson, R. G., Faust, J. R., Goldstein, J. L. and Brown, M. S. (1982). Appearance of crystalloid endoplasmic reticulum in compactin-resistant Chinese hamster cells with a 500-fold increase in 3-hydroxy-3-methylglutaryl-coenzyme A reductase. *Proc Natl Acad Sci U S A* **79**, 1185-9.

Chiu, C. G., St-Pierre, P., Nabi, I. R. and Wiseman, S. M. (2008). Autocrine motility factor receptor: a clinical review. *Expert Rev Anticancer Ther* **8**, 207-17.

Cipolat, S., Martins de Brito, O., Dal Zilio, B. and Scorrano, L. (2004). OPA1 requires mitofusin 1 to promote mitochondrial fusion. *Proc Natl Acad Sci U S A* **101**, 15927-32.

Cohen, M. M., Leboucher, G. P., Livnat-Levanon, N., Glickman, M. H. and Weissman, A. M. (2008). Ubiquitin-proteasome-dependent degradation of a mitofusin, a critical regulator of mitochondrial fusion. *Mol Biol Cell* **19**, 2457-64.

Collins, T. J., Berridge, M. J., Lipp, P. and Bootman, M. D. (2002). Mitochondria are morphologically and functionally heterogeneous within cells. *Embo J* **21**, 1616-27.

Colombini, M. (2004). VDAC: the channel at the interface between mitochondria and the cytosol. *Mol Cell Biochem* **256-257**, 107-15.

Cribbs, J. T. and Strack, S. (2007). Reversible phosphorylation of Drp1 by cyclic AMP-dependent protein kinase and calcineurin regulates mitochondrial fission and cell death. *EMBO Rep* **8**, 939-44.

Csordas, G., Renken, C., Varnai, P., Walter, L., Weaver, D., Buttle, K. F., Balla, T., Mannella, C. A. and Hajnoczky, G. (2006). Structural and functional features and significance of the physical linkage between ER and mitochondria. *J Cell Biol* **174**, 915-21.

Csordas, G., Thomas, A. P. and Hajnoczky, G. (1999). Quasi-synaptic calcium signal transmission between endoplasmic reticulum and mitochondria. *Embo J* **18**, 96-108.

de Brito, O. M. and Scorrano, L. (2008). Mitofusin 2: a mitochondria-shaping protein with signaling roles beyond fusion. *Antioxid Redox Signal* **10**, 621-33.

de Virgilio, M., Weninger, H. and Ivessa, N. E. (1998). Ubiquitination is required for the retro-translocation of a short-lived luminal endoplasmic reticulum glycoprotein to the cytosol for degradation by the proteasome. *J Biol Chem* **273**, 9734-43.

DeLaBarre, B. and Brunger, A. T. (2003). Complete structure of p97/valosin-containing protein reveals communication between nucleotide domains. *Nat Struct Biol* **10**, 856-63.

Dempsey, E. W. (1953). Electron microscopy of the visceral yolk-sac epithelium of the guinea pig. *Am J Anat* **93**, 331-63.

DeVay, R. M., Dominguez-Ramirez, L., Lackner, L. L., Hoppins, S., Stahlberg, H. and Nunnari, J. (2009). Coassembly of Mgm1 isoforms requires cardiolipin and mediates mitochondrial inner membrane fusion. *J Cell Biol* **186**, 793-803.

Dixit, G., Mikoryak, C., Hayslett, T., Bhat, A. and Draper, R. K. (2008). Cholera toxin up-regulates endoplasmic reticulum proteins that correlate with sensitivity to the toxin. *Exp Biol Med (Maywood)* **233**, 163-75.

Dobashi, Y., Watanabe, H., Sato, Y., Hirashima, S., Yanagawa, T., Matsubara, H. and Ooi, A. (2006). Differential expression and pathological significance of autocrine motility factor/glucose-6-phosphate isomerase expression in human lung carcinomas. *J Pathol* **210**, 431-40.

Ellgaard, L. and Helenius, A. (2003). Quality control in the endoplasmic reticulum. *Nat Rev Mol Cell Biol* **4**, 181-91.

Fairbank, M., St-Pierre, P. and Nabi, I. R. (2009). The complex biology of autocrine motility factor/phosphoglucose isomerase (AMF/PGI) and its receptor, the gp78/AMFR E3 ubiquitin ligase. *Mol Biosyst* **5**, 793-801.

Fang, S., Ferrone, M., Yang, C., Jensen, J. P., Tiwari, S. and Weissman, A. M. (2001a). The tumor autocrine motility factor receptor, gp78, is a ubiquitin protein ligase implicated in degradation from the endoplasmic reticulum. *Proc Natl Acad Sci U S A* **98**, 14422-7.

Fang, S., Ferrone, M., Yang, C., Jensen, J. P., Tiwari, S. and Weissman, A. M. (2001b). The tumor autocrine motility factor receptor, gp78, is a ubiquitin protein ligase implicated in degradation from the endoplasmic reticulum. *Proc Natl Acad Sci U S A* **98**, 14422-14427.

Feldman, M. and van der Goot, F. G. (2009). Novel ubiquitin-dependent quality control in the endoplasmic reticulum. *Trends Cell Biol* **19**, 357-63.

Fernandez, J., Yaman, I., Sarnow, P., Snider, M. D. and Hatzoglou, M. (2002). Regulation of internal ribosomal entry site-mediated translation by phosphorylation of the translation initiation factor eIF2alpha. *J Biol Chem* **277**, 19198-205.

Fisher, E. A. and Ginsberg, H. N. (2002). Complexity in the secretory pathway: the assembly and secretion of apolipoprotein B-containing lipoproteins. *J Biol Chem* **277**, 17377-80.

Flierman, D., Ye, Y., Dai, M., Chau, V. and Rapoport, T. A. (2003). Polyubiquitin serves as a recognition signal, rather than a ratcheting molecule, during retrotranslocation of proteins across the endoplasmic reticulum membrane. *J Biol Chem* **278**, 34774-82.

Freemont, P. S. (2000). RING for destruction? *Curr Biol* **10**, R84-7.

Frenkel, Z., Shenkman, M., Kondratyev, M. and Lederkremer, G. Z. (2004). Separate roles and different routing of calnexin and ERp57 in endoplasmic reticulum quality control revealed by interactions with asialoglycoprotein receptor chains. *Mol Biol Cell* **15**, 2133-42.

Friedlander, R., Jarosch, E., Urban, J., Volkwein, C. and Sommer, T. (2000). A regulatory link between ER-associated protein degradation and the unfolded-protein response. *Nat Cell Biol* **2**, 379-84.

Fu, M., Li, L., Albrecht, T., Johnson, J. D., Kojic, L. D. and Nabi, I. R. (2011). Autocrine motility factor/phosphoglucose isomerase regulates ER stress and cell death through control of ER calcium release. *Cell Death Differ* **18**, 1057-70.

Funasaka, T., Hu, H., Yanagawa, T., Hogan, V. and Raz, A. (2007). Down-regulation of phosphoglucose isomerase/autocrine motility factor results in mesenchymal-to-epithelial transition of human lung fibrosarcoma cells. *Cancer Res* **67**, 4236-43.

Gafni, J., Munsch, J. A., Lam, T. H., Catlin, M. C., Costa, L. G., Molinski, T. F. and Pessah, I. N. (1997). Xestospongins: potent membrane permeable blockers of the inositol 1,4,5-trisphosphate receptor. *Neuron* **19**, 723-33.

Gandhi, S., Wood-Kaczmar, A., Yao, Z., Plun-Favreau, H., Deas, E., Klupsch, K., Downward, J., Latchman, D. S., Tabrizi, S. J., Wood, N. W. et al. (2009). PINK1-

associated Parkinson's disease is caused by neuronal vulnerability to calcium-induced cell death. *Mol Cell* **33**, 627-38.

Gandre-Babbe, S. and van der Bliek, A. M. (2008). The novel tail-anchored membrane protein Mff controls mitochondrial and peroxisomal fission in mammalian cells. *Mol Biol Cell* **19**, 2402-12.

Goetz, J. G., Genty, H., St-Pierre, P., Dang, T., Joshi, B., Sauve, R., Vogl, W. and Nabi, I. R. (2007a). Reversible interactions between smooth domains of the endoplasmic reticulum and mitochondria are regulated by physiological cytosolic Ca2+ levels. *J Cell Sci* **120**, 3553-64.

Goetz, J. G., Genty, H., St. Pierre, P., Dang, T., Joshi, B., Sauvé, R., Vogl, W. and Nabi, I. R. (2007b). Reversible interactions between smooth domains of the endoplasmic reticulum and mitochondria are regulated by physiological cytosolic calcium levels. *J Cell Science* **120**, 3553-3564.

Goetz, J. G. and Nabi, I. R. (2006a). Interaction of the smooth endoplasmic reticulum and mitochondria. *Biochem Soc Trans* **340**, 370-373.

Goetz, J. G. and Nabi, I. R. (2006b). Interaction of the smooth endoplasmic reticulum and mitochondria. *Biochem Soc Trans* **34**, 370-3.

Griparic, L., Kanazawa, T. and van der Bliek, A. M. (2007). Regulation of the mitochondrial dynamin-like protein Opa1 by proteolytic cleavage. *J Cell Biol* **178**, 757-64.

Grynkiewicz, G., Poenie, M. and Tsien, R. Y. (1985). A new generation of Ca2+ indicators with greatly improved fluorescence properties. *J Biol Chem* **260**, 3440-50.

Gurney, M. E., Heinrich, S. P., Lee, M. R. and Yin, H. S. (1986). Molecular cloning and expression of neuroleukin, a neurotrophic factor for spinal and sensory neurons. *Science* **234**, 566-74.

Haga, A., Funasaka, T., Deyashiki, Y. and Raz, A. (2008). Autocrine motility factor stimulates the invasiveness of malignant cells as well as up-regulation of matrix metalloproteinase-3 expression via a MAPK pathway. *FEBS Lett* **582**, 1877-82.

Haga, A., Funasaka, T., Niinaka, Y., Raz, A. and Nagase, H. (2003). Autocrine motility factor signaling induces tumor apoptotic resistance by regulations Apaf-1 and Caspase-9 apoptosome expression. *Int J Cancer* **107**, 707-14.

Hajnoczky, G., Csordas, G., Madesh, M. and Pacher, P. (2000). Control of apoptosis by IP(3) and ryanodine receptor driven calcium signals. *Cell Calcium* **28**, 349-63.

Hajnoczky, G., Csordas, G. and Yi, M. (2002). Old players in a new role: mitochondria-associated membranes, VDAC, and ryanodine receptors as contributors to

calcium signal propagation from endoplasmic reticulum to the mitochondria. *Cell Calcium* **32**, 363-77.

Harding, H. P., Zhang, Y. and Ron, D. (1999). Protein translation and folding are coupled by an endoplasmic-reticulum-resident kinase. *Nature* **397**, 271-4.

He, C. and Klionsky, D. J. (2009). Regulation mechanisms and signaling pathways of autophagy. *Annu Rev Genet* **43**, 67-93.

Head, B., Griparic, L., Amiri, M., Gandre-Babbe, S. and van der Bliek, A. M. (2009). Inducible proteolytic inactivation of OPA1 mediated by the OMA1 protease in mammalian cells. *J Cell Biol* **187**, 959-66.

Herlan, M., Bornhovd, C., Hell, K., Neupert, W. and Reichert, A. S. (2004). Alternative topogenesis of Mgm1 and mitochondrial morphology depend on ATP and a functional import motor. *J Cell Biol* **165**, 167-73.

Hershko, A. and Ciechanover, A. (1998). The ubiquitin system. *Annu Rev Biochem* **67**, 425-79.

Hirata, M., Suematsu, E., Hashimoto, T., Hamachi, T. and Koga, T. (1984). Release of Ca2+ from a non-mitochondrial store site in peritoneal macrophages treated with saponin by inositol 1,4,5-trisphosphate. *Biochem J* **223**, 229-36.

Hu, J., Shibata, Y., Voss, C., Shemesh, T., Li, Z., Coughlin, M., Kozlov, M. M., Rapoport, T. A. and Prinz, W. A. (2008). Membrane proteins of the endoplasmic reticulum induce high-curvature tubules. *Science* **319**, 1247-50.

Hu, J., Shibata, Y., Zhu, P. P., Voss, C., Rismanchi, N., Prinz, W. A., Rapoport, T. A. and Blackstone, C. (2009). A class of dynamin-like GTPases involved in the generation of the tubular ER network. *Cell* **138**, 549-61.

Huser, J. and Blatter, L. A. (1999). Fluctuations in mitochondrial membrane potential caused by repetitive gating of the permeability transition pore. *Biochem J* **343 Pt 2**, 311-7.

Iino, M. (1990). Biphasic Ca2+ dependence of inositol 1,4,5-trisphosphate-induced Ca release in smooth muscle cells of the guinea pig taenia caeci. *J Gen Physiol* **95**, 1103-22.

Ishihara, N., Fujita, Y., Oka, T. and Mihara, K. (2006). Regulation of mitochondrial morphology through proteolytic cleavage of OPA1. *Embo J* **25**, 2966-77.

Ishihara, N., Nomura, M., Jofuku, A., Kato, H., Suzuki, S. O., Masuda, K., Otera, H., Nakanishi, Y., Nonaka, I., Goto, Y. et al. (2009). Mitochondrial fission factor Drp1 is essential for embryonic development and synapse formation in mice. *Nat Cell Biol* **11**, 958-66.

Iwawaki, T., Hosoda, A., Okuda, T., Kamigori, Y., Nomura-Furuwatari, C., Kimata, Y., Tsuru, A. and Kohno, K. (2001). Translational control by the ER transmembrane kinase/ribonuclease IRE1 under ER stress. *Nat Cell Biol* **3**, 158-64.

Jakob, C. A., Burda, P., Roth, J. and Aebi, M. (1998). Degradation of misfolded endoplasmic reticulum glycoproteins in Saccharomyces cerevisiae is determined by a specific oligosaccharide structure. *J Cell Biol* **142**, 1223-33.

Jan, C. R., Wu, S. N. and Tseng, C. J. (1999). A further investigation of ATP-induced calcium mobilization in MDCK cells. *Chin J Physiol* **42**, 33-9.

Jarosch, E., Taxis, C., Volkwein, C., Bordallo, J., Finley, D., Wolf, D. H. and Sommer, T. (2002). Protein dislocation from the ER requires polyubiquitination and the AAA-ATPase Cdc48. *Nat Cell Biol* **4**, 134-9.

Johnston, J. A., Ward, C. L. and Kopito, R. R. (1998). Aggresomes: a cellular response to misfolded proteins. *J Cell Biol* **143**, 1883-98.

Jones, A. L. and Armstrong, D. T. (1965). Increased cholesterol biosynthesis following phenobarbital induced hypertrophy of agranular endoplasmic reticulum in liver. *Proc Soc Exp Biol Med* **119**, 1136-9.

Joshi, B., Li, L. and Nabi, I. R. (2010). A role for KAI1 in promotion of cell proliferation and mammary gland hyperplasia by the gp78 ubiquitin ligase. *J Biol Chem* **285**, 8830-9.

Jouaville, L. S., Ichas, F., Holmuhamedov, E. L., Camacho, P. and Lechleiter, J. D. (1995). Synchronization of calcium waves by mitochondrial substrates in Xenopus laevis oocytes. *Nature* **377**, 438-41.

Kamhi-Nesher, S., Shenkman, M., Tolchinsky, S., Fromm, S. V., Ehrlich, R. and Lederkremer, G. Z. (2001a). A novel quality control compartment derived from the endoplasmic reticulum. *Mol Biol Cell* **12**, 1711-23.

Kamhi-Nesher, S., Shenkman, M., Tolchinsky, S., Fromm, S. V., Ehrlich, R. and Lederkremer, G. Z. (2001b). A novel quality control compartment derived from the endoplasmic reticulum. *Mol Biol Cell* **12**, 1711-23.

Kang, R. S., Daniels, C. M., Francis, S. A., Shih, S. C., Salerno, W. J., Hicke, L. and Radhakrishnan, I. (2003). Solution structure of a CUE-ubiquitin complex reveals a conserved mode of ubiquitin binding. *Cell* **113**, 621-30.

Kano, F., Kondo, H., Yamamoto, A., Tanaka, A. R., Hosokawa, N., Nagata, K. and Murata, M. (2005). The maintenance of the endoplasmic reticulum network is regulated by p47, a cofactor of p97, through phosphorylation by cdc2 kinase. *Genes Cells* **10**, 333-44.

Karbowski, M. Mitochondria on guard: role of mitochondrial fusion and fission in the regulation of apoptosis. *Adv Exp Med Biol* **687**, 131-42.

Karbowski, M., Neutzner, A. and Youle, R. J. (2007). The mitochondrial E3 ubiquitin ligase MARCH5 is required for Drp1 dependent mitochondrial division. *J Cell Biol* **178**, 71-84.

Koegl, M., Hoppe, T., Schlenker, S., Ulrich, H. D., Mayer, T. U. and Jentsch, S. (1999). A novel ubiquitination factor, E4, is involved in multiubiquitin chain assembly. *Cell* **96**, 635-44.

Kojic, L. D., Joshi, B., Lajoie, P., Le, P. U., Cox, M. E., Turbin, D. A., Wiseman, S. M. and Nabi, I. R. (2007). Raft-dependent Endocytosis of Autocrine Motility Factor Is Phosphatidylinositol 3-Kinase-dependent in Breast Carcinoma Cells. *J Biol Chem* **282**, 29305-13.

Kojic, L. D., Wiseman, S. M., Ghaidi, F., Joshi, B., Nedev, H., Saragovi, H. U. and Nabi, I. R. (2008). Raft-dependent endocytosis of autocrine motility factor/phosphoglucose isomerase: a potential drug delivery route for tumor cells. *PLoS ONE* **3**, e3597.

Kornmann, B., Currie, E., Collins, S. R., Schuldiner, M., Nunnari, J., Weissman, J. S. and Walter, P. (2009). An ER-mitochondria tethering complex revealed by a synthetic biology screen. *Science* **325**, 477-81.

Koshiba, T., Detmer, S. A., Kaiser, J. T., Chen, H., McCaffery, J. M. and Chan, D. C. (2004). Structural basis of mitochondrial tethering by mitofusin complexes. *Science* **305**, 858-62.

Kothe, M., Ye, Y., Wagner, J. S., De Luca, H. E., Kern, E., Rapoport, T. A. and Lencer, W. I. (2005). Role of p97 AAA-ATPase in the retrotranslocation of the cholera toxin A1 chain, a non-ubiquitinated substrate. *J Biol Chem* **280**, 28127-32.

Koumenis, C., Naczki, C., Koritzinsky, M., Rastani, S., Diehl, A., Sonenberg, N., Koromilas, A. and Wouters, B. G. (2002). Regulation of protein synthesis by hypoxia via activation of the endoplasmic reticulum kinase PERK and phosphorylation of the translation initiation factor eIF2alpha. *Mol Cell Biol* **22**, 7405-16.

Le, P. U., Benlimame, N., Lagana, A., Raz, A. and Nabi, I. R. (2000). Clathrin-mediated endocytosis and recycling of autocrine motility factor receptor to fibronectin fibrils is a limiting factor for NIH-3T3 cell motility. *J Cell Sci* **113 (Pt 18)**, 3227-40.

Le, P. U., Guay, G., Altschuler, Y. and Nabi, I. R. (2002). Caveolin-1 is a negative regulator of caveolae-mediated endocytosis to the endoplasmic reticulum. *J Biol Chem* **277**, 3371-9.

Le, P. U. and Nabi, I. R. (2003). Distinct caveolae-mediated endocytic pathways target the Golgi apparatus and the endoplasmic reticulum. *J Cell Sci* **116**, 1059-71.

Lederkremer, G. Z. (2009). Glycoprotein folding, quality control and ER-associated degradation. *Curr Opin Struct Biol* **19**, 515-23.

Lee, C. and Chen, L. B. (1988). Dynamic behavior of endoplasmic reticulum in living cells. *Cell* **54**, 37-46.

Lee, J. N., Song, B., DeBose-Boyd, R. A. and Ye, J. (2006a). Sterol-regulated degradation of Insig-1 mediated by the membrane-bound ubiquitin ligase gp78. *J Biol Chem* **281**, 39308-15.

Lee, J. N., Song, B., DeBose-Boyd, R. A. and Ye, J. (2006b). Sterol-regulated Degradation of Insig-1 Mediated by the Membrane-bound Ubiquitin Ligase gp78. *J Biol Chem* **281**, 39308-39315.

Lee, R. J., Liu, C. W., Harty, C., McCracken, A. A., Latterich, M., Romisch, K., DeMartino, G. N., Thomas, P. J. and Brodsky, J. L. (2004). Uncoupling retro-translocation and degradation in the ER-associated degradation of a soluble protein. *Embo J* **23**, 2206-15.

Lenk, U., Yu, H., Walter, J., Gelman, M. S., Hartmann, E., Kopito, R. R. and Sommer, T. (2002). A role for mammalian Ubc6 homologues in ER-associated protein degradation. *J Cell Sci* **115**, 3007-14.

Li, G., Zhao, G., Zhou, X., Schindelin, H. and Lennarz, W. J. (2006). The AAA ATPase p97 links peptide N-glycanase to the endoplasmic reticulum-associated E3 ligase autocrine motility factor receptor. *Proc Natl Acad Sci U S A* **103**, 8348-53.

Li, G., Zhou, X., Zhao, G., Schindelin, H. and Lennarz, W. J. (2005). Multiple modes of interaction of the deglycosylation enzyme, mouse peptide N-glycanase, with the proteasome. *PNAS* **102**, 15809-15814.

Li, W., Tu, D., Brunger, A. T. and Ye, Y. (2007). A ubiquitin ligase transfers preformed polyubiquitin chains from a conjugating enzyme to a substrate. *Nature* **446**, 333-7.

Li, Z., Okamoto, K., Hayashi, Y. and Sheng, M. (2004). The importance of dendritic mitochondria in the morphogenesis and plasticity of spines and synapses. *Cell* **119**, 873-87.

Liang, J. S., Kim, T., Fang, S., Yamaguchi, J., Weissman, A. M., Fisher, E. A. and Ginsberg, H. N. (2003). Overexpression of the tumor autocrine motility factor receptor Gp78, a ubiquitin protein ligase, results in increased ubiquitinylation and decreased secretion of apolipoprotein B100 in HepG2 cells. *J Biol Chem* **278**, 23984-8.

Lilley, B. N. and Ploegh, H. L. (2005). Multiprotein complexes that link dislocation, ubiquitination, and extraction of misfolded proteins from the endoplasmic reticulum membrane. *PNAS* **102**, 14296-14301.

Liotta, L. A., Mandler, R., Murano, G., Katz, D. A., Gordon, R. K., Chiang, P. K. and Schiffmann, E. (1986). Tumor cell autocrine motility factor. *Proc Natl Acad Sci U S A* **83**, 3302-6.

Luo, S., Baumeister, P., Yang, S., Abcouwer, S. F. and Lee, A. S. (2003). Induction of Grp78/BiP by translational block: activation of the Grp78 promoter by ATF4 through and upstream ATF/CRE site independent of the endoplasmic reticulum stress elements. *J Biol Chem* **278**, 37375-85.

Lytton, J., Westlin, M. and Hanley, M. R. (1991). Thapsigargin inhibits the sarcoplasmic or endoplasmic reticulum Ca-ATPase family of calcium pumps. *J Biol Chem* **266**, 17067-71.

Marsh, B. J., Mastronarde, D. N., Buttle, K. F., Howell, K. E. and McIntosh, J. R. (2001). Organellar relationships in the Golgi region of the pancreatic beta cell line, HIT-T15, visualized by high resolution electron tomography. *Proc Natl Acad Sci U S A* **98**, 2399-406.

Martin, B. R., Giepmans, B. N., Adams, S. R. and Tsien, R. Y. (2005a). Mammalian cell-based optimization of the biarsenical-binding tetracysteine motif for improved fluorescence and affinity. *Nat Biotechnol* **23**, 1308-14.

Martin, B. R., Giepmans, B. N. G., Adams, S. R. and Tsien, R. Y. (2005b). Mammalian cell-based optimization of the biarsenical-binding tetracysteine motif for improved fluorescence and affinity. *Nat Biotechnol* **23**, 1308-1314.

Matsuda, N., Sato, S., Shiba, K., Okatsu, K., Saisho, K., Gautier, C. A., Sou, Y. S., Saiki, S., Kawajiri, S., Sato, F. et al. (2010). PINK1 stabilized by mitochondrial depolarization recruits Parkin to damaged mitochondria and activates latent Parkin for mitophagy. *J Cell Biol* **189**, 211-21.

Meeusen, S., McCaffery, J. M. and Nunnari, J. (2004). Mitochondrial fusion intermediates revealed in vitro. *Science* **305**, 1747-52.

Meldolesi, J. and Pozzan, T. (1998). The endoplasmic reticulum Ca2+ store: a view from the lumen. *Trends Biochem Sci* **23**, 10-4.

Mendes, C. C., Gomes, D. A., Thompson, M., Souto, N. C., Goes, T. S., Goes, A. M., Rodrigues, M. A., Gomez, M. V., Nathanson, M. H. and Leite, M. F. (2005). The type III inositol 1,4,5-trisphosphate receptor preferentially transmits apoptotic Ca2+ signals into mitochondria. *J Biol Chem* **280**, 40892-900.

Merz, S. and Westermann, B. (2009). Genome-wide deletion mutant analysis reveals genes required for respiratory growth, mitochondrial genome maintenance and mitochondrial protein synthesis in Saccharomyces cerevisiae. *Genome Biol* **10**, R95.

Messerschmitt, M., Jakobs, S., Vogel, F., Fritz, S., Dimmer, K. S., Neupert, W. and Westermann, B. (2003). The inner membrane protein Mdm33 controls mitochondrial morphology in yeast. *J Cell Biol* **160**, 553-64.

Meusser, B., Hirsch, C., Jarosch, E. and Sommer, T. (2005). ERAD: the long road to destruction. *Nat Cell Biol* **7**, 766-72.

Meyer, H. H., Wang, Y. and Warren, G. (2002). Direct binding of ubiquitin conjugates by the mammalian p97 adaptor complexes, p47 and Ufd1-Npl4. *Embo J* **21**, 5645-52.

Miyazaki, S., Shirakawa, H., Nakada, K. and Honda, Y. (1993). Essential role of the inositol 1,4,5-trisphosphate receptor/Ca2+ release channel in Ca2+ waves and Ca2+ oscillations at fertilization of mammalian eggs. *Dev Biol* **158**, 62-78.

Molinari, M., Calanca, V., Galli, C., Lucca, P. and Paganetti, P. (2003). Role of EDEM in the release of misfolded glycoproteins from the calnexin cycle. *Science* **299**, 1397-400.

Montero, M., Alonso, M. T., Carnicero, E., Cuchillo-Ibanez, I., Albillos, A., Garcia, A. G., Garcia-Sancho, J. and Alvarez, J. (2000). Chromaffin-cell stimulation triggers fast millimolar mitochondrial Ca2+ transients that modulate secretion. *Nat Cell Biol* **2**, 57-61.

Mori, A., Yamashita, S., Uchino, K., Suga, T., Ikeda, T., Takamatsu, K., Ishizaki, M., Koide, T., Kimura, E., Mita, S. et al. (2011). Derlin-1 overexpression ameliorates mutant SOD1-induced endoplasmic reticulum stress by reducing mutant SOD1 accumulation. *Neurochem Int* **58**, 344-53.

Morito, D., Hirao, K., Oda, Y., Hosokawa, N., Tokunaga, F., Cyr, D. M., Tanaka, K., Iwai, K. and Nagata, A. K. (2008a). Gp78 cooperates with RMA1 in endoplasmic reticulum-associated degradation of CFTRDeltaF508. *Mol Biol Cell* **19**, 1328-36.

Morito, D., Hirao, K., Oda, Y., Hosokawa, N., Tokunaga, F., Cyr, D. M., Tanaka, K., Iwai, K. and Nagata, K. (2008b). Gp78 Cooperates with RMA1 in Endoplasmic Reticulum-associated Degradation of CFTR{Delta}F508. *Mol. Biol. Cell* **19**, 1328-1336.

Mosesson, Y., Shtiegman, K., Katz, M., Zwang, Y., Vereb, G., Szollosi, J. and Yarden, Y. (2003). Endocytosis of receptor tyrosine kinases is driven by monoubiquitylation, not polyubiquitylation. *J Biol Chem* **278**, 21323-6.

Mozdy, A. D., McCaffery, J. M. and Shaw, J. M. (2000). Dnm1p GTPase-mediated mitochondrial fission is a multi-step process requiring the novel integral membrane component Fis1p. *J Cell Biol* **151**, 367-80.

Nabi, I. R. and Raz, A. (1987). Cell shape modulation alters glycosylation of a metastatic melanoma cell-surface antigen. *Int J Cancer* **40**, 396-402.

Nabi, I. R. and Raz, A. (1988). Loss of metastatic responsiveness to cell shape modulation in a newly characterized B16 melanoma adhesive cell variant. *Cancer Res* **48**, 1258-64.

Nabi, I. R., Watanabe, H. and Raz, A. (1990a). Identification of B16-F1 melanoma autocrine motility-like factor receptor. *Cancer Res* **50**, 409-414.

Nabi, I. R., Watanabe, H. and Raz, A. (1990b). Identification of B16-F1 melanoma autocrine motility-like factor receptor. *Cancer Res* **50**, 409-14.

Nabi, I. R., Watanabe, H., Silletti, S. and Raz, A. (1991). Tumor cell autocrine motility factor receptor. *Exs* **59**, 163-77.

Narendra, D. P., Jin, S. M., Tanaka, A., Suen, D. F., Gautier, C. A., Shen, J., Cookson, M. R. and Youle, R. J. (2010). PINK1 is selectively stabilized on impaired mitochondria to activate Parkin. *PLoS Biol* **8**, e1000298.

Oda, Y., Okada, T., Yoshida, H., Kaufman, R. J., Nagata, K. and Mori, K. (2006). Derlin-2 and Derlin-3 are regulated by the mammalian unfolded protein response and are required for ER-associated degradation. *J Cell Biol* **172**, 383-93.

Okuda-Shimizu, Y. and Hendershot, L. M. (2007). Characterization of an ERAD pathway for nonglycosylated BiP substrates, which require Herp. *Mol Cell* **28**, 544-54.

Onishi, Y., Tsukada, K., Yokota, J. and Raz, A. (2003). Overexpression of autocrine motility factor receptor (AMFR) in NIH3T3 fibroblasts induces cell transformation. *Clin Exp Metastasis* **20**, 51-8.

Ono, T., Isobe, K., Nakada, K. and Hayashi, J. I. (2001). Human cells are protected from mitochondrial dysfunction by complementation of DNA products in fused mitochondria. *Nat Genet* **28**, 272-5.

Orci, L., Brown, M. S., Goldstein, J. L., Garcia-Segura, L. M. and Anderson, R. G. (1984). Increase in membrane cholesterol: a possible trigger for degradation of HMG CoA reductase and crystalloid endoplasmic reticulum in UT-1 cells. *Cell* **36**, 835-45.

Oyadomari, S., Yun, C., Fisher, E. A., Kreglinger, N., Kreibich, G., Oyadomari, M., Harding, H. P., Goodman, A. G., Harant, H., Garrison, J. L. et al. (2006).

Cotranslocational degradation protects the stressed endoplasmic reticulum from protein overload. *Cell* **126**, 727-39.

Pacher, P., Sharma, K., Csordas, G., Zhu, Y. and Hajnoczky, G. (2008). Uncoupling of ER-mitochondrial calcium communication by transforming growth factor-beta. *Am J Physiol Renal Physiol* **295**, F1303-12.

Papp, S., Dziak, E., Michalak, M. and Opas, M. (2003). Is all of the endoplasmic reticulum created equal? The effects of the heterogeneous distribution of endoplasmic reticulum Ca2+-handling proteins. *J Cell Biol* **160**, 475-9.

Park, M. K., Ashby, M. C., Erdemli, G., Petersen, O. H. and Tepikin, A. V. (2001). Perinuclear, perigranular and sub-plasmalemmal mitochondria have distinct functions in the regulation of cellular calcium transport. *Embo J* **20**, 1863-74.

Park, S., Isaacson, R., Kim, H. T., Silver, P. A. and Wagner, G. (2005). Ufd1 exhibits the AAA-ATPase fold with two distinct ubiquitin interaction sites. *Structure (Camb)* **13**, 995-1005.

Park, Y. Y., Lee, S., Karbowski, M., Neutzner, A., Youle, R. J. and Cho, H. (2010). Loss of MARCH5 mitochondrial E3 ubiquitin ligase induces cellular senescence through dynamin-related protein 1 and mitofusin 1. *J Cell Sci* **123**, 619-26.

Pearce, M. M., Wang, Y., Kelley, G. G. and Wojcikiewicz, R. J. (2007). SPFH2 mediates the endoplasmic reticulum-associated degradation of inositol 1,4,5-trisphosphate receptors and other substrates in mammalian cells. *J Biol Chem* **282**, 20104-15.

Perkins, G., Renken, C., Martone, M. E., Young, S. J., Ellisman, M. and Frey, T. (1997). Electron tomography of neuronal mitochondria: three-dimensional structure and organization of cristae and membrane contacts. *J Struct Biol* **119**, 260-72.

Petaja-Repo, U. E., Hogue, M., Laperriere, A., Bhalla, S., Walker, P. and Bouvier, M. (2001). Newly synthesized human delta opioid receptors retained in the endoplasmic reticulum are retrotranslocated to the cytosol, deglycosylated, ubiquitinated, and degraded by the proteasome. *J Biol Chem* **276**, 4416-23.

Pfeiffer, D. R., Gunter, T. E., Eliseev, R., Broekemeier, K. M. and Gunter, K. K. (2001). Release of Ca2+ from mitochondria via the saturable mechanisms and the permeability transition. *IUBMB Life* **52**, 205-12.

Piccini, M., Vitelli, F., Bruttini, M., Pober, B. R., Jonsson, J. J., Villanova, M., Zollo, M., Borsani, G., Ballabio, A. and Renieri, A. (1998). FACL4, a new gene encoding long-chain acyl-CoA synthetase 4, is deleted in a family with Alport syndrome, elliptocytosis, and mental retardation. *Genomics* **47**, 350-8.

Piccoli, C., Sardanelli, A., Scrima, R., Ripoli, M., Quarato, G., D'Aprile, A., Bellomo, F., Scacco, S., De Michele, G., Filla, A. et al. (2008). Mitochondrial respiratory dysfunction in familiar parkinsonism associated with PINK1 mutation. *Neurochem Res* **33**, 2565-74.

Pilon, M., Schekman, R. and Romisch, K. (1997). Sec61p mediates export of a misfolded secretory protein from the endoplasmic reticulum to the cytosol for degradation. *Embo J* **16**, 4540-8.

Ponting, C. P. (2000). Proteins of the endoplasmic-reticulum-associated degradation pathway: domain detection and function prediction. *Biochem J* **351 Pt 2**, 527-35.

Pozzan, T., Rizzuto, R., Volpe, P. and Meldolesi, J. (1994). Molecular and cellular physiology of intracellular calcium stores. *Physiol Rev* **74**, 595-636.

Protzel, C., Kakies, C., Kleist, B., Poetsch, M. and Giebel, J. (2008). Down-regulation of the metastasis suppressor protein KAI1/CD82 correlates with occurrence of metastasis, prognosis and presence of HPV DNA in human penile squamous cell carcinoma. *Virchows Arch* **452**, 369-75.

Pye, V. E., Beuron, F., Keetch, C. A., McKeown, C., Robinson, C. V., Meyer, H. H., Zhang, X. and Freemont, P. S. (2007). Structural insights into the p97-Ufd1-Npl4 complex. *Proc Natl Acad Sci U S A* **104**, 467-72.

Rakovic, A., Grunewald, A., Kottwitz, J., Bruggemann, N., Pramstaller, P. P., Lohmann, K. and Klein, C. (2011). Mutations in PINK1 and Parkin impair ubiquitination of Mitofusins in human fibroblasts. *PLoS ONE* **6**, e16746.

Rapizzi, E., Pinton, P., Szabadkai, G., Wieckowski, M. R., Vandecasteele, G., Baird, G., Tuft, R. A., Fogarty, K. E. and Rizzuto, R. (2002). Recombinant expression of the voltage-dependent anion channel enhances the transfer of Ca2+ microdomains to mitochondria. *J Cell Biol* **159**, 613-24.

Raposo, G., van Santen, H. M., Leijendekker, R., Geuze, H. J. and Ploegh, H. L. (1995a). Misfolded major histocompatibility complex class I molecules accumulate in an expanded ER-Golgi intermediate compartment. *Journal of Cell Biology* **131**, 1403-1419.

Raposo, G., van Santen, H. M., Leijendekker, R., Geuze, H. J. and Ploegh, H. L. (1995b). Misfolded major histocompatibility complex class I molecules accumulate in an expanded ER-Golgi intermediate compartment. *J Cell Biol* **131**, 1403-19.

Registre, M., Goetz, J. G., St Pierre, P., Pang, H., Lagace, M., Bouvier, M., Le, P. U. and Nabi, I. R. (2004). The gene product of the gp78/AMFR ubiquitin E3 ligase cDNA is selectively recognized by the 3F3A antibody within a subdomain of the endoplasmic reticulum. *Biochem Biophys Res Commun* **320**, 1316-22.

Ribeiro, C. M., McKay, R. R., Hosoki, E., Bird, G. S. and Putney, J. W., Jr. (2000). Effects of elevated cytoplasmic calcium and protein kinase C on endoplasmic reticulum structure and function in HEK293 cells. *Cell Calcium* **27**, 175-85.

Richly, H., Rape, M., Braun, S., Rumpf, S., Hoege, C. and Jentsch, S. (2005). A series of ubiquitin binding factors connects CDC48/p97 to substrate multiubiquitylation and proteasomal targeting. *Cell* **120**, 73-84.

Rizzuto, R., Brini, M., Murgia, M. and Pozzan, T. (1993). Microdomains with high Ca2+ close to IP3-sensitive channels that are sensed by neighboring mitochondria. *Science* **262**, 744-7.

Rizzuto, R., Duchen, M. R. and Pozzan, T. (2004). Flirting in little space: the ER/mitochondria Ca2+ liaison. *Sci STKE* **2004**, re1.

Rizzuto, R., Pinton, P., Carrington, W., Fay, F. S., Fogarty, K. E., Lifshitz, L. M., Tuft, R. A. and Pozzan, T. (1998). Close contacts with the endoplasmic reticulum as determinants of mitochondrial Ca2+ responses. *Science* **280**, 1763-6.

Rojo, M., Legros, F., Chateau, D. and Lombes, A. (2002). Membrane topology and mitochondrial targeting of mitofusins, ubiquitous mammalian homologs of the transmembrane GTPase Fzo. *J Cell Sci* **115**, 1663-74.

Ross, C. A., Meldolesi, J., Milner, T. A., Satoh, T., Supattapone, S. and Snyder, S. H. (1989). Inositol 1,4,5-trisphosphate receptor localized to endoplasmic reticulum in cerebellar Purkinje neurons. *Nature* **339**, 468-70.

Roy, L., Bergeron, J. J., Lavoie, C., Hendriks, R., Gushue, J., Fazel, A., Pelletier, A., Morre, D. J., Subramaniam, V. N., Hong, W. et al. (2000). Role of p97 and syntaxin 5 in the assembly of transitional endoplasmic reticulum. *Mol Biol Cell* **11**, 2529-42.

Rutledge, A. C., Qiu, W., Zhang, R., Kohen-Avramoglu, R., Nemat-Gorgani, N. and Adeli, K. (2009). Mechanisms targeting apolipoprotein B100 to proteasomal degradation: evidence that degradation is initiated by BiP binding at the N terminus and the formation of a p97 complex at the C terminus. *Arterioscler Thromb Vasc Biol* **29**, 579-85.

Santel, A. and Fuller, M. T. (2001). Control of mitochondrial morphology by a human mitofusin. *J Cell Sci* **114**, 867-74.

Schroder, M. and Kaufman, R. J. (2005). ER stress and the unfolded protein response. *Mutat Res* **569**, 29-63.

Schulz, L. C. and Bahr, J. M. (2003). Glucose-6-phosphate isomerase is necessary for embryo implantation in the domestic ferret. *Proc Natl Acad Sci U S A* **100**, 8561-6.

Schumacher, M. M., Choi, J. Y. and Voelker, D. R. (2002). Phosphatidylserine transport to the mitochondria is regulated by ubiquitination. *J Biol Chem* **277**, 51033-42.

Schwieger, I., Lautz, K., Krause, E., Rosenthal, W., Wiesner, B. and Hermosilla, R. (2008). Derlin-1 and p97/valosin-containing protein mediate the endoplasmic reticulum-associated degradation of human V2 vasopressin receptors. *Mol Pharmacol* **73**, 697-708.

Scorrano, L., Penzo, D., Petronilli, V., Pagano, F. and Bernardi, P. (2001). Arachidonic acid causes cell death through the mitochondrial permeability transition. Implications for tumor necrosis factor-alpha aopototic signaling. *J Biol Chem* **276**, 12035-40.

Sharp, A. H., Snyder, S. H. and Nigam, S. K. (1992). Inositol 1,4,5-trisphosphate receptors. Localization in epithelial tissue. *J Biol Chem* **267**, 7444-9.

Shen, Y., Ballar, P. and Fang, S. (2006). Ubiquitin ligase gp78 increases solubility and facilitates degradation of the Z variant of alpha-1-antitrypsin. *Biochem Biophys Res Commun* **349**, 1285-93.

Shi, Y., Vattem, K. M., Sood, R., An, J., Liang, J., Stramm, L. and Wek, R. C. (1998). Identification and characterization of pancreatic eukaryotic initiation factor 2 alpha-subunit kinase, PEK, involved in translational control. *Mol Cell Biol* **18**, 7499-509.

Shibata, Y., Shemesh, T., Prinz, W. A., Palazzo, A. F., Kozlov, M. M. and Rapoport, T. A. (2010). Mechanisms determining the morphology of the peripheral ER. *Cell* **143**, 774-88.

Shibata, Y., Voeltz, G. K. and Rapoport, T. A. (2006). Rough sheets and smooth tubules. *Cell* **126**, 435-9.

Shibata, Y., Voss, C., Rist, J. M., Hu, J., Rapoport, T. A., Prinz, W. A. and Voeltz, G. K. (2008). The reticulon and DP1/Yop1p proteins form immobile oligomers in the tubular endoplasmic reticulum. *J Biol Chem* **283**, 18892-904.

Shih, S. C., Prag, G., Francis, S. A., Sutanto, M. A., Hurley, J. H. and Hicke, L. (2003a). A ubiquitin-binding motif required for intramolecular monoubiquitylation, the CUE domain. *Embo J* **22**, 1273-81.

Shih, S. C., Prag, G., Francis, S. A., Sutanto, M. A., Hurley, J. H. and Hicke, L. (2003b). A ubiquitin-binding motif required for intramolecular monoubiquitylation, the CUE domain. *Embo J* **22**, 1273-1281.

Shimizu, K., Tani, M., Watanabe, H., Nagamachi, Y., Niinaka, Y., Shiroishi, T., Ohwada, S., Raz, A. and Yokota, J. (1999a). The autocrine motility factor receptor gene encodes a novel type of seven transmembrane protein. *FEBS Lett* **456**, 295-300.

Shimizu, K., Tani, M., Watanabe, H., Nagamachi, Y., Niinaka, Y., Shiroishi, T., Ohwada, S., Raz, A. and Yokota, J. (1999b). The autocrine motility factor receptor gene encodes a novel type of seven transmembrane protein. *FEBS Letters* **456**, 295-300.

Shiraishi, K., Okada, A., Shirakawa, H., Nakanishi, S., Mikoshiba, K. and Miyazaki, S. (1995). Developmental changes in the distribution of the endoplasmic reticulum and inositol 1,4,5-trisphosphate receptors and the spatial pattern of Ca2+ release during maturation of hamster oocytes. *Dev Biol* **170**, 594-606.

Shore, G. C. and Tata, J. R. (1977). Two fractions of rough endoplasmic reticulum from rat liver. I. Recovery of rapidly sedimenting endoplasmic reticulum in association with mitochondria. *J Cell Biol* **72**, 714-25.

Shoshan-Barmatz, V., Zalk, R., Gincel, D. and Vardi, N. (2004). Subcellular localization of VDAC in mitochondria and ER in the cerebellum. *Biochim Biophys Acta* **1657**, 105-14.

Shuai, J. W. and Jung, P. (2003). Optimal ion channel clustering for intracellular calcium signaling. *Proc Natl Acad Sci U S A* **100**, 506-10.

Silletti, S., Paku, S. and Raz, A. (1998). Autocrine motility factor and the extracellular matrix. II. Degradation or remodeling of substratum components directs the motile response of tumor cells. *Int J Cancer* **76**, 129-35.

Silletti, S., Watanabe, H., Hogan, V., Nabi, I. R. and Raz, A. (1991). Purification of B16-F1 melanoma autocrine motility factor and its receptor. *Cancer Res* **51**, 3507-11.

Simard, D. and Nabi, I. R. (1996). Inverse relation of autocrine motility factor receptor and E-cadherin expression following MDCK epithelial cell transformation. *Biochem Biophys Res Commun* **219**, 122-7.

Simmen, T., Aslan, J. E., Blagoveshchenskaya, A. D., Thomas, L., Wan, L., Xiang, Y., Feliciangeli, S. F., Hung, C. H., Crump, C. M. and Thomas, G. (2005). PACS-2 controls endoplasmic reticulum-mitochondria communication and Bid-mediated apoptosis. *Embo J* **24**, 717-29.

Simpson, P. B., Mehotra, S., Lange, G. D. and Russell, J. T. (1997). High density distribution of endoplasmic reticulum proteins and mitochondria at specialized Ca2+ release sites in oligodendrocyte processes. *J Biol Chem* **272**, 22654-61.

Skulachev, V. P. (2001). Mitochondrial filaments and clusters as intracellular power-transmitting cables. *Trends Biochem Sci* **26**, 23-9.

Smirnova, E., Shurland, D. L., Ryazantsev, S. N. and van der Bliek, A. M. (1998). A human dynamin-related protein controls the distribution of mitochondria. *J Cell Biol* **143**, 351-8.

Snapp, E. L., Hegde, R. S., Francolini, M., Lombardo, F., Colombo, S., Pedrazzini, E., Borgese, N. and Lippincott-Schwartz, J. (2003). Formation of stacked ER cisternae by low affinity protein interactions. *J Cell Biol* **163**, 257-69.

Sommer, J. R. and Johnson, E. A. (1970). Comparative ultrastructure of cardiac cell membrane specializations. A review. *Am J Cardiol* **25**, 184-94.

Song, B. L., Sever, N. and DeBose-Boyd, R. A. (2005). Gp78, a membrane-anchored ubiquitin ligase, associates with Insig-1 and couples sterol-regulated ubiquitination to degradation of HMG CoA reductase. *Mol Cell* **19**, 829-40.

Spiliotis, E. T., Pentcheva, T. and Edidin, M. (2002a). Probing for Membrane Domains in the Endoplasmic Reticulum: Retention and Degradation of Unassembled MHC Class I Molecules. *Mol. Biol. Cell* **13**, 1566-1581.

Spiliotis, E. T., Pentcheva, T. and Edidin, M. (2002b). Probing for membrane domains in the endoplasmic reticulum: retention and degradation of unassembled MHC class I molecules. *Mol Biol Cell* **13**, 1566-81.

Sprocati, T., Ronchi, P., Raimondi, A., Francolini, M. and Borgese, N. (2006). Dynamic and reversible restructuring of the ER induced by PDMP in cultured cells. *J Cell Sci* **119**, 3249-60.

Sriburi, R., Jackowski, S., Mori, K. and Brewer, J. W. (2004). XBP1: a link between the unfolded protein response, lipid biosynthesis, and biogenesis of the endoplasmic reticulum. *J Cell Biol* **167**, 35-41.

Starkov, A. A., Chinopoulos, C. and Fiskum, G. (2004). Mitochondrial calcium and oxidative stress as mediators of ischemic brain injury. *Cell Calcium* **36**, 257-64.

Stirling, C. J. and Lord, J. M. (2006). Quality control: linking retrotranslocation and degradation. *Curr Biol* **16**, R1035-7.

Stone, S. J. and Vance, J. E. (2000). Phosphatidylserine synthase-1 and -2 are localized to mitochondria-associated membranes. *J Biol Chem* **275**, 34534-40.

Straub, S. V., Giovannucci, D. R. and Yule, D. I. (2000). Calcium wave propagation in pancreatic acinar cells: functional interaction of inositol 1,4,5-trisphosphate receptors, ryanodine receptors, and mitochondria. *J Gen Physiol* **116**, 547-60.

Subramanian, K. and Meyer, T. (1997). Calcium-induced restructuring of nuclear envelope and endoplasmic reticulum calcium stores. *Cell* **89**, 963-71.

Sudjana-Sugiaman, E., Eggertsen, G. and Bjorkhem, I. (1994). Stimulation of HMG-CoA reductase as a consequence of phenobarbital-induced primary stimulation of cholesterol 7 alpha-hydroxylase in rat liver. *J Lipid Res* **35**, 319-27.

Sun, F., Zhang, R., Gong, X., Geng, X., Drain, P. F. and Frizzell, R. A. (2006). Derlin-1 promotes the efficient degradation of the cystic fibrosis transmembrane conductance regulator (CFTR) and CFTR folding mutants. *J Biol Chem* **281**, 36856-63.

Szabadkai, G., Bianchi, K., Varnai, P., De Stefani, D., Wieckowski, M. R., Cavagna, D., Nagy, A. I., Balla, T. and Rizzuto, R. (2006). Chaperone-mediated coupling of endoplasmic reticulum and mitochondrial Ca2+ channels. *J Cell Biol* **175**, 901-11.

Szabadkai, G., Simoni, A. M. and Rizzuto, R. (2003). Mitochondrial Ca2+ uptake requires sustained Ca2+ release from the endoplasmic reticulum. *J Biol Chem* **278**, 15153-61.

Taguchi, N., Ishihara, N., Jofuku, A., Oka, T. and Mihara, K. (2007). Mitotic phosphorylation of dynamin-related GTPase Drp1 participates in mitochondrial fission. *J Biol Chem* **282**, 11521-9.

Takei, K., Stukenbrok, H., Metcalf, A., Mignery, G. A., Sudhof, T. C., Volpe, P. and De Camilli, P. (1992). Ca2+ stores in Purkinje neurons: endoplasmic reticulum subcompartments demonstrated by the heterogeneous distribution of the InsP3 receptor, Ca(2+)-ATPase, and calsequestrin. *J Neurosci* **12**, 489-505.

Tcherpakov, M., Delaunay, A., Toth, J., Kadoya, T., Petroski, M. D. and Ronai, Z. e. A. (2009). Regulation of Endoplasmic Reticulum-associated Degradation by RNF5-dependent Ubiquitination of JNK-associated Membrane Protein (JAMP). *J Biol Chem* **284**, 12099-12109.

Terasaki, M., Jaffe, L. A., Hunnicutt, G. R. and Hammer, J. A., 3rd. (1996). Structural change of the endoplasmic reticulum during fertilization: evidence for loss of membrane continuity using the green fluorescent protein. *Dev Biol* **179**, 320-8.

Terasaki, M., Runft, L. L. and Hand, A. R. (2001). Changes in organization of the endoplasmic reticulum during Xenopus oocyte maturation and activation. *Mol Biol Cell* **12**, 1103-16.

Thastrup, O., Cullen, P. J., Drobak, B. K., Hanley, M. R. and Dawson, A. P. (1990). Thapsigargin, a tumor promoter, discharges intracellular Ca2+ stores by specific inhibition of the endoplasmic reticulum Ca2(+)-ATPase. *Proc Natl Acad Sci U S A* **87**, 2466-70.

Tieu, Q. and Nunnari, J. (2000). Mdv1p is a WD repeat protein that interacts with the dynamin-related GTPase, Dnm1p, to trigger mitochondrial division. *J Cell Biol* **151**, 353-66.

Tieu, Q., Okreglak, V., Naylor, K. and Nunnari, J. (2002). The WD repeat protein, Mdv1p, functions as a molecular adaptor by interacting with Dnm1p and Fis1p during mitochondrial fission. *J Cell Biol* **158**, 445-52.

Tinel, H., Cancela, J. M., Mogami, H., Gerasimenko, J. V., Gerasimenko, O. V., Tepikin, A. V. and Petersen, O. H. (1999). Active mitochondria surrounding the pancreatic acinar granule region prevent spreading of inositol trisphosphate-evoked local cytosolic Ca(2+) signals. *Embo J* **18**, 4999-5008.

Tirasophon, W., Welihinda, A. A. and Kaufman, R. J. (1998). A stress response pathway from the endoplasmic reticulum to the nucleus requires a novel bifunctional protein kinase/endoribonuclease (Ire1p) in mammalian cells. *Genes Dev* **12**, 1812-24.

Tondera, D., Czauderna, F., Paulick, K., Schwarzer, R., Kaufmann, J. and Santel, A. (2005). The mitochondrial protein MTP18 contributes to mitochondrial fission in mammalian cells. *J Cell Sci* **118**, 3049-59.

Travers, K. J., Patil, C. K., Wodicka, L., Lockhart, D. J., Weissman, J. S. and Walter, P. (2000). Functional and genomic analyses reveal an essential coordination between the unfolded protein response and ER-associated degradation. *Cell* **101**, 249-58.

Tsai, Y. C., Mendoza, A., Mariano, J. M., Zhou, M., Kostova, Z., Chen, B., Veenstra, T., Hewitt, S. M., Helman, L. J., Khanna, C. et al. (2007). The ubiquitin ligase gp78 promotes sarcoma metastasis by targeting KAI1 for degradation. *Nat Med* **13**, 1504-9.

Tsutsumi, S., Gupta, S. K., Hogan, V., Tanaka, N., Nakamura, K. T., Nabi, I. R. and Raz, A. (2003a). The enzymatic activity of phosphoglucose isomerase is not required for its cytokine function. *FEBS Lett* **534**, 49-53.

Tsutsumi, S., Hogan, V., Nabi, I. R. and Raz, A. (2003b). Overexpression of the autocrine motility factor/phosphoglucose isomerase induces transformation and survival of NIH-3T3 fibroblasts. *Cancer Res* **63**, 242-9.

Twig, G., Elorza, A., Molina, A. J., Mohamed, H., Wikstrom, J. D., Walzer, G., Stiles, L., Haigh, S. E., Katz, S., Las, G. et al. (2008). Fission and selective fusion govern mitochondrial segregation and elimination by autophagy. *Embo J* **27**, 433-46.

Uchiyama, K., Totsukawa, G., Puhka, M., Kaneko, Y., Jokitalo, E., Dreveny, I., Beuron, F., Zhang, X., Freemont, P. and Kondo, H. (2006). p37 is a p97 adaptor required for Golgi and ER biogenesis in interphase and at the end of mitosis. *Dev Cell* **11**, 803-16.

Vance, J. E. (1990). Phospholipid synthesis in a membrane fraction associated with mitochondria. *J Biol Chem* **265**, 7248-56.

Vembar, S. S. and Brodsky, J. L. (2008). One step at a time: endoplasmic reticulum-associated degradation. *Nat Rev Mol Cell Biol* **9**, 944-57.

Vendelin, M., Eimre, M., Seppet, E., Peet, N., Andrienko, T., Lemba, M., Engelbrecht, J., Seppet, E. K. and Saks, V. A. (2004). Intracellular diffusion of adenosine phosphates is locally restricted in cardiac muscle. *Mol Cell Biochem* **256-257**, 229-41.

Ventura-Clapier, R., Garnier, A. and Veksler, V. (2004). Energy metabolism in heart failure. *J Physiol* **555**, 1-13.

Voeltz, G. K. and Prinz, W. A. (2007). Sheets, ribbons and tubules - how organelles get their shape. *Nat Rev Mol Cell Biol* **8**, 258-64.

Voeltz, G. K., Prinz, W. A., Shibata, Y., Rist, J. M. and Rapoport, T. A. (2006). A class of membrane proteins shaping the tubular endoplasmic reticulum. *Cell* **124**, 573-86.

Voeltz, G. K., Rolls, M. M. and Rapoport, T. A. (2002). Structural organization of the endoplasmic reticulum. *EMBO Rep* **3**, 944-50.

Wahlman, J., DeMartino, G. N., Skach, W. R., Bulleid, N. J., Brodsky, J. L. and Johnson, A. E. (2007). Real-time fluorescence detection of ERAD substrate retrotranslocation in a mammalian in vitro system. *Cell* **129**, 943-55.

Wakabayashi, J., Zhang, Z., Wakabayashi, N., Tamura, Y., Fukaya, M., Kensler, T. W., Iijima, M. and Sesaki, H. (2009). The dynamin-related GTPase Drp1 is required for embryonic and brain development in mice. *J Cell Biol* **186**, 805-16.

Wakana, Y., Takai, S., Nakajima, K., Tani, K., Yamamoto, A., Watson, P., Stephens, D. J., Hauri, H. P. and Tagaya, M. (2008). Bap31 is an itinerant protein that moves between the peripheral endoplasmic reticulum (ER) and a juxtanuclear compartment related to ER-associated Degradation. *Mol Biol Cell* **19**, 1825-36.

Wang, B., Heath-Engel, H., Zhang, D., Nguyen, N., Thomas, D. Y., Hanrahan, J. W. and Shore, G. C. (2008). BAP31 interacts with Sec61 translocons and promotes retrotranslocation of CFTRDeltaF508 via the derlin-1 complex. *Cell* **133**, 1080-92.

Wang, H.-J., Benlimame, N. and Nabi, I. R. (1997a). The AMF-R tubule is a smooth ilimaquinone-sensitive subdomain of the endoplasmic reticulum. *Journal of Cell Science* **110**, 3043-3053.

Wang, H. J., Benlimame, N. and Nabi, I. (1997b). The AMF-R tubule is a smooth ilimaquinone-sensitive subdomain of the endoplasmic reticulum. *J Cell Sci* **110 (Pt 24)**, 3043-53.

Wang, H. J., Guay, G., Pogan, L., Sauve, R. and Nabi, I. R. (2000). Calcium regulates the association between mitochondria and a smooth subdomain of the endoplasmic reticulum. *J Cell Biol* **150**, 1489-98.

Wang, Q. and Chang, A. (2003). Substrate recognition in ER-associated degradation mediated by Eps1, a member of the protein disulfide isomerase family. *Embo J* **22**, 3792-802.

Wang, Q., Li, L. and Ye, Y. (2006). Regulation of retrotranslocation by p97-associated deubiquitinating enzyme ataxin-3. *J Cell Biol* **174**, 963-71.

Watanabe, H., Carmi, P., Hogan, V., Raz, T., Silletti, S., Nabi, I. R. and Raz, A. (1991). Purification of human tumor cell autocrine motility factor and molecular cloning of its receptor. *J Biol Chem* **266**, 13442-8.

Watanabe, H., Takehana, K., Date, M., Shinozaki, T. and Raz, A. (1996). Tumor cell autocrine motility factor is the neuroleukin/phosphohexose isomerase polypeptide. *Cancer Res* **56**, 2960-3.

Wesche, J., Rapak, A. and Olsnes, S. (1999). Dependence of ricin toxicity on translocation of the toxin A-chain from the endoplasmic reticulum to the cytosol. *J Biol Chem* **274**, 34443-9.

Westermann, B. (2010). Mitochondrial fusion and fission in cell life and death. *Nat Rev Mol Cell Biol* **11**, 872-84.

Wiertz, E. J., Jones, T. R., Sun, L., Bogyo, M., Geuze, H. J. and Ploegh, H. L. (1996a). The human cytomegalovirus US11 gene product dislocates MHC class I heavy chains from the endoplasmic reticulum to the cytosol. *Cell* **84**, 769-79.

Wiertz, E. J., Tortorella, D., Bogyo, M., Yu, J., Mothes, W., Jones, T. R., Rapoport, T. A. and Ploegh, H. L. (1996b). Sec61-mediated transfer of a membrane protein from the endoplasmic reticulum to the proteasome for destruction. *Nature* **384**, 432-8.

Wilkinson, C. R., Seeger, M., Hartmann-Petersen, R., Stone, M., Wallace, M., Semple, C. and Gordon, C. (2001). Proteins containing the UBA domain are able to bind to multi-ubiquitin chains. *Nat Cell Biol* **3**, 939-43.

Wilson, B. S., Pfeiffer, J. R., Smith, A. J., Oliver, J. M., Oberdorf, J. A. and Wojcikiewicz, R. J. (1998). Calcium-dependent clustering of inositol 1,4,5-trisphosphate receptors. *Mol Biol Cell* **9**, 1465-78.

Wojcik, C., Yano, M. and DeMartino, G. N. (2004). RNA interference of valosin-containing protein (VCP/p97) reveals multiple cellular roles linked to ubiquitin/proteasome-dependent proteolysis. *J Cell Sci* **117**, 281-92.

Xu, J. H., Guo, X. Z., Ren, L. N., Shao, L. C. and Liu, M. P. (2008). KAI1 is a potential target for anti-metastasis in pancreatic cancer cells. *World J Gastroenterol* **14**, 1126-32.

Xu, P., Duong, D. M., Seyfried, N. T., Cheng, D., Xie, Y., Robert, J., Rush, J., Hochstrasser, M., Finley, D. and Peng, J. (2009). Quantitative proteomics reveals the function of unconventional ubiquitin chains in proteasomal degradation. *Cell* **137**, 133-45.

Yakirevich, E. and Naot, Y. (2000). Cloning of a glucose phosphate isomerase/neuroleukin-like sperm antigen involved in sperm agglutination. *Biol Reprod* **62**, 1016-23.

Yanagawa, T., Watanabe, H., Takeuchi, T., Fujimoto, S., Kurihara, H. and Takagishi, K. (2004). Overexpression of autocrine motility factor in metastatic tumor cells: possible association with augmented expression of KIF3A and GDI-beta. *Lab Invest* **84**, 513-22.

Yang, J. M., Peng, Z. H., Si, S. H., Liu, W. W., Luo, Y. H. and Ye, Z. Y. (2008). KAI1 gene suppresses invasion and metastasis of hepatocellular carcinoma MHCC97-H cells in vitro and in animal models. *Liver Int* **28**, 132-9.

Ye, Y., Meyer, H. H. and Rapoport, T. A. (2001). The AAA ATPase Cdc48/p97 and its partners transport proteins from the ER into the cytosol. *Nature* **414**, 652-6.

Ye, Y., Meyer, H. H. and Rapoport, T. A. (2003). Function of the p97-Ufd1-Npl4 complex in retrotranslocation from the ER to the cytosol: dual recognition of nonubiquitinated polypeptide segments and polyubiquitin chains. *J Cell Biol* **162**, 71-84.

Ye, Y., Shibata, Y., Kikkert, M., van Voorden, S., Wiertz, E. and Rapoport, T. A. (2005a). Inaugural Article: Recruitment of the p97 ATPase and ubiquitin ligases to the site of retrotranslocation at the endoplasmic reticulum membrane. *PNAS* **102**, 14132-14138.

Ye, Y., Shibata, Y., Kikkert, M., van Voorden, S., Wiertz, E. and Rapoport, T. A. (2005b). Inaugural Article: Recruitment of the p97 ATPase and ubiquitin ligases to the site of retrotranslocation at the endoplasmic reticulum membrane. *Proc Natl Acad Sci U S A* **102**, 14132-8.

Ye, Y., Shibata, Y., Yun, C., Ron, D. and Rapoport, T. A. (2004). A membrane protein complex mediates retro-translocation from the ER lumen into the cytosol. *Nature* **429**, 841-7.

Yi, M., Weaver, D. and Hajnoczky, G. (2004). Control of mitochondrial motility and distribution by the calcium signal: a homeostatic circuit. *J Cell Biol* **167**, 661-72.

Yonashiro, R., Ishido, S., Kyo, S., Fukuda, T., Goto, E., Matsuki, Y., Ohmura-Hoshino, M., Sada, K., Hotta, H., Yamamura, H. et al. (2006). A novel mitochondrial ubiquitin ligase plays a critical role in mitochondrial dynamics. *Embo J* **25**, 3618-26.

Yoshida, H. (2007). ER stress and diseases. *FEBS J* **274**, 630-58.

Yoshida, H., Matsui, T., Hosokawa, N., Kaufman, R. J., Nagata, K. and Mori, K. (2003). A time-dependent phase shift in the mammalian unfolded protein response. *Dev Cell* **4**, 265-71.

Yu, F. L., Liao, M. H., Lee, J. W. and Shih, W. L. (2004). Induction of hepatoma cells migration by phosphoglucose isomerase/autocrine motility factor through the upregulation of matrix metalloproteinase-3. *Biochem Biophys Res Commun* **314**, 76-82.

Zhang, Y. and Chan, D. C. (2007). Structural basis for recruitment of mitochondrial fission complexes by Fis1. *Proc Natl Acad Sci U S A* **104**, 18526-30.

Zhong, X. and Pittman, R. N. (2006). Ataxin-3 binds VCP/p97 and regulates retrotranslocation of ERAD substrates. *Hum Mol Genet* **15**, 2409-20.

Zhong, X., Shen, Y., Ballar, P., Apostolou, A., Agami, R. and Fang, S. (2004). AAA ATPase p97/valosin-containing protein interacts with gp78, a ubiquitin ligase for endoplasmic reticulum-associated degradation. *J Biol Chem* **279**, 45676-84.

Zimmermann, B. (2000). Control of InsP3-induced Ca2+ oscillations in permeabilized blowfly salivary gland cells: contribution of mitochondria. *J Physiol* **525 Pt 3**, 707-19.

Ziviani, E., Tao, R. N. and Whitworth, A. J. Drosophila parkin requires PINK1 for mitochondrial translocation and ubiquitinates mitofusin. *Proc Natl Acad Sci U S A* **107**, 5018-23.